

Electronic Thesis and Dissertation Repository

10-5-2022 9:00 AM

Probing the genetic code with Leucine tRNA variants

Peter Anderson Hall, *The University of Western Ontario*

Supervisor: O'donoghue, Patrick, *The University of Western Ontario*

Co-Supervisor: Brandl, Christopher J, *The University of Western Ontario*

A thesis submitted in partial fulfillment of the requirements for the Master of Science degree in Biochemistry

© Peter Anderson Hall 2022

Follow this and additional works at: <https://ir.lib.uwo.ca/etd>



Part of the [Molecular Biology Commons](#)

Recommended Citation

Hall, Peter Anderson, "Probing the genetic code with Leucine tRNA variants" (2022). *Electronic Thesis and Dissertation Repository*. 8956.

<https://ir.lib.uwo.ca/etd/8956>

This Dissertation/Thesis is brought to you for free and open access by Scholarship@Western. It has been accepted for inclusion in Electronic Thesis and Dissertation Repository by an authorized administrator of Scholarship@Western. For more information, please contact wlsadmin@uwo.ca.

Abstract

Mistranslation is an error in protein synthesis whereby the amino acids specified by the genetic code are misplaced by others in the growing polypeptide chain. The anticodon of tRNA^{Leu} can be altered allowing for the misincorporation of leucine at non-leucine codons. Observing the effect of tRNA^{Leu} variants on the viability of yeast and mammalian cells will provide information on their ability to cause mistranslation and potential relationship to genetic diseases. To explore this, a random pool of tRNA^{Leu} anticodon variants was expressed in *Saccharomyces cerevisiae*. Furthermore, three mutant tRNA^{Leu} already sequenced from humans were expressed in murine Neuro 2A blastoma cells. There was slow growth in yeast when tRNA^{Leu} with proline (NGG) and arginine (GCG) anticodons were expressed. In N2a cells tRNA^{Leu}_{GAA} lowered protein synthesis while tRNA^{Leu}_{CCA} increased it. The effect of each tRNA^{Leu} anticodon variant varied depended on the anticodon with no obvious correlation to known biological factors.

Keywords

transfer RNA, aminoacyl tRNA synthetase, translation, mistranslation, *Saccharomyces cerevisiae*, murine neuro-2a blastoma cells, proteotoxicity, protein synthesis, ribosome, doxycycline

Summary for lay audience

DNA is the genetic library of our cells. It stores all the essential data for creating proteins and other biological materials that allow for cells to function. To translate DNA into protein, it first must be transcribed into messenger RNA (mRNA). A protein called RNA polymerase II runs along DNA and adds nucleotides until an mRNA chain is created. This mRNA is delivered a macromolecular complex called the ribosome. A molecule known as Eukaryotic translation factor 1A (eEF1A) delivers tRNAs to the ribosome. tRNAs are another type of RNA which deliver amino acids, the building blocks of proteins, to the ribosome to allow protein synthesis.

This study endeavors to change a component of tRNAs called the anticodon to leucine carrying tRNAs. The anticodon is located at the bottom of the tRNA molecule and can base-pair with specific three nucleotide sequences in mRNA known as codons. Through changing the anticodon, the leucine carrying tRNA (tRNA^{Leu}) can bind to non-leucine codons and add leucine to a protein instead of another amino acid. This creates an abnormal protein which is likely harmful to cells but could provide benefits under certain circumstances. tRNA^{Leu} is special as they can change their anticodon and still carry its cognate (leucine) amino acid.

It is important to study the effects of the tRNA^{Leu} anticodon mutants as they have been found in some humans. Therefore, it is important to observe the effects of these tRNAs on yeast and mammalian cells to relate the data collected to human disease. Using these tRNAs to create abnormal proteins could help in engineering synthetic proteins with unique functions, or in making a codon ambiguously decode two amino acids. The results of this study show that certain tRNA^{Leu} variants with proline and arginine anticodons cause yeast cells to grow very slow. There are also human tRNA^{Leu} variants that mistranslate phenylalanine and methionine. These tRNAs either protein synthesis or increase toxicity when protein degradation is halted.

Co-authorship

Julie Genereaux constructed the tRNA^{Leu} anticodon variant plasmids. Victoria Clarke was responsible for the trypsin digest of yeast cell lysates for mass spec analysis. Paula Pittock performed the LC MS/MS analysis of these trypsin digested samples. Jeremy Lant provided the tRNA^{Ser}_{AGA} and tRNA^{Ser}_{AAA} plasmids.

Acknowledgements

I would like to acknowledge my two supervisors Dr. Christopher John Brandl and Dr. Patrick O'Donoghue for letting me work for both of their labs. They have both been beyond generous in helping me complete my work every step of the way. I would also like to thank both Jeremy Lant and Farah Hasan in mentoring me in my work with human tRNA^{Leu} variants and mammalian cell culturing. Without them I would not have been able to complete this study. The same can be said for Julie Genereaux who taught me how to culture *E. coli* and yeast cells. She also helped me to clone yeast tRNA^{Leu} genes into yeast plasmids. I also need to thank Victoria Clarke for doing the trypsin digest and Paula Pittock for performing the LC-MS/MS experiment and assisting in the analysis of the spectra. I also must thank Matthew Berg and Ecaterina Cozma for giving me advice on how to interpret my data. Lastly, I want to thank my committee members Bogumil Karas and Murray Junop for all the excellent advice they gave me on this project.

Table of Contents

Abstract.....	ii
Summary for Lay Audience.....	iii
Co-Authorship.....	iv
Acknowledgements.....	v
Table of contents.....	vii
List of Figures.....	ix
List of Tables.....	x
List of Abbreviations.....	xiv
1 Introduction.....	2
1.1 Overview of translation.....	4
1.2 Genetic code.....	6
1.3 tRNA structure.....	7
1.4 tRNA modifications.....	8
1.5 Amino-acyl tRNA synthetases.....	8
1.6 tRNA ^{Leu} identity elements.....	9
1.7 Ribosome stalling.....	9
1.8 Tolerance to mistranslation in diverse cells	10
1.9 Mistranslating tRNAs and disease.....	11
1.10 tRNA ^{Leu} variants as a probe to explore genetic code evolution	12
1.11 tRNA expression system.....	12
1.12 Detecting mistranslation.....	14
1.13 Objectives	15

2	Materials and Methods	
2.1	Plasmids.....	17
2.2	Yeast strains and growth	18
2.3	Mass spectrometry.....	20
2.4	Synthesis by overlap PCR.....	20
2.5	Mammalian plasmids.....	21
2.6	Cell transfection.....	22
2.7	Fluorescence microscopy and data analysis.....	23
2.8	Cytotoxicity analysis.....	23
3	Results.....	24
3.1	Inducible expression of tRNA ^{Leu} variant tRNA ^{Leu} _{UGG}	25
3.2	Addition of G26A mutation to tRNA ^{Leu} variant.....	28
3.3	Growth rate analysis of tRNA ^{Leu} variant yeast strains.....	31
3.4	Trends in the growth curve data.....	36
3.5	Mass spectrometry of tRNA ^{Leu} variant yeast strains.....	41
3.6	Selecting the mammalian tRNA variants.....	44
3.7	Mammalian cell fluorescence after proteasome inhibition.....	45
3.8	Cytotoxicity analysis of tRNA ^{Leu} variant cell lines.....	49
4	Discussion.....	55
4.1	Safe expression of tRNA ^{Leu} variants in yeast.....	56
4.2	tRNA ^{Leu} identity in yeast.....	56
4.3	Comparing GC content of the anticodon.....	57
4.4	Type of amino acid substitution.....	58
4.5	Codon and anticodon context.....	60
4.6	Changes in protein synthesis and the toxic effect of human tRNA ^{Leu} variants.....	62
4.7	Conclusion.....	63
	References.....	74
	Supplemental figures	82
	Supplemental Tables.....	91

Curriculum Vitae.....	93
-----------------------	----

List of Figures

Figure 1: Diagram of tRNA ^{Leu} wild type and tRNA ^{Leu} variant delivering leucine at the ribosome.....	2
Figure 2: Representation of translation at the ribosome.....	4
Figure 3: Diagram of wild type tRNA ^{Leu}	7
Figure 4: Diagram of the doxycycline TetO promoter inducible tRNA expression system.....	13
Figure 5: Representative growth curve images for tRNA ^{Leu} _{UAA} expressing yeast cells and tRNA ^{Leu} _{UGG} expressing yeast cells	26
Figure 6: Scatter plot of 24 hour growth curve data for yeast cells transformed with tRNA ^{Leu} _{UAA} and mutant tRNA ^{Leu} _{UGG} (Pro).....	27
Figure 7: Comparing the Area under curve in tRNA ^{Leu} _{UAA} , tRNA ^{Leu} _{UGG} (Pro) and tRNA ^{Leu} _{UGG} (G26A) expressing yeast cells.....	29
Figure 8: Growth rate analysis of 38 different tRNA ^{Leu} anticodon variant expressing yeast strains.....	32
Figure 9: Representative growth curves of yeast cells expressing the wild-type tRNA ^{Leu} _{UAA} (A) and the tRNA ^{Leu} _{CGG} (Pro) variant (B).....	33
Figure 10: Linear correlation of potential codon usage against the doubling time of the tRNA ^{Leu} anticodon variant strain.....	37
Figure 11: Linear correlation of GC content of the anticodon against the doubling time of the tRNA ^{Leu} anticodon variant strain.....	38
Figure 12: Comparing the doubling time of the tRNA ^{Leu} anticodon variants with the BLOSUM62 matrix.....	39
Figure 13: Mass spectrometry profiles of Saccharopepsin peptide found in tRNA ^{Leu} _{CGG} and wild type tRNA ^{Leu} _{UAA} yeast cells.....	43

Figure 14: The Comparison of eGFP fluorescence between wild type tRNA^{Leu}_{AAG} and tRNA^{Leu}_{AAA}(G36A) (phenylalanine anticodon) N2_a cells.....46

Figure 15: The comparison of GFP fluorescence between the wild type tRNA^{Leu}_{CAA}, tRNA^{Leu}_{CCA} (A35C) (tryptophan anticodon) and tRNA^{Leu}_{GAA} (C34G) (phenylalanine anticodon) N2_a cells...47

Figure 16: The comparison of eGFP fluorescence in tRNA^{Leu}_{AAG} and tRNA^{Leu}_{AAA} (G36A) (phenylalanine anticodon) N2_a cells under different concentrations of MG132.....50

Figure 17: The comparison of eGFP fluorescence in wild-type tRNA^{Leu}_{CAA}, tRNA^{Leu}_{CCA} (A35C) (tryptophan anticodon) and tRNA^{Leu}_{GAA} (C34G) (phenylalanine anticodon) N2_a cells under different MG132 concentrations.....51

Figure 18: The comparison of relative cytotoxicity caused by wild type tRNA^{Leu}_{CAA}, tRNA^{Leu}_{CCA} (A35C) (tryptophan anticodon) and tRNA^{Leu}_{GAA} (C34G) (phenylalanine anticodon) towards N2_a cells under different MG132 concentrations.53

Figure 19: The comparison of relative cytotoxicity induced by tRNA^{Leu}_{AAG} and tRNA^{Leu}_{AAA}(G36A) (phenylalanine anticodon) in N2_a cells under different MG132 concentrations.....54

List of Tables

Table 1: The 64-codon genetic code.....	5
Table 2: List of Yeast oligos used to amplify tRNA ^{Leu} genes from plasmids.....	17
Table 3: Description of yeast strains used in this study.....	18
Table 4: Heat map of the growth rate of each tRNA ^{Leu} anticodon variant yeast strain.....	34
Table 5: Description of proteins with leucine mistranslation identified via LC-MS/MS	42
Table 6: The profiles for the three human tRNA ^{Leu} anticodon variants.....	44

List of abbreviations

%	Percent
°C	Degrees Celsius
A	Adenine
A600	Absorbance at 600 nm
aaRS	Aminoacyl-tRNA synthetase
Ala	Alanine
Arg	Arginine
AUC	Area under curve
BLAST	Basic local alignment search tool
bp	Base pair
C	Cytosine
Cys	Cysteine
Da	Dalton
DNA	Deoxyribonucleic acid
Dnmt2	tRNA (cytosine38-C5)-methyltransferase
DOX	Doxycycline
eEf1A	Eukaryotic translation elongation factor 1 alpha 1
eiF2	Eukaryotic initiation factor 2
eiF2a	Eukaryotic translation initiation factor 2
ER	Endoplasmic reticulum
G	Guanine

eGFP	Enhanced green fluorescent protein
Glu	Glutamic acid
Gly	Glycine
I	Inosine
LB	Lysogeny broth
LC-MS/MS spectrometry	Liquid chromatography-coupled tandem mass spectrometry
Leu	Leucine
LeuRS	Leucyl-tRNA synthetase
Lys	Lysine
m/z	Mass to charge
tRNA ^{Leu}	Leucine tRNA
m ⁵ C	5-methylcytidine
m ⁷ G	7-methylguanosine
Met	Methionine
mL	Millilitre
mM	Millimolar
mol	Mole
mRNA	Messenger ribonucleic acid
MS	Mass spectrometry
N2 _a	Murine Neuro2A Blastoma cells
NaCl	Sodium chloride
ncm5U	5-carbamoylmethyluridine

mcm5U	5-methoxycarbonylmethyluridine
mcm5s2U	5-methoxycarbonylmethyl-2-thiouridine
Nm	Nanometer
PCR	Polymerase chain reaction
PDB	Protein database
pH	Potential of hydrogen
ppm	Parts per million
polyQ	Polyglutamine
Pro	Proline
Rat1	5'-3' exoribonuclease 2
RNA	Ribonucleic acid
rRNA	Ribosomal ribonucleic acid
RTD	Rapid tRNA decay
Ser	Serine
SNP	Single nucleotide polymorphism
TetO	Tetracycline operator
TetR	Tetracycline repressor
tRNA	Transfer ribonucleic acid
Trp	Tryptophan
U	Uracil
Val	Valine
WT	Wild type
Xm1	5'-3' exoribonuclease 1

YCplac111(Leu2)

Yeast centromeric plasmid with a leu 2 marker

YPD

Yeast extract-peptone-dextrose media

μg

Microgram

μl

Microliter

μM

Micromol

Chapter 1

1.0 Introduction

In biochemical terms, mistranslation is the addition of an amino acid that does not match the sequence outlined in the genome, to a growing peptide due to an error in tRNA amino-acylation or an improper tRNA-codon interaction (1). In terms of errors in tRNA amino-acylation, an amino-acyl tRNA synthetase (AARS) may add a non-cognate amino acid to a tRNA or add the correct amino acid to a tRNA with an incorrect anticodon. A properly amino-acylated wild-type tRNA may also base-pair with a non-cognate codon, leading to the addition of a non-template amino acid to the growing polypeptide chain (2). This is important as while these mistranslation events are tolerated by cells, they may cause proteotoxic stress, which may be either highly detrimental or even lethal to the cells (3). This proteotoxic stress can come from the aggregation of mistranslated protein which then activates the unfolded protein response pathway (4). The impact of mistranslation events on a host organism is also dependent on which amino acid is mis-incorporated at the ribosome and the level of mis-incorporation. Thus, it is important to use tRNA variants to find out how each misincorporation event is tolerated by the host organism (i.e., *Saccharomyces cerevisiae*). Mistranslation events that are not tolerated by cells, may have a potential relationship to disease and those that are tolerated may provide evidence about the evolution of the genetic code.

I investigated tRNA^{Leu} variants, which have a different anticodon compared to wild type leucine anticodons (Fig 1.). tRNA^{Leu}, tRNA^{Ser} and tRNA^{Ala} do not have their aminoacylation defined by the anticodon (5). The anticodon is a minor identity element in yeast tRNA^{Leu} aminoacylation. The major identity elements include nucleotide base pairs in the acceptor stem, adenine at the discriminator base (nucleotide 73) and the extended variable arm (6). Since the anticodon of a tRNA is not a major identity element, it can be modified to allow leucine mistranslation at different codons, creating statistical proteins with leucine amino acid replacements (7). Statistical proteins are the myriad of proteins that can be translated from one gene if mistranslation errors are factored in (7). In this case one gene could produce a greater number of proteins if leucine is mis-incorporated at random codons. It is difficult to anticipate how these statistical proteins will fold and how that will impact their function. It could cause the mistranslated proteins to

aggregate, or alter the proteins function by completely removing all functionality, or potentially alter the binding to its substrate (8).

An A14G mutation of the mitochondrial tRNA^{Leu}_{UUR} has been linked to mitochondrial encephalomyopathy (9). However, the random mistranslation of methionine at different codons buffers cell stress caused by an excess of reactive oxygen species (10). The serine tRNA (tRNA^{Ser}) of the yeast species *Candida albicans* (*C. albicans*) also has adopted the leucine codon (CAG) (11). Thus, there are mistranslation events that are a detriment to the host organism, but there are also mistranslation events which can benefit it. Therefore, a key goal of my work was to measure the effect of every tRNA^{Leu} variant on yeast and naturally occurring human tRNA^{Leu} variants in mammalian cells. The information from this study will have a broad impact on how we understand mistranslation, how tRNAs affect human health and the continuing evolution of the genetic code in eukaryotic organisms. My studies in yeast use a tRNA^{Leu}, that is based on tRNA^{Leu}_{UAA-1-2} gene from *S. cerevisiae* (12). This gene was modified to have a G26A mutation, and degenerate anticodons (representing all possible anticodon sequences). This allows for an exploration of mistranslation of leucine at every codon. Furthermore, the human tRNAs, tRNA-Leu (anticodon AAG) 3-1 and tRNA-Leu (anticodon CAA) 3-1 were also used for this study. They were modified after mutations categorized in the genomic tRNA database (GtRNADB) (13).

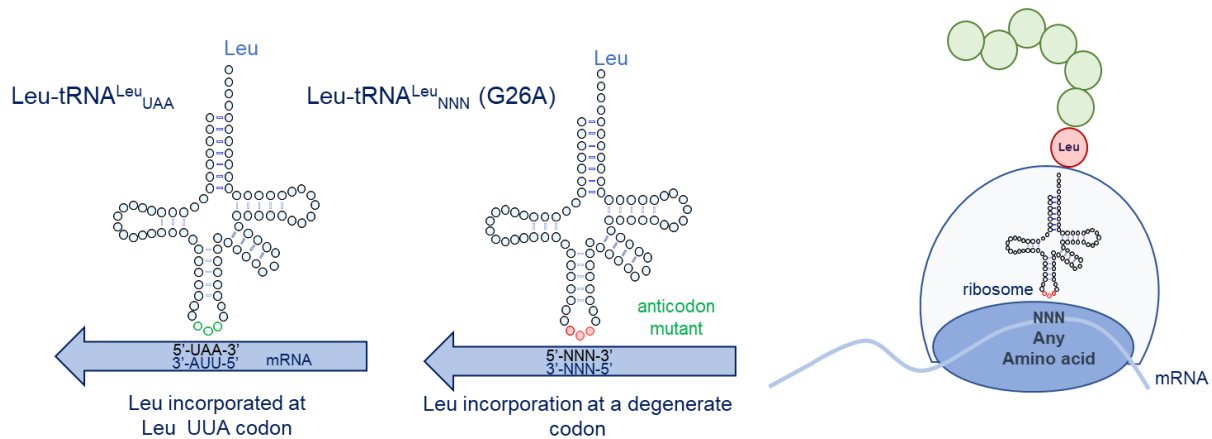


Figure 1: Diagram of tRNA^{Leu} wild type and tRNA^{Leu} variant delivering leucine at the ribosome. On the left are diagrams showing a wild-type tRNA^{Leu} and the tRNA^{Leu} anticodon variant base pairing with an mRNA molecule. On the right is a drawing of the mutant tRNA mistranslating leucine at the anticodon.

Literature Review

1.1 Overview of translation:

The central dogma of molecular biology describes the information flow that occurs in all cells from the DNA sequences in genes to their encoded proteins. Transcription is the conversion of information stored in DNA to messenger RNA (mRNA). This mRNA is then processed from pre-mRNA into mature mRNA (14). For the mRNA to travel from the nucleus to the cytosol without being degraded it must be given a 5' 7-methylguanosine (m7G) cap and a poly-adenosine tail so that neither end is degraded. This is primarily a eukaryotic process, as prokaryotic mRNA is translated before it is fully transcribed to reduce the risk of degradation (15). Translation is the next step, where the mRNA is translated into protein (Fig 2.). In mRNAs, every three nucleotides starting with the start codon, normally AUG, is a codon that specifies a particular amino acid (16). On the ribosome, tRNAs anneal at particular codons via base pairing their three-nucleotide anticodon sequence and transfer an amino acid from their 3' end to the growing polypeptide chain of a nascent protein (17).

In eukaryotes the ribosome consists of two subunits, the larger 60S subunit and the smaller 40S subunit (18). The larger 60S ribosome consists of 3 rRNAs (ribosomal RNAs) and 46 proteins (18). The smaller 40S ribosome consists of one rRNA molecule and 33 proteins (18). In bacteria the ribosome components are the 50S and 30s subunits (18). At the start of translation, the protein eIF2 (eukaryotic initiation factor 2) forms a ternary complex with GTP (guanine triphosphate) and Met-tRNA_i^{Met} (initiator methionine tRNA) (19). This ternary complex then binds to the 40S subunit to create a 43s preinitiation complex which also contains eIF3 and eIF5. This new complex then scans the mRNA after it has been activated by the eIF4F complex until the methionine codon (AUG) is in the P site of the 40S subunit (19).

The 40S subunit contains three translation sites, the A site where the new tRNA enters, the P site which holds the tRNA that carries the growing polypeptide and the E site where the tRNA exits (20). Upon recognition of the AUG codon, GTP is hydrolyzed thereby allowing the release of eIF2 followed by eIF5, eIF3 and eIF1 (19). After this the 60S ribosomal subunit joins the 40S subunit to form the 80S complex, which is used for translation. The 80S complex then travels along the ribosome and eIF2a (eukaryotic translation initiation factor) delivers new tRNAs to the

ribosome (19). The tRNAs enter at the A site where a peptide bond between the new amino acid and the growing polypeptide chain is catalyzed. The tRNA then moves to the P-site where it transfers the growing protein to the next tRNA delivered by eEF1a (eukaryotic translation elongation factor). Finally, it enters the E site where it is removed. When one of the three stop codons (UAA, UAG, or UGA) is recognized by the ERF1 (eukaryotic release factor 1), translation is terminated, the new protein is sent off for processing and all the components of the translation complex are recycled (21).

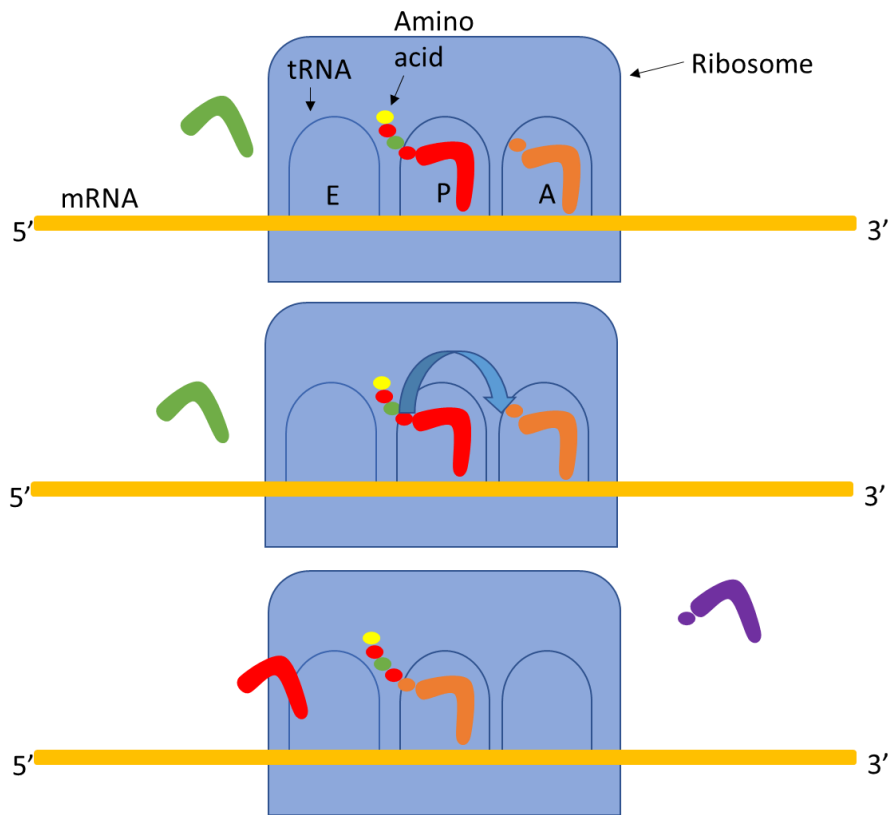


Figure 2: Representation of translation at the ribosome. First a new amino-acyl-tRNA (orange) enters the A site. A tRNA (red) carrying the growing polypeptide chain is already present in the P site. The tRNA (green) that was previously in the P site leaves when entering the E site. There can only be two tRNAs present in the ribosome. While in the A site the old tRNA transfers its polypeptide chain to the new tRNA, which increases the size of the protein. The old tRNA then leaves, the new tRNA enters the P site and another new tRNA (purple) travels to the A site.

1.2 Genetic code:

The genetic code consists of four nucleotide bases: adenine (A), cytosine (C), guanine (G), and thymine (T). When the genetic code stored in DNA is transcribed into RNA, the base uracil (U) takes the place of thymine. Adenine and guanine are purines which contain two nitrogenous rings, while uracil, cytosine and thymine are pyrimidines that contain one ring. These four bases are utilized by the cells as three base codon combinations. There are a total of 64 possible combinations ($4^{\text{bases}^3 \text{nucleotides}} = 64$ codons) (Table 1.). These codons are separated into boxes which contain four codons. Amino acids can be assigned to as few as 1 and as many as six codons.

Table 1: The 64 codon genetic code. The first nucleotide is in the left-most column, the second nucleotide is in the top row and third nucleotide in the right-most column. All 21 amino acids are shown beside their assigned codon. Since my project concerns tRNAs I have included U in place of T.

	U	C	A	G	
U	UUU Phe	UCU Ser	UAU Tyr	UGU Cys	U
	UUC Phe	UCC Ser	UAC Tyr	UGC Cys	C
	UUA Leu	UCA Ser	UAA stop	UGA stop	A
	UUG Leu	UCG Ser	UAG stop	UGG Trp	G
C	CUU Leu	CCU Pro	CAU His	CGU Arg	U
	CUC Leu	CCC Pro	CAC His	CGC Arg	C
	CUA Leu	CCA Pro	CAA Gln	CGA Arg	A
	CUG Leu	CCG Pro	CAG Gln	CGG Arg	G
A	AUU Ile	ACU Thr	AAU Asn	AGU Ser	U
	AUC Ile	ACC Thr	AAC Asn	AGC Ser	C
	AUA Ile	ACA Thr	AAA Lys	AGA Arg	A
	AUG Met	ACG Thr	AAG Lys	AGG Arg	G
G	GUU Val	GCU Ala	GAU Asp	GGU Gly	U
	GUC Val	GCC Ala	GAC Asp	GGC Gly	C
	GUA Val	GCA Ala	GAA Glu	GGA Gly	A
	GUG Val	GCG Ala	GAG Glu	GGG Gly	G

This along with the base pairing rules give the genetic code a high degree of degeneracy and flexibility. Nucleotides normally base pair A to U and C to G. However, when both a tRNA and mRNA codon are aligned at the ribosome, U can base pair to G and A nucleotides. Inversely, G can base pair to U and C (22). This can only occur between nucleotide 34 of the tRNA (first base of the anticodon) and the third base of the codon, which follows Crick's wobble hypothesis (23). This allows for tRNAs with U or G at position 34 to bind two codons (24). Furthermore, when A34 is modified to inosine it can base pair with U, A, or C. This allows for the tRNA to bind to three different codons. Three codons are devoted to stop codons. Instead of tRNAs entering these positions, release factors such as ERF1 enter this site and stop translation (25).

1.3 tRNA structure:

The transfer RNA (tRNA) secondary structure is commonly represented by a cloverleaf diagram (Fig 3A.). Transfer RNAs are usually 72-95 nucleotides in length (26). In the human genome there are over 500 tRNA genes (13). The tRNA structure is created by internal base pairing. This structure is made of an acceptor stem and three nucleotide arms referred to as the D arm (left), the TΨC arm (right) and the anticodon arm (bottom) (27). There is also a short fifth arm, which is extended in serine and leucine tRNAs (27). At the end of every tRNA is the nucleotide sequence CCA, which is encoded in the genome in several bacteria and some eukaryotes, or added by a CCA adding enzyme (tRNA nucleotidyl transferase) (28). The tertiary structure is often referred to as being L-shaped as its tertiary structure is mostly formed by interactions between the D arm and TΨC arm which results in an L shaped structure (29) (Fig 3B.). At the two opposite ends of the L shape are the acceptor stem and the anticodon arm (30),(31). There are variations to this L-shaped structure as mitochondrial DNA can sometimes omit the D or TΨC arms (32). There are 21 high confidence tRNA^{Leu} encoding genes in yeast cells and 31 in human cells (13).

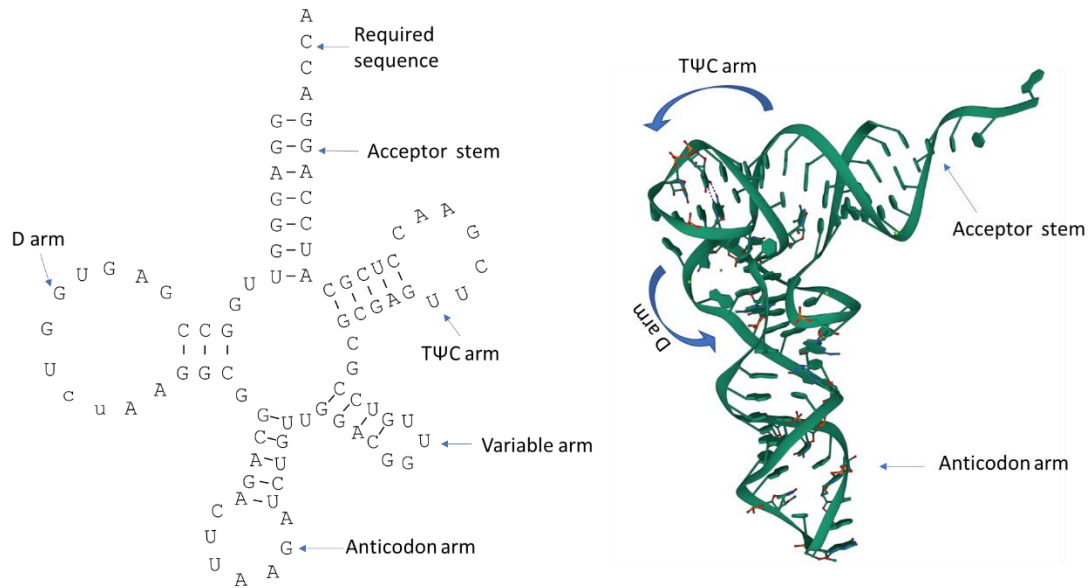


Figure 3: 2D diagram of wild type tRNA^{Leu} and 3D diagram of tRNA^{Phe}. A) Shown above on the left is the 2D structure of tRNA^{Leu}_{UAA} (yeast) B) and on the right is 3D representation of a phenylalanine tRNA taken from the protein data bank (4TNA) (33).

1.4 tRNA modifications:

RNA modifications are important for directing biochemical pathways, giving the RNA a unique function, or targeting it for degradation. To date there are 150 types of RNA modifications that are recorded from many different organisms (34). In human nuclear tRNA's there are an average of 13 modifications per tRNA molecule, but this number is highly variable depending on the tRNA (35). tRNA modifications in the anticodon stem and loop are particularly important for regulating translation. For example, Chou et al. (36) found that 2'O-methylations at position 32 and 34 of the anticodon, affects the ability of the tRNA to occupy the ribosome. Furthermore ncm⁵U (5-carbamoylmethyluridine), mcm⁵U (5-methoxycarbonylmethyluridine) or mcm⁵s²U (5-methoxycarbonylmethyl-2-thiouridine) modifications at the wobble codon have a substantial impact on translation and protein homeostasis (36). Klassen et al. (37), found that a lack of these modifications increases stress sensitivity in yeast and causes an increase in +1 ribosomal frameshifting. Eukaryotic tRNAs which have this modification include tRNA^{Leu}_{UAA}, tRNA^{Lys}_{UUU}, tRNA^{Glu}_{UUC} and tRNA^{Gln}_{UUG} (38).

Studies involving budding yeast have shown that in many tRNAs U34 is an important modification site as 9 of the 24 ribonucleoside modifications are located there (39). This is likely because site 34 is an important wobble position of the tRNA. Furthermore inosine modifications at position 34 allow for super-wobble base pairing as inosine base pairs to adenine, cytosine, and uridine (24). This A to I editing is performed by the tRNA-specific adenosine deaminase 2 (ADAT2)-ADAT3 complex (40). Another important aspect of tRNA modifications is that they can prevent rapid tRNA mediated decay. For example, Schaefer et al. (41) found that Dnmt2 (tRNA (cytosine38-C5)-methyltransferase) provides methylation of tRNAs at position 38 which protects them against degradation. Berg et al. (42), found that the G26A mutation targeted the toxic tRNA^{Ser}_{UGG} for rapid tRNA decay. This is because G26 is the site of a N(2),N(2)-dimethyl modification that protects the tRNA from degradation by the Rat1(5'-3' exoribonuclease 2) and Xrn1 (5'-3' exoribonuclease 1) exoribonucleases (43).

1.5 Amino acyl tRNA synthetases:

Amino-acyl tRNA synthetases (AARS) are a group of enzymes that facilitate the transfer of an amino acid to a tRNA. This can be summed up as a 2-step reaction. In the first part, the enzyme uses ATP to adenylate the amino acid (44). It is the breaking of this phospho-diester bond that provides the energy for tRNA amino-acylation (45). In the second step of the reaction the amino acid is removed from the adeno-mono phosphate and the amino acid is added to the tRNA (46). AARS have specific active sites that fit cognate amino acids and tRNAs. Select amino acids in these active sites allow certain tRNAs to fit (46). AARS recognize tRNA identity elements that are usually specific tRNA nucleotides, or parts of the tRNA structure (i.e., the extended variable arm) (5). Certain AARS also have their own editing domain. This domain recognizes tRNAs that are paired with non-cognate amino acids and removes the amino acid (47). The editing domain for leucyl-tRNA synthetase (LeuRS) is the CP1 domain, making LeuRS a class Ia AARS (48).

Identity elements can be structural elements like the variable arm in tRNA^{Ser} and tRNA^{Leu}, or a specific sequence, often the anticodon arm (5). Each tRNA can be grouped into an iso-acceptor family, that all share certain identity element(s) that allow them to be recognized by the same cognate AARS. In eukaryotes each tRNA is charged with a specific amino acid by its cognate AARS (49). AARS aminoacylate specific tRNAs based on identity elements found in the tRNA sequences and structures. These identity elements may include the placement of specific

nucleotides in the sequence (e.g., discriminator base 73), base pairs at specific locations, (e.g., the G3:U70 base pair that confers alanine selectivity), an extension in the length of the variable arm (as in serine and leucine tRNAs) or parts of the anticodon sequence itself (50). For many, but not all AARS the anticodon is a major identity element (5).

1.6 tRNA^{Leu} identity elements:

In *Escherichia coli* (*E. coli*), yeast, and mammalian cells the shared major identity elements for leucine tRNAs (tRNA^{Leu}) are an extension of the variable arm and A at discriminator base 73 (5),(50),(19). The specific identity elements for tRNA^{Leu} in yeast include A35 and G37 in the anticodon loop. The variable arm is not sequence-specific in recognition, rather its conformation fits the LeuRS (50). The substitution of A35 with G results in a 2-fold decrease in catalytic efficiency, while a substitution of A35 with C or U causes a more moderate decrease in tRNA^{Leu} aminoacylation (5). Comparatively, G37 is a much stronger identity element, as its substitution with other nucleotides caused a 10-20 fold decrease in tRNA^{Leu} aminoacylation. Therefore, the anticodon of tRNA^{Leu} can be altered at all 3 bases without eliminating leucine aminoacylation in yeast. Thus, many different tRNA^{Leu} anti-codon variants should have the ability to mis-incorporate leucine at multiple codons. In human tRNA^{Leu} the specific identity elements are base pairs A3:G70, A4:U69 and G5:C68 in the acceptor stem C20a in the D-arm, and the variable arm structure (24). For humans, the variable arm has orientation specificity and sequence specificity that is used by human LeuRS to discriminate between tRNA^{Leu} and tRNA^{Ser} (24).

1.7 Ribosome stalling:

Ribosome stalling can occur during the elongation phase if the ribosome stops at a codon. Reasons for stalling include mRNAs with premature stop codons, removed stop codons, and mRNA with a secondary structure that blocks translation (51). When these stalling events are reached, the ribosome facilitates nonsense mRNA decay (NMD), nonstop mRNA decay (NSD) and no-go decay (NGD) (51). Ishimura et al. (52), found that both a mutation in the novel binding protein GTPBP2 (GTP Binding Protein 2) and a tRNA mutation will cause ribosome stalling. These two mutations are associated with neurodegeneration in mice (52). Furthermore, the N¹ methylation of G37 is necessary for some tRNAs to prevent +1 ribosomal frameshifting and a lack of this modification can also cause translation to stall (53). This modification has an

important role in preventing ribosome stalling by the under methylated tRNA^{Pro}_{NGG} and tRNA^{Arg}_{CCG} (53). Furthermore, when under significant cells stress, cells may insert damaged or uncharged tRNAs at the ribosome, which can lead to ribosome stalling (54).

1.8 Tolerance to mistranslation in diverse cells:

Elevated levels of mistranslation are tolerated to a surprisingly large degree by diverse cell types. For example, organisms mistranslate with methionine under conditions of oxidative stress (55). Mistranslation is tolerated up to a rate of 10% in *E. coli* (56). tRNA-dependent mistranslation of proline codons with alanine was tolerated without significant growth defects at approximately 6% in yeast cells and 3% in mammalian cells (57), (58). Mistranslation can also increase protein diversity, potentially creating proteins with a wider array of functions than the homogenous form. For example, a heterogenous group of antibodies could be created by inducing mistranslation allowing recognition even if the antigen were to change its structure (59). The pathogenic yeast species *C. albicans* naturally mistranslates the leucine codon CUG. This is because a serine tRNA in *C. albicans* has adopted a CAG anticodon (60). This evolution of the genetic code assists *C. albicans* in evading host cell immune responses by mistranslation of the cell wall protein β -glucan (61) This CUG codon mistranslation also allows for the synthesis of two different adhesin Als3 proteins, which increases their hydrophobicity and adhesion on other yeast cells. The benefits of mistranslation can also be extended to synthetic biology. For example, Goto and Suga (62), were able to mis-acylate the initiator tRNA^{iMet} to incorporate non-canonical amino acids at the N-terminus, which allow for the formation of cyclic peptides.

1.9 Mistranslating tRNAs and disease:

It has been reported that tRNAs with a mutant anticodon are contributors to disease. For example, Santos et al. (63) found mutant serine tRNAs which mistranslate serine for leucine and alanine, had increased expression in mouse tumor cells as compared to non-tumor cells (8-fold higher for tRNA^{Ser} (alanine anticodon) and 8.4 fold higher for tRNA^{Ser} (leucine anticodon)). They also found that both tRNAs were essential for the activation of the UPR (unfolded protein response), which is an essential pathway for tumor cell survival (63). Furthermore, mitochondrial tRNA^{Leu}_{UUR} (R=A or G) with point mutations at G-14 and C-20, is associated with mitochondrial

myopathy, encephalopathy, lactic acidosis, and stroke-like episodes and maternally inherited diabetes with deafness (64).

Lant et al. (65), found that tRNA^{Ser}_{AAA} causes defects in aggregation and degradation of Huntington's disease causing polyQ protein aggregates in mammalian cells. The mistranslating cells showed synthetic toxicity with proteasome inhibition and were also resistant to the inhibitor of integrated stress response inhibitor (ISRIB) (65). These studies support an emerging link between tRNAs that cause mistranslation and their ability to impact human disease at the molecular level. Therefore, it is important to investigate the ability of naturally occurring human tRNA^{Leu} anticodon mutants to cause mistranslation and impact disease. In the human population, genome and targeted sequencing efforts have revealed a diversity of both common and rare tRNA variants (66),(58),(67). Among these natural variants are tRNA^{Leu} anticodon mutants, including tRNA^{Leu}_{AAA} (G36A) (phenylalanine anticodon), tRNA^{Leu}_{CCA} (A35C) (tryptophan anticodon) and tRNA^{Leu}_{GAA} (C34G) (phenylalanine anticodon). tRNA^{Leu}_{AAA} (G36A) and tRNA^{Leu}_{GAA} (C34G) have the potential to mistranslate leucine at phenylalanine codons. tRNA^{Leu}_{CCA} (A35C) has the potential to mistranslate leucine at the tryptophan codon UGG. All three of these tRNAs will be analyzed for their effect on mammalian cells.

1.10 tRNA^{Leu} variants as a probe to explore genetic code evolution:

tRNA^{Leu} variants alter the proteome and allow for mistranslation at codons other than leucine. This allows for insight into how tRNA^{Leu} variants can alter the codon identity of an organism if they are tolerated by the cell. Schultz and Yarus (68), theorized that if a tRNA mutation changes its codon identity, the tRNA can then adopt that codon even if another tRNA is already decoding it. Any codons that cannot accept this ambiguous decoding, will change their identity so they are decoded by another tRNA. Mühlhausen et al. (69) proposed another theory that a tRNA can be lost and the codon it was assigned to can then be recaptured by another tRNA. These theories are supported by the ambiguous decoding of the CUG codon found in both *C. albicans* (70), *Candida zeylanoids* (71) and *Pachysolen tannophilus* (69). Thus, it is possible that if tRNA^{Leu} variants with no effect on yeast cells were to occur naturally, they could change the identity of a codon to leucine. Woese (7), theorized that the ambiguous decoding of codons with two separate amino acids would allow for the generation of many different statistical proteins (7). Statistical proteins are created through the random mistranslation of certain codons with non-cognate amino

acids thanks to the mistranslating tRNAs which carry to non-cognate tRNAs (42). Wals and Ovaa (59) have predicted that mistranslating tRNAs could be used in the future to develop antibodies with randomly introduced missense mutations that would allow for them to evolve with constantly adapting disease antigens.

1.11 tRNA expression system:

Berg et al. (72), inserted a G26A mutation into tRNA^{Ser}_{UGG} (proline to serine) and found that it decreased the toxicity of tRNA^{Ser}_{UGG} in *S. cerevisiae*. The G26A mutation reduces the toxicity of tRNA^{Leu} variants, as this mutation removes a key methylation site that protects the tRNA from the rapid tRNA decay pathway (43). Berg et al. (73) then developed a tRNA expression system based on the tet-off system (74). In this system Berg et al. (73), cloned the tRNA^{Ser}_{UGG}G26A upstream of a TetO promoter (also inserted into the YCplac111(Leu2) vector). This new plasmid was transformed into a yeast strain with a TetR-VP16 fusion gene inserted into the genome. This fusion gene expresses the TetR-VP16 activator protein which binds to the tet gene in the absence of doxycycline and allows for its expression (74). This TetO promoter induced transcription reads over the tRNA gene, thereby reducing transcription of the tRNA. When doxycycline is added, the TetR-VP16 activator protein disassociates from the TetO promoter, which then allows tRNA expression. At approximately 0.01 µg/mL concentration of doxycycline, half of normal tRNA expression is allowed, while at 1.0 µg/mL full tRNA expression is allowed (73). All these components work together to allow the expression of a less toxic tRNA with the rate of tRNA transcription dependent on the concentration of doxycycline (Fig 4.).

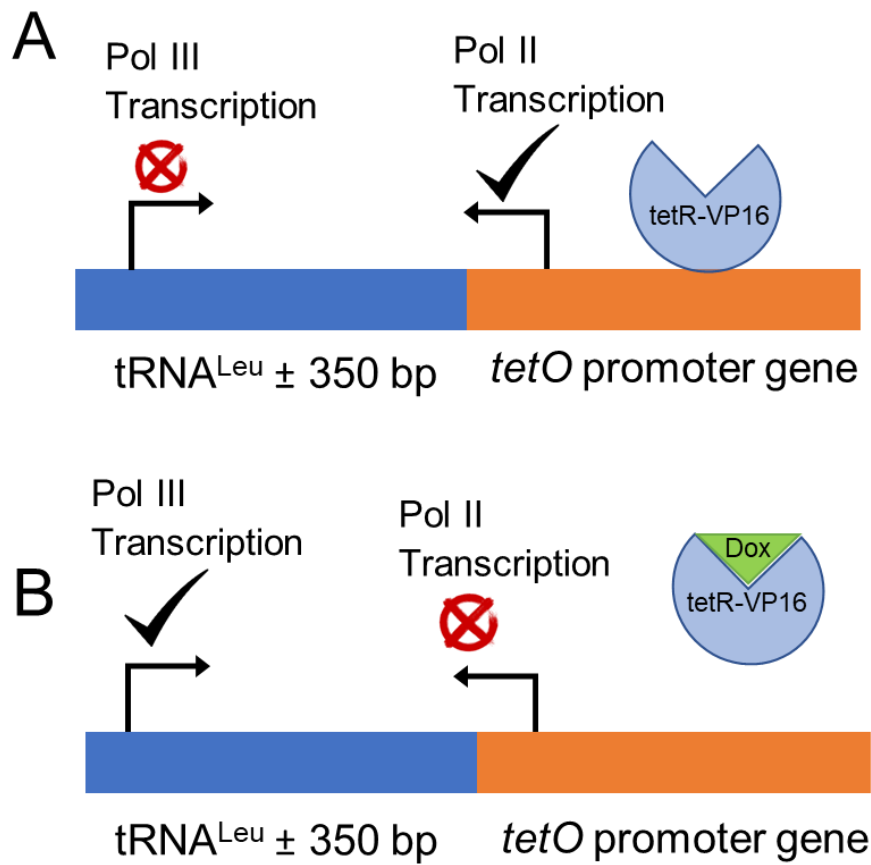


Figure 4: Diagram of the doxycycline TetO promoter inducible tRNA expression system. In the top diagram the TetR-VP16 fusion protein is bound to the tet promoter. This blocks native pol III transcription at the tRNA^{Leu} gene (A). In the bottom diagram doxycycline has bound to the fusion protein and removed it from the TetO promoter. This allows transcription of the tRNA gene (B).

1.12 Detecting mistranslation:

One of the most effective methods to detect mistranslation is to grow cells transformed with a mutant tRNA plasmid and a wild type tRNA plasmid, lyse the cells, purify protein, perform a trypsin digest on the protein and perform mass spectrometry analysis (3). The mass spectrometry results can then be used to compare the % of mistranslation in the mutant strain compared to the wild type strain (42). There is also a less specific way of detecting mistranslation. The growth rate of tRNA variant expressing cells can be recorded as A_{600} . Growth rate can be computed as area under curve or doubling time using the program “Growthcurver” (75). Area under the curve is essentially the measure of the area under the growth curve of a strain. A greater area indicates a higher growth rate. Doubling time is a measure of how many minutes it takes for cells to double in population. Cells cultures with a high doubling time have a low growth rate. The impact of the tRNA on the growth rate of the cells is estimates mistranslation (42). The same can be done by spotting mutant tRNA and wild type tRNA colonies onto plates (42). Cells will grow into large, medium, and small colonies.

Mistranslation can also be measured within the cells by expressing a fluorescent protein like enhanced green fluorescent protein (eGFP) or mCherry. A mutation is added in the sequence of the fluorescent protein, so it does not emit light. The tRNA variant can restore fluorescence by correcting the sequence. If fluorescence is detected, then mistranslation has occurred. This gives a method of detecting the relative % of mistranslation if the fluorescence rate is measured in comparison to a no-tRNA control (58).

1.13 Objectives

The question my thesis addresses is whether tRNA^{Leu} variants cause a shift in cellular protein homeostasis when they are expressed in either yeast or mammalian cells. This study aims to discover the effect of numerous tRNA^{Leu} variants on *S. cerevisiae*. Yeast is an excellent eukaryotic organism owing to its rapid growth and advance suite of genetic tools. It allows for us to discover the effect of various tRNA^{Leu} variants easily. The goal is to use the information gained to determine what tRNA^{Leu} variants negatively contribute to the survival of a eukaryotic cells and those that do not affect cell viability. This could provide important information for how natural human tRNA variants affect health and disease. Furthermore, the development of

tRNA^{Leu} variants could be an important synthetic biology tool. Each tRNA can be used to alter the proteome in unique ways to change any amino acid to leucine.

The second objective is to view how these tRNA variants impact cellular viability when expressed in mammalian cells. It has already been shown that some serine tRNA variants alter the protein homeostasis of the cell (58),(65). This could possibly contribute to or worsen an already existing illness (i.e., Huntington's disease). Viewing the affect that my tRNAs have on mammalian cells is an important step in seeing if leucine tRNA variants could alter cellular viability and thus the health of an organism.

Chapter 2 Materials and Methods

2.1 Plasmids:

See Supplemental Table 2 for a list of plasmid descriptions

The plasmids that allowed titratable expression of tRNA^{Leu} in yeast cells, have the YCpLAC111(LEU2 cen) vector as their background (76). This plasmid has a LEU2 gene which allows for the synthesis of leucine, removing the requirement of leucine in the medium (77). The tRNA^{Leu}_{UAA} gene (wild-type leucine tRNA) was amplified by PCR from the plasmid pCB4043(3) and tRNA^{Leu}_{UGG} was amplified from pCB4045 (Supp Table 1). The forward primer (UL0676) adds an *Eco*-RI site to the 5' side of the tRNA gene and the reverse primer (YI6283) adds a *Not*I site to the 3' side of the tRNA gene (Table 2.). The PCR products were purified after separation on a low melt agarose gel by phenol extraction and ethanol precipitation. To clone these tRNA genes, the PCR products were digested with *Not*I and *Eco*RI. The TetO promoter gene, previously described in (73), was digested out of the pCB4695 vector using *Not*I and *Bam*HI. The YCpLAC111 vector was cut with the *Bam*HI and *Eco*RI restriction enzymes. Both inserts were triple ligated into YCpLac111(LEU2 cen) to create pCB4721 (tRNA^{Leu}_{UAA}) and pCB4727 (tRNA^{Leu}_{UGG}). The tRNA^{Leu}_{UGG}G26A plasmid was created by PCR of the template pCB4043 using two step PCR with UL0676/UL0677 as the outside primers and XJ7581/XJ7586 as the inside primers. This PCR product was then cloned into pGEM-T Vector (78) and subsequently the YCplac33 vector (79).

Plasmids were amplified by transforming them into *E. coli* SCS1 cells and then using an alkaline lysis mini prep procedure to isolate the plasmid DNA (72). The tRNA^{Leu}_{UAA} gene with randomized anticodons (N34, N35, N36) and with the G26A mutation was purchased from GeneArt (Supp. Fig 1). Once the oligo pool arrived it was PCR amplified with YI6283 reverse primer and UL0676 forward primer. These random tRNA^{Leu} variants were digested with *Eco*RI and *Not*I. The oligos were cloned into *Eco*RI and *Not*I digested pCB4714 vector (which already contained the TetO promoter gene). This random pool of tRNA^{Leu}_{NNN} G26A was transformed into *E. coli* SCS1. An index plate of clones was sent to Genewiz in (South Plainfield, NJ) for

sequencing. The individual yeast cultures were then mini-prepped (80) to extract the plasmid DNA. These individual plasmids were then used for growth curve analysis (Supp Table 1.).

Table 2: List of Yeast oligos used to amplify tRNA^{Leu} genes from plasmids

Yeast oligos	MW (g/mol)	Tm (°C)	Sequence
UL0676	9182.0	50	TGTTGGAATTCCAGTGGCTCCACGACCAAT
UL0677	8835.6	54	AGGAAGCTTTGCAGGGGGTAGTTTCGGT
YI6283	9400.1	54	AGGGCGGCCGCAGGGGTAGTTTCGGTAGTG
XJ7582	7384.8	60.7	AGTCTGCtGCCTTAGACCACTCGG
XJ7581	9702.2	64.3	TGGTCTAAGGCAGCAGACTTGGGATCTGTTG

2.2 Yeast strains and growth:

The original yeast strain that the plasmids were transformed into is CY8652, a derivative of crossing yeast strains CY7020 (3) and CY8636 (Table 3.). CY8652 contains the gene expressing the TetR-VP16 fusion protein which allows for *TetO*-inducible tRNA expression (81). The yeast strain containing pCB4721 was named CY9113. The strain with pCB4727 was given the label CY9114. All the yeast strains created by transformation of random tRNA^{Leu} oligos, had CY8652 as the parental strain. The yeast strains were grown in synthetic medium supplemented with all essential amino acids (Trp, His, Met, Lys and Ade) and containing 2% glucose at 30 °C. All the tRNA^{Leu} transformed yeast cells were grown in triplicate. The growth of these yeast cells was observed by measuring the A₆₀₀ of the cells in a plate reader for 24 hours. They were grown under doxycycline concentrations of 0, 0.01 and 1.0 µg/mL to regulate expression of the tRNA.

This data was processed using the R program “Growthcurver” which computed the doubling time and area under the curve (75). All the comparisons of the doubling time/area under curve between the tRNA^{Leu} variant and wild type tRNA^{Leu} yeast strains were tested for significance using Welch’s t-test which take unequal variances into account.

Table 3: Description of yeast strains used in this study.

Yeast strain	Description
CY7020	Yeast strain with URA3 gene (synthesizes uracil)
CY8636	Yeast strain incorporated with TetO activator protein (TetR-VP16)
CY8652	Yeast strain incorporated with TetR-VP16 gene and URA3 gene
CY9113	Yeast strain transformed with pCB4721 (tRNA ^{Leu} _{UAA} upstream of <i>tetO</i> promoter in YCPLAC111)
CY9114	Yeast strain transformed with pCB4727 (tRNA ^{Leu} _{UGG} upstream of TetO promoter in YCPLAC111)

2.3 Mass spectrometry:

The tRNA^{Leu}_{CGG} plasmid (proline anticodon), tRNA^{Leu}_{AGG} plasmid (proline anticodon), tRNA^{Leu}_{UAC} plasmid (valine anticodon) and wild-type tRNA^{Leu}_{UAA} plasmid were transformed into CY8652 cells. The yeast strains were grown in 2mL of yeast peptone media without leucine and uracil and with 2% glucose. These cultures were grown in 3 biological replicates for 31.25 hours (tRNA^{Leu}_{UAC} -3, tRNA^{Leu}_{UAA} -1 and 3) and 59 hours (tRNA^{Leu}_{CGG} 1-3, tRNA^{Leu}_{AGG} 1-3, tRNA^{Leu}_{UAC} 1-2 and tRNA^{Leu}_{UAA} -2). These starter cultures were then added to culture flasks also filled with 20 mL of yeast peptone media without leucine and uracil and with 2% glucose. Yeast cells transformed with the tRNA^{Leu}_{CGG} plasmid and the tRNA^{Leu}_{AGG} plasmid have a slow growth rate in comparison to the wild-type strain. To compensate for the slow growth rate, 2 mL of each starter culture was added to separate 20mL flasks. Conversely, the yeast cells transformed with

the tRNA^{Leu}_{UAC} plasmid grow at a similar rate to the wild-type strain, so only 1mL of the tRNA^{Leu}_{UAC} and wild-type starter culture was added to separate 20ml of media flasks. These cultures grew at 30.0 °C until the $A_{600} = 0.6$. Afterwards dox was added to each culture, to reach a final concentration of 2 µg/mL. These cultures were grown 25.5 hours when the cells were pelleted by centrifugation. These pellets were then frozen at -80 °C until they could be used for protein extraction. The cells of each tRNA plasmid strain were then lysed using glass beads and given 300 µL of denaturing lysis buffer (50mM Tris HCl pH 8.0, 200mM NaCl, 0.5mM EDTA). The protein concentration was measured using a Bradford assay with reagents purchased from Bio-Rad (Hercules, CA). This assay involves adding Coomassie brilliant blue G-250 dye to the protein samples. This dye binds to basic and aromatic amino acids. Upon binding to the amino acids, the dye changes color (red to blue) and begins absorbing light at 590nm. This absorbance is measured and used to calculate the concentration of protein in the sample.

Once the protein concentration of each strain was determined, 100µg of protein was aliquoted to be run on an 0.8% SDS PAGE gel (82). The samples were suspended in 1x Laemmli (pH 6.8) buffer (83), heated at 95°C for 5 mins and separated by SDS PAGE. The sample was then loaded at 30 µL of volume. The proteins bands were then excised and transferred to 3% acetic acid solution where they would be digested using trypsin by Victoria Clarke of the functional proteomics facility. Paula Pittock of the Schulich biological mass spectrometry laboratory then performed LC MS/MS on the digested peptides. The trypsin digested peptides were reconstituted in 20µL of 0.1% formic acid and then 4µL was inserted to a ACQUITY MClass nano UPLC (Waters Corporation, Milford, MA) system using an ACQUITY UPLC MClass Symmetry C18 trap column (Waters Corporation, Milford, MA) at a flow rate of 5µL/min for 6 minutes using 99% buffer A (100% H₂O, 0.1% formic acid) and 1% buffer B (100% Acetonitrile + 0.1% formic acid). The purified protein was then sent through a nano spray ionization source with a source voltage of 2.3 KV and combined with a Orbitrap Elite mass spectrometer (Thermo Electron Corp., Waltham, MA). X-calibur software (Thermo, v. 2.2) was used to control the mass spectrometer and used the FT/IT/CID top 10 scheme. The mass to charge ratio recorded by MS scan was 375-1500 at a resolution of 60,000 at m/z 400, positive ion, profile, full MS mode in the orbitrap (FT) using a lock mass (445.120025 m/z). The top 10 abundant multiply charged ions were automatically selected for subsequent collisional induced dissociation, with charge

state filtering permitting only ions of +2 and higher charged states. Normalized collision energy was 35, and precursor ions were then left out from further selection for 20 seconds.

The raw data was put through the Peaks X+ software (Bioinformatic Solutions Inc.) by Paula Pittock and the spectra was searched against yeast protein sequences from the Uniprot database using a contaminants database (CRAPome) (84). The FDR was 1.0% and at least 1 peptide filtering was used. An amount of 3 missed cleavages (MC) were allowed for searching tryptic peptides. Fixed modification of carboxyamidomethylation (CAM) Cysteine, and variable modifications of deamidation (N/Q), oxidation (M), with a parent mass error tolerance of 10.0 ppm and fragment mass error tolerance of 0.2 Da were used, allowing non-specific cleavage at one end of the peptide. A Homology Match (Spider) was used to identify point amino acid changes (mutations).

2.4 Synthesis by overlap PCR:

See Supplemental table 2 for human tRNA primers

Synthesis by overlap PCR (SOEPCR) was used to create the wild type and mutant human tRNA^{Leu} inserts (65). Primers which annealed 500 bp upstream and downstream of the target gene (tRNA^{Leu}) were designed. These primers were used in the first round of PCR on genomic DNA from HEK 293 cells. These first round tRNA products then underwent a second round of PCR. For the wild type tRNA^{Leu} these first round gene products were amplified with a 300bp upstream and downstream primer pair. These primers were designed to have a *Pci*-I site inserted at either end. For the mutant tRNA^{Leu} variants the first-round product was amplified twice. Once with a 300bp upstream forward primer and second with a 300 bp downstream reverse mutant primer. The mutant primer anneals to the section of the DNA containing the tRNA anticodon and inserts a mutation at one nucleotide. This PCR step is then repeated with the opposite set of primers. These two separate halves with the mutation are then joined using PCR without the primers. After 5 rounds of PCR without primers, the 300 +/- bp primers are added to amplify to complete tRNA^{Leu} variant PCR product. The PCR then continued for another 24 rounds. Afterwards the tRNA genes were run on a 1.5% agarose gel. The GenepHlow Gel/PCR kit (FroggaBio) was then used to extract the tRNA inserts from the gel. The tRNA inserts were reconstituted in 35µL H₂O

2.5 Mammalian plasmids:

The human tRNA^{Leu} genes and their variants were cut with the *Pci*-I restriction enzyme and ligated into a *Pci*-I cut WT-PAN vector (85). The WT-PAN vector contains a kanamycin resistance gene and a fluorescent fusion gene of enhanced green fluorescent protein (eGFP) – GlySerLinker – mCherry. The level of fluorescence acted as a reporter to indicate the relative level of protein synthesis in mouse neuroblastoma (N2_a) cells (ATCC #CCL-131) transfected with WT-PAN plasmids each bearing a wild-type or mutant tRNA^{Leu} allele. The level of fluorescent protein synthesis in tRNA^{Leu} variant expressing N2_a cells were compared to the wild-type tRNA^{Leu} expressing N2_a cells. The wild-type human tRNA^{Leu} genes were tRNA^{Leu}_{AAG} and tRNA^{Leu}_{CAA}. The tRNA^{Leu} variants are tRNA^{Leu}_{AAG} G36A (tRNA^{Leu}_{AAA}), tRNA^{Leu}_{CAA} A35C (tRNA^{Leu}_{CCA}) and tRNA^{Leu}_{GAA} C34G (tRNA^{Leu}_{GAA}). tRNA^{Leu}_{AAA} and tRNA^{Leu}_{GAA} have phenylalanine anticodons, while tRNA^{Leu}_{CCA} has a tryptophan anticodon. These ligations were transformed into *E. coli* DH5 α cells. The transformants had their plasmid tRNA^{Leu} DNA amplified directly by the cells, by extending the initial 95 °C denaturation step in PCR. The *Pci*-I \pm 300 bp primer set was used to amplify the primer DNA from the cells. The amplified DNA was run on an 1.5% SDS PAGE gel and if the DNA length (750 bp) matched the ladder length it meant the tRNA^{Leu} had been properly cloned into the WT-PAN vector. The transformants which passed the screen were grown overnight in LB media (at 37 °C) and mini-prepped (using the Presto Mini plasmid kit (FroggaBio)) the next day. The plasmid DNA was sent to Genewiz (South Plainfield, NJ) for sequencing. If the sequencing showed the tRNA was present without mutations and was inserted in the correct orientation the plasmid could then be used in the mammalian cell studies.

2.6 Cell transfection:

Murine Neuro-2_a neuroblastoma (N2_a) cells (purchased from ATCC) were grown in Dulbecco's modified eagle media (DMEM) (+ 10% FBS + 1% Strep/Pen) media in a t-75 flask. N2_a cells are derived from neuroblastoma cells (located in the adrenal gland) in mice (*Mus musculus*). Once approximately 80% confluent, these cells were passaged and plated on a 96 well plate. Enough wells were plated so there were 3 biological replicates for each tRNA plasmid under each different MG132 concentration (10, 1.0, 0.1 and 0 μ g/mL MG132). After one day of growth (at

37°C) the plated N2_a cells were transfected with the human tRNA^{Leu} WT-PAN plasmids. These included the tRNA^{Leu}_{AAA} (G36A), tRNA^{Leu}_{CCA} (A35C), tRNA^{Leu}GAA (A34G), tRNA^{Leu}_{CAA} and tRNA^{Leu}_{AAG} plasmids. The tRNA^{Ser}_{AGA} 2-3 and tRNA^{Ser}_{AAA} 2-3 plasmids provided by Lant et al. (65) were used as a control. Two separate mixtures were prepared for each plasmid. One set of seven mixtures consisted of the 7 plasmids with added lipofectamine p3000 and DMEM. In all the plasmid DNA mixtures, the amount of the added plasmid was made equal to 100ng. The other seven mixtures consisted of lipofectamine 3000 and DMEM. Both mixtures were shaken and incubated separately at room temperature (approximately 25°C) for five minutes. For each plasmid 60µL of the DNA mixture was added to the 60µL of lipofectamine mixture and the mixture was shaken and incubated at room temperature for 20 minutes. In this mixture the concentration of the plasmid was 10 ng/µL. 10uL (100ng per well) of this mixture were then added to each sample well of the 96 well plate. 84 wells were plated as 2 wild type tRNA^{Leu}, 1 wild type tRNA^{Ser}, 3 tRNA^{Leu} variant and 1 tRNA^{Ser} variant plasmid were transfected.

2.7 Fluorescence microscopy and data analysis:

The fluorescent images of N2A cells transfected with wild type tRNA^{Leu}, wild type tRNA^{Ser}, tRNA^{Leu} variant and tRNA^{Ser} variant WT-PAN plasmids, were taken after 24 hours using an EVOS FL auto fluorescent microscope (Thermo Fisher Scientific). The images were captured at 470 ± 22 nm (GFP) and 510 ± 42 nm (RFP), using corresponding filter cubes. This was done using the ImageJ/Fiji software (86), (87). Fluorescence was quantitated per cell using the same imageJ/fiji macros as Lant et al. (65). Images were taken 24-hours post transfection and then 4 hours after adding MG132 proteasome inhibitor (MG132 dissolved in DMSO to reach 25mg/mL MG132 conc.) (sigma-Aldrich). Each cell line was treated under 4 different MG132 concentrations (10, 1.0, 0.1 and 0 µg/mL) and there were 3 biological replicates for each condition. For the 0 µg/mL condition only DMSO was added instead of the MG132 solution. MG132 is a proteasome inhibitor which slows the degradation of proteins inside the cell and indirectly inhibits protein synthesis (88). Previous work found that the accumulation of misfolded caused by MG132 protein was toxic to N2_a cells (65). All comparison between the mean fluorescence of a tRNA anticodon variant and wild type tRNA variant cell lines were tested for significance using the ANOVA single factor test.

2.8 Cytotoxicity analysis:

The toxicity induced by the tRNA^{Leu} and tRNA^{Ser} variants in comparison to wild type tRNA^{Leu} and tRNA^{Ser} was analyzed by transfecting N2_a cells with the previously described WT-PAN plasmids containing wild-type or mutant tRNAs and using the CytoTox-Glo Cytotoxicity assay (Promega, Madison WI). For each cell line, 3 biological replicates were used. Cell lines were assayed 24 hours post transfection. Furthermore, all cells had been treated with 0, 0.1, 1.0 and 10.0 µg/mL of MG132. The Cells were held in the 37 °C incubator during the 4-hour period. Following fluorescent imaging, luminescent agent was added to conduct a cell toxicity assay using the CytoTox-Glo assay. After 20 minutes Luminescence readings were taken using a plate reader. The digitonin reagent (160 µg/mL) was then added and after another 20 minutes the luminescence readings were taken. All comparison between the cytotoxicity induced by the tRNA anticodon variant and wild-type tRNA variant were tested for significance using Welch's t-test.

Chapter 3 Results

3.0 Project Goals

The goal of this project was to observe the effects of expressing different tRNA^{Leu} anticodon variants in eukaryotic cells (yeast and mammalian). In *S. cerevisiae*, the aim was to cover all 64 possible anticodons, but due to time constraints 38 were covered. In mammalian cells 3 tRNA^{Leu} anticodon variants were covered and these had been observed in the human population. This will provide insight on tRNA^{Leu} anticodon variants that could be linked to genetic disease, changes in codon identity and have applications generating statistical proteins. tRNA^{Leu} anticodon variants create statistical proteins by mis-incorporating leucine at different codons during translation. Depending on where in the structure the misincorporation occurred, the resulting statistical proteins can have altered activity, substrate specificity, or no impact on structure or function (42). To control the expression of tRNA^{Leu} variants the tRNAs were cloned into a plasmid as part of a dox-inducible vector. Controlling the expression of the tRNA^{Leu} variant was necessary to see if any resulting change in yeast cells can be controlled by changing the level of tRNA expression.

3.1 Inducible expression of tRNA^{Leu} variant tRNA^{Leu}_{UGG}

To begin this process there needed to be an initial trial to see if the expression of one toxic tRNA^{Leu} could be expressed using the dox-inducible system, and have its growth compared to a wild type tRNA^{Leu}_{UAA}. In the dox-inducible system, the expression of the TetO promoter gene downstream of the tRNA gene blocks the expression of the tRNA. When doxycycline is added the expression of the TetO promoter is blocked, thereby allowing expression of the tRNA gene. As the concentration of doxycycline is increased so is the expression of the tRNA. This system had already been used by Berg et al. (81) to regulate the expression of a toxic tRNA^{Ser}_{UGG} tRNA in *S. cerevisiae* so its growth rate could be compared to yeast cells expressing the wild-type serine tRNA. In this study this dox system is being adapted to compare the growth rate of yeast cells expressing tRNA^{Leu} anticodon variants to cells expressing the wild-type tRNA^{Leu} (tRNA^{Leu}_{UAA}). The yeast strains that contained wild-type tRNA^{Leu}_{UAA} and mutant tRNA^{Leu}_{UGG} (Pro anticodon) plasmids were grown in the presence of 0, 0.625, 1.25, 2.5, 5.0 and 10.0 µg/mL

of dox. At 10 $\mu\text{g}/\text{mL}$ dox there was a significant 90% decrease ($p = 0.007$) in the growth rate (measured by area under curve) in $\text{tRNA}^{\text{Leu}}_{\text{UGG}}$ expressing cells vs. wild-type cells (Fig 5, Fig 6A.). Since there was so little growth from the $\text{tRNA}^{\text{Leu}}_{\text{UGG}}$ cells, area under the growth curve was used to measure growth rate instead of cell culture doubling time (min^{-1}). To reduce the toxicity in the $\text{tRNA}^{\text{Leu}}_{\text{UGG}}$ strain, the concentration of the doxycycline was lowered, to reduce the expression of the tRNA^{Leu} anticodon variant. However, the same result was found when comparing the growth rate of the wild-type cells from the previous trial to $\text{tRNA}^{\text{Leu}}_{\text{UGG}}$ cells grown under lower dox concentrations (0, 0.00625, 0.0125, 0.025, 0.05, and 0.1 $\mu\text{g}/\text{mL}$) (Fig 6B.). Once again, the tRNA^{Leu} anticodon variant strain showed almost no growth in comparison to the wild-type strain. These results showed that $\text{tRNA}^{\text{Leu}}_{\text{UGG}}$ (Pro) induces low to almost no growth in yeast cells. It was logical to presume there may be other tRNAs like $\text{tRNA}^{\text{Leu}}_{\text{UGG}}$ (Pro) that eliminate cell survivability when expressed in *S. cerevisiae*. It was then necessary to reduce the toxicity of the tRNA^{Leu} variants so the effect of the tRNA^{Leu} variants on yeast cell growth can be compared to the wild-type tRNA.

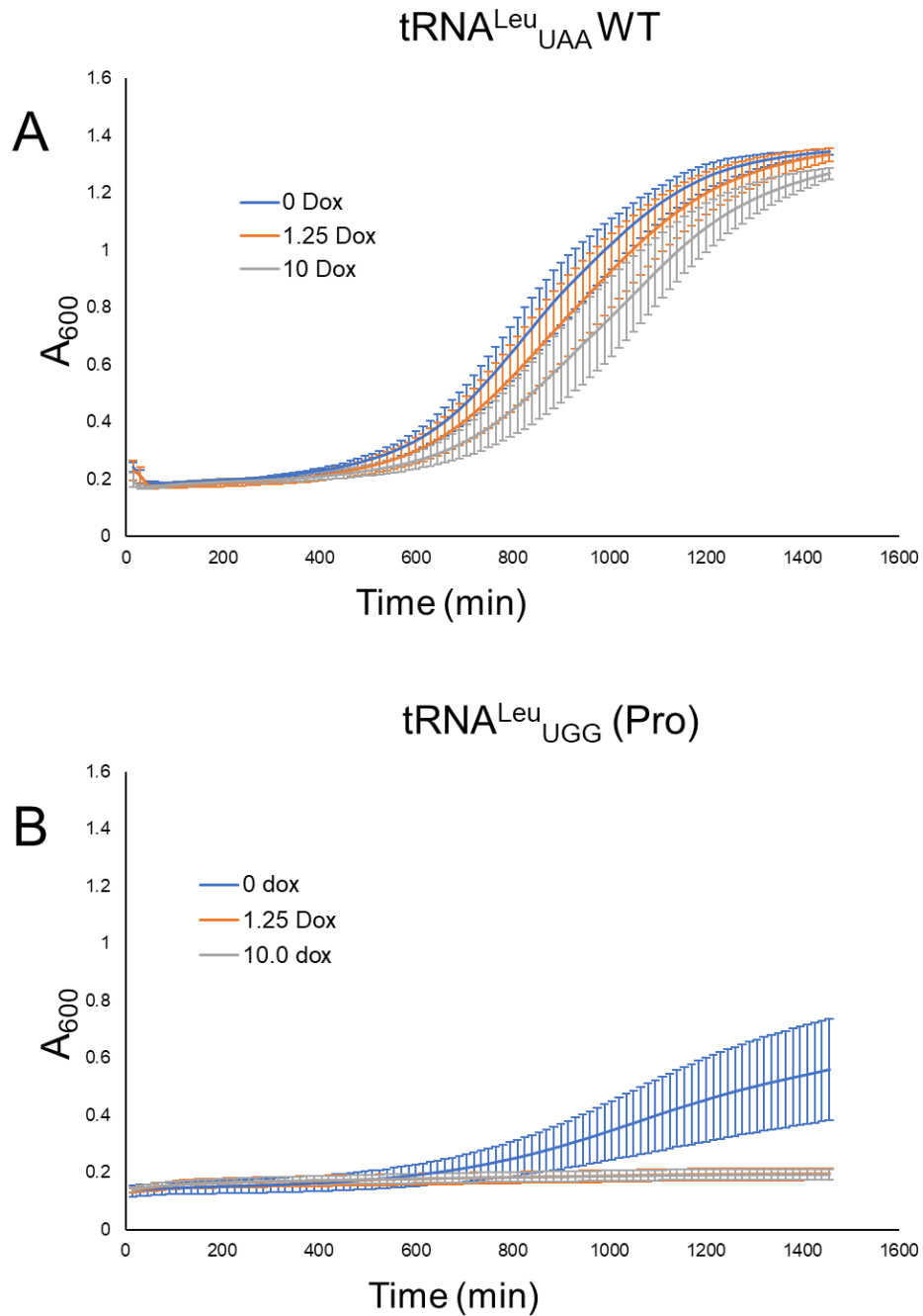


Figure 5: Representative growth curve images for tRNA^{Leu}_{UAA} expressing yeast cells A) and tRNA^{Leu}_{UGG} (Pro) expressing yeast cells B). The wild-type and tRNA^{Leu} anticodon variant strains were grown 24 hours at 30°C in minimal medium lacking uracil and containing 0, 1.25 or 10 µg/mL doxycycline. Growth was measured by recording A₆₀₀ at 15 minute intervals. The blue curve represents 0 µg/mL dox concentration and the orange and grey curve represent 1.25 and 10.0 µg/mL dox concentrations.

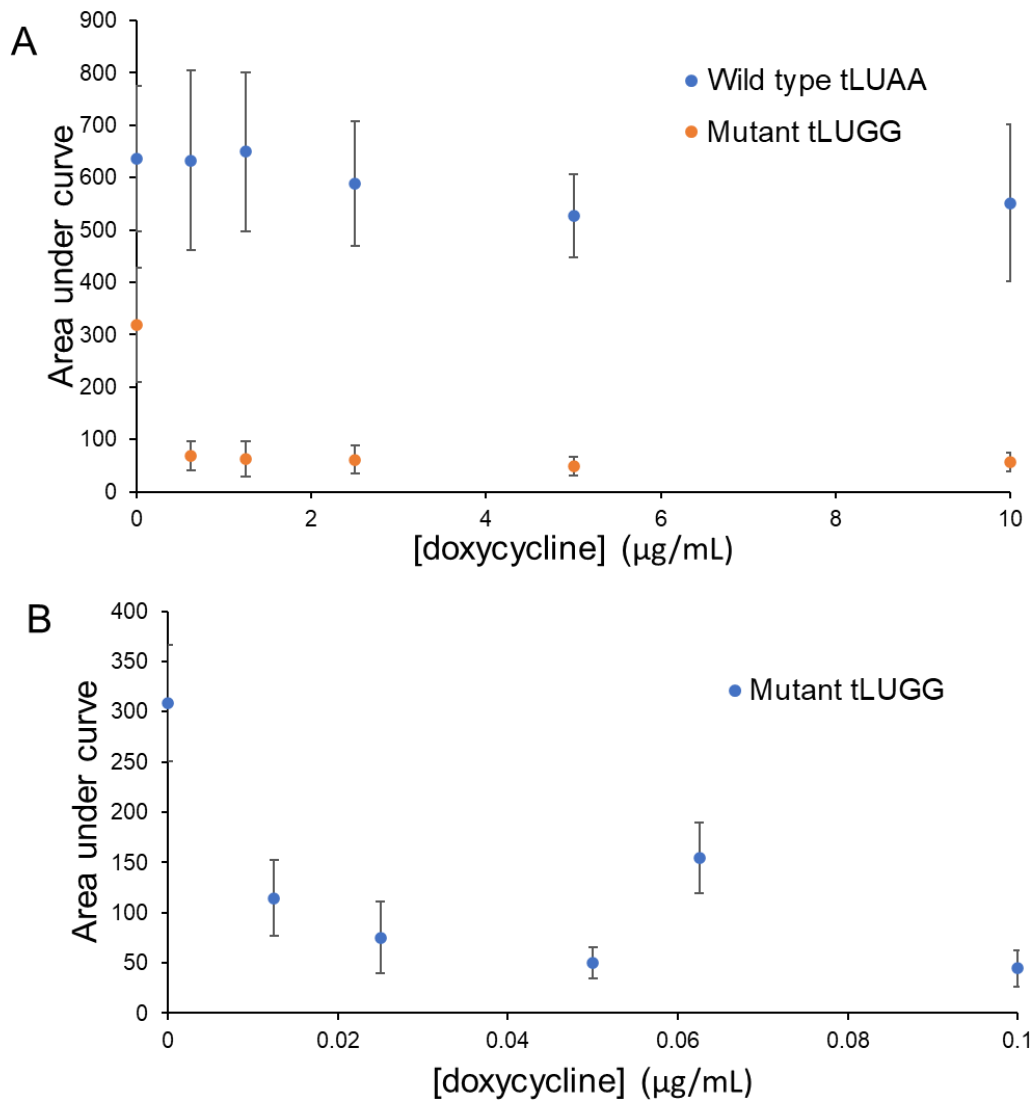


Figure 6: Scatter plot of 24-hour growth curve data for yeast cells transformed with plasmids expressing tRNA^{Leu}_{UAA} or mutant tRNA^{Leu}_{UGG} (Pro). A) Growth curve analysis of wild type (tRNA^{Leu}_{UAA}) and mutant (tRNA^{Leu}_{UGG} (Pro)) yeast strains at doxycycline concentrations from 0 to 10 µg/mL. The Area under the curve is represented on the y-axis and the doxycycline concentration is represented on the x-axis. B) Growth curve analysis of mutant yeast strain (tRNA^{Leu}_{UGG}) from 0 to 0.1 µg/mL dox.

3.2 Addition of G26A mutation to tRNA^{Leu} variant

To reduce the toxicity of tRNA^{Leu} variant strains like the tRNA^{Leu}_{UGG} (Pro) strain, a guanine residue at position 26 of the tRNA was substituted for adenine (G26A mutation). Replacing G at position 26 with A26 in the RNA removes an important methylation site that prevents the tRNA from entering the rapid tRNA decay pathway (43). Targeting the mutant tRNA for the rapid tRNA decay pathway reduces the toxic effect of the tRNA, which then allows for the yeast cells to grow. This strategy had been previously used by Berg et al. (42) to limit the toxicity of a tRNA^{Ser} variant in *S. cerevisiae*. Limiting the toxicity of the tRNA^{Leu} variants was necessary to compare the growth rate of the yeast cells that express them to yeast cells that express the wild-type tRNA^{Leu}. A strain with a G26A mutation in tRNA^{Leu}_{UGG} was grown and its growth was measured and compared to the wild-type strain and the tRNA^{Leu}_{UGG} (no G26A) strain at a dox concentration of 0 µg/mL. The cells transformed with the G26A-plasmid grew at 59% of the growth rate of wild-type cells (p= 0.0002) (Fig 7.). However, since cells transformed with the tRNA^{Leu}_{UGG} G26A plasmid grew at a 1.85 (p= 0.0008) fold higher rate than tRNA^{Leu}_{UGG} cells, the G26A mutation made tRNA^{Leu}_{UGG} plasmid less toxic to *S. cerevisiae*. This confirmed that the G26A mutation reduced the toxicity of the tRNA^{Leu} variants but did not remove their slow growth phenotype. This allowed for a detailed view of how each tRNA^{Leu} variant comparatively effects yeast cells. Thus, all yeast tRNA^{Leu} anticodon variants were given the G26A mutation to reduce their toxicity to *S. cerevisiae*.

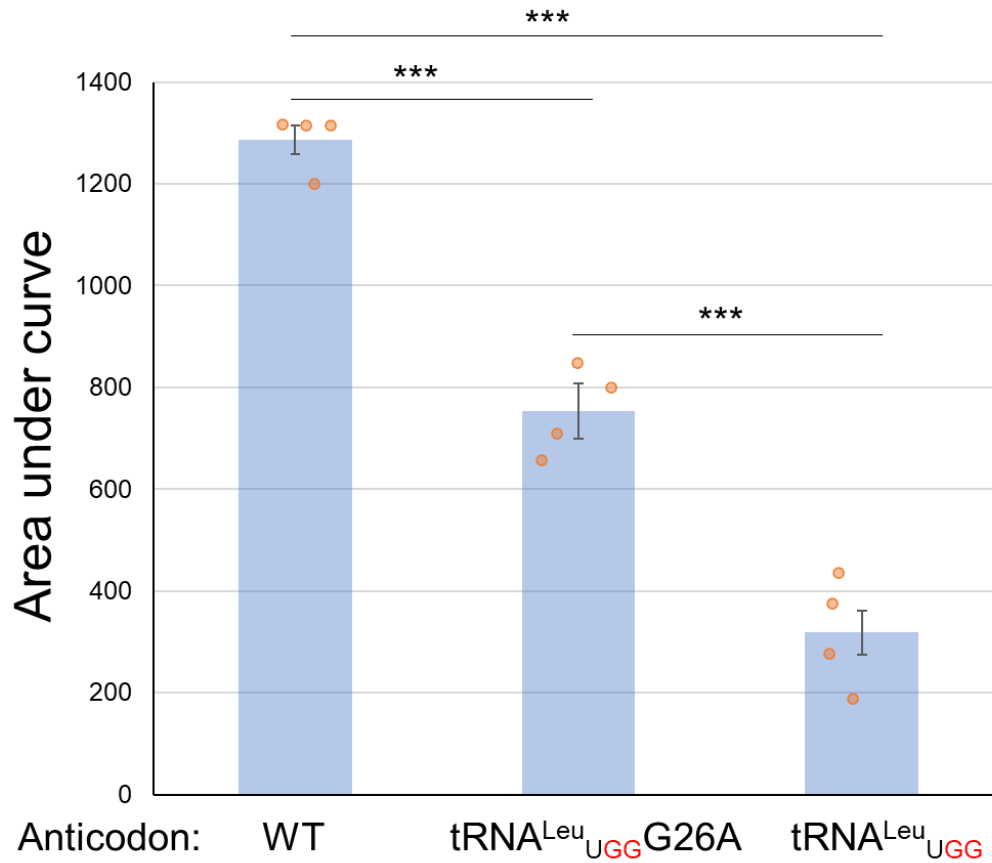


Figure 7: Comparing the Area under curve in tRNA^{Leu}_{UAA}, tRNA^{Leu}_{UGG} (Pro) and tRNA^{Leu}_{UGG} (G26A) expressing yeast cells. The yeast strains expressing tRNA^{Leu}_{UAA} (n = 4), tRNA^{Leu}_{UGG} (Pro) (n = 4) and tRNA^{Leu}_{UGG} (G26A) (n = 4) were grown for 24 hours at 30 °C without doxycycline. The A₆₀₀ of each strain was recorded using a Biotek Epoch 2 micro-plate reader (Santa Clara, CA). This growth curve data was converted to area under curve using the program “Growthcurver” (75). Stars indicate p-values from Welch’s t-test. (n.s. = no significant difference, * p < 0.05, ** p < 0.01, *** p < 0.001).

3.3 Growth rate analysis of tRNA^{Leu} variant yeast strains

Moving on from the initial trial experiments, 38 tRNA^{Leu} variants differing in their anticodon sequence were cloned into the dox-inducible vector and transformed into yeast cells. The initial goal was to test all 64 tRNA^{Leu} anticodon variants, but due to time restraints 38 tRNAs were obtained. The growth (A_{600}) of these cells was monitored for 24 hours and the area under curve and doubling time were calculated using the program “Growthcurver” (75). Doubling time is a measure of how long it takes for a population of cells to double in size. Each strain was grown under three different doxycycline concentrations (0, 0.01 and 1.0 $\mu\text{g}/\text{mL}$). Berg et al. (81), had previously found these conditions match almost no tRNA expression (there is always some leakiness), half tRNA expression and full tRNA expression (81). At least 3 different biological replicates were grown per tRNA^{Leu} variant anticodon plasmid and doxycycline concentration. The only exception was the tRNA^{Leu}_{UAA} strain with an anticodon which matches the stop codon UAA, which was grown in duplicate for each dox concentration due to time restraints.

In terms of the growth rate of each strain, it varied depending on the tRNA^{Leu} anticodon variant plasmid. The growth rate of each strain was measured by its doubling time (Fig 8.). The doubling time of each strain was compared to the doubling time of the wild-type strain. In both cases the data from the 1.0 $\mu\text{g}/\text{mL}$ dox condition was analyzed. This is because this was the condition where full tRNA expression was allowed (81). After comparing the doubling times of the tRNA^{Leu} variants strains to the wild-type strain (tRNA^{Leu}_{UAA}), the results were separated into three categories. The first category were the mutant strains which had no significant change in doubling time ($p > 0.05$) compared to the wild-type. The second category were three strains that grew significantly ($p < 0.05$) faster (lower doubling time) than the wild-type. The third category were 12 strains that grew significantly ($p < 0.05$) slower (higher doubling time) than the wild-type. Significance was calculated using Welch’s t-test, which accounts for unequal variance between groups (89).

In the third category there were some extreme examples of tRNA^{Leu} anticodon variant yeast strains that grew slower than the wild-type strain. Yeast cells with the proline anticodons (NGG) all grew far slower than the wild-type cells. For example, cells expressing tRNA^{Leu}_{CGG} had a 2.0-fold ($p = 9.8\text{E}-07$) higher doubling time at 1.0 $\mu\text{g}/\text{mL}$ dox than the wild-type cells (Fig 9.) and

tRNA^{Leu}_{AGG} cells had a 1.7-fold higher doubling time ($p = 0.00066$) than the wild-type cells at 1.0 $\mu\text{g/mL}$ dox. The other exceptionally slow growing cell line was a yeast strain transformed with the tRNA^{Leu}_{GCG} (Arg anticodon) variant which had a 2.1-fold ($p = 7.6\text{E-}05$) higher doubling time than wild-type cells at 1.0 $\mu\text{g/mL}$ dox (Table 4.). Surprisingly, other tRNA^{Leu} Arg anticodon strains like tRNA^{Leu}_{CCU} did not share the same significant increase in doubling time ($p = 0.37$) as the tRNA^{Leu}_{GCG} strain. This indicates that the anticodon affects the growth phenotype as well as the type of amino acid substitution.

Furthermore, the three yeast strains that grew significantly faster than the wild-type strain had a tRNA^{Leu} anticodon plasmid with a tyrosine (ATA), valine (GAC) and another leucine (CAA) anti-codon. While this difference in growth for all three strains was lower than 10%, it could indicate that these three tRNA^{Leu} variants may have some beneficial effect on yeast cell growth. There are cases where an increase in mistranslation can benefit cell viability (i.e., increased methionine mistranslation can reduce oxidative stress (55)), so it could be that these strains somehow have a slight positive effect on cell division.

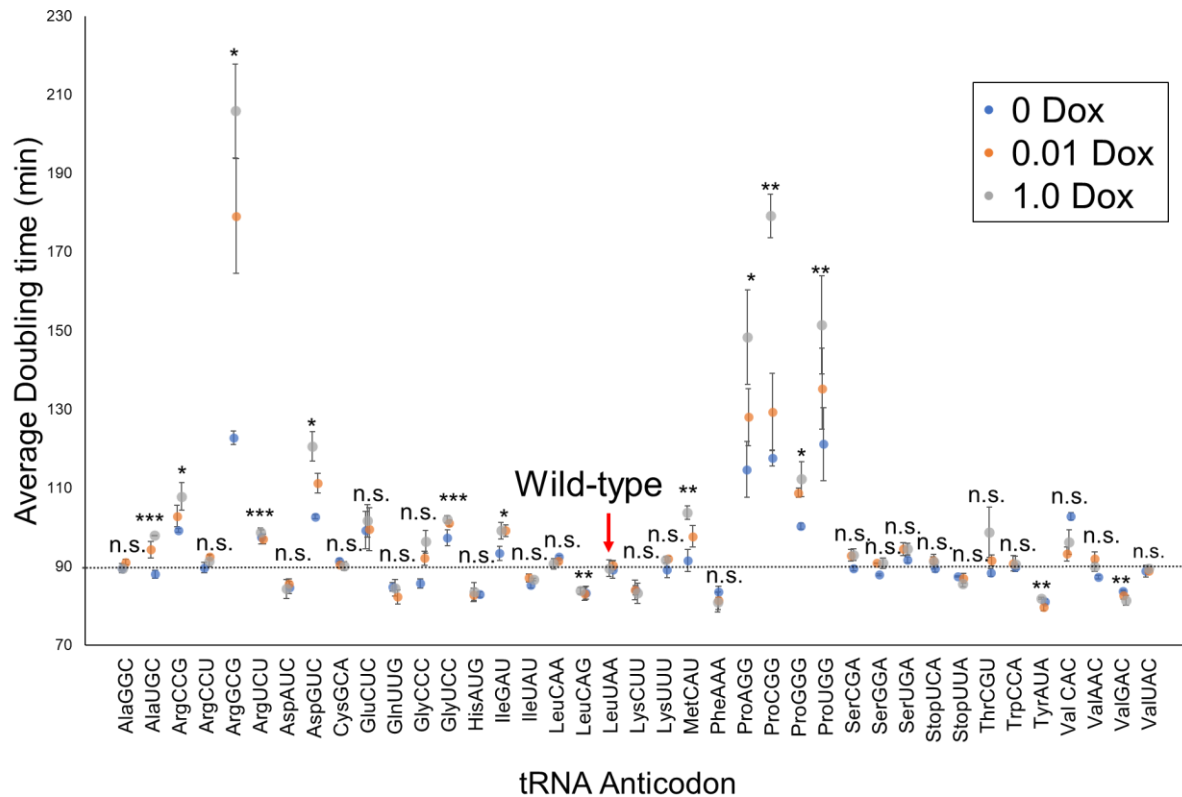


Figure 8: Growth rate analysis of 38 different tRNA^{Leu} anticodon variant and wild-type tRNA^{Leu} expressing yeast strains. Shown here are the doubling times (from 24-hour recorded growth) of the 38 yeast strains that express tRNA^{Leu} variants. The doubling of the wild-type strain (tRNA^{Leu}_{UAA}) is also shown. They are arranged in alphabetical order according to the assigned amino acid (x-axis). Each tRNA^{Leu} yeast strain is represented as points which differ in their doubling time. Each strain was grown in triplicate (n = 3) except the strain transformed with the tRNA^{Leu}_{UUA} plasmid (2 biological replicates). Furthermore, five biological replicates (n = 5) were used to find the average for both the wild-type strain and tRNA^{Leu}_{UGG} (Pro). The black dotted line matches the doubling time of the wild-type strain (tRNA^{Leu}_{UAA}). The legend on the top right indicates the dox concentration (μg/mL) that the strains were grown under. The blue dots are cells grown at 0 μg/mL dox, the orange dots are cells grown at 0.01 μg/mL dox and the grey dots are cells grown at 1.0 μg/mL dox. The Welch's t-test was used to calculate significance of the difference in doubling time between the tRNA^{Leu} anticodon variant and wild-type strain. (n.s. = no significant difference, * p < 0.05, ** p < 0.01, *** p < 0.001).

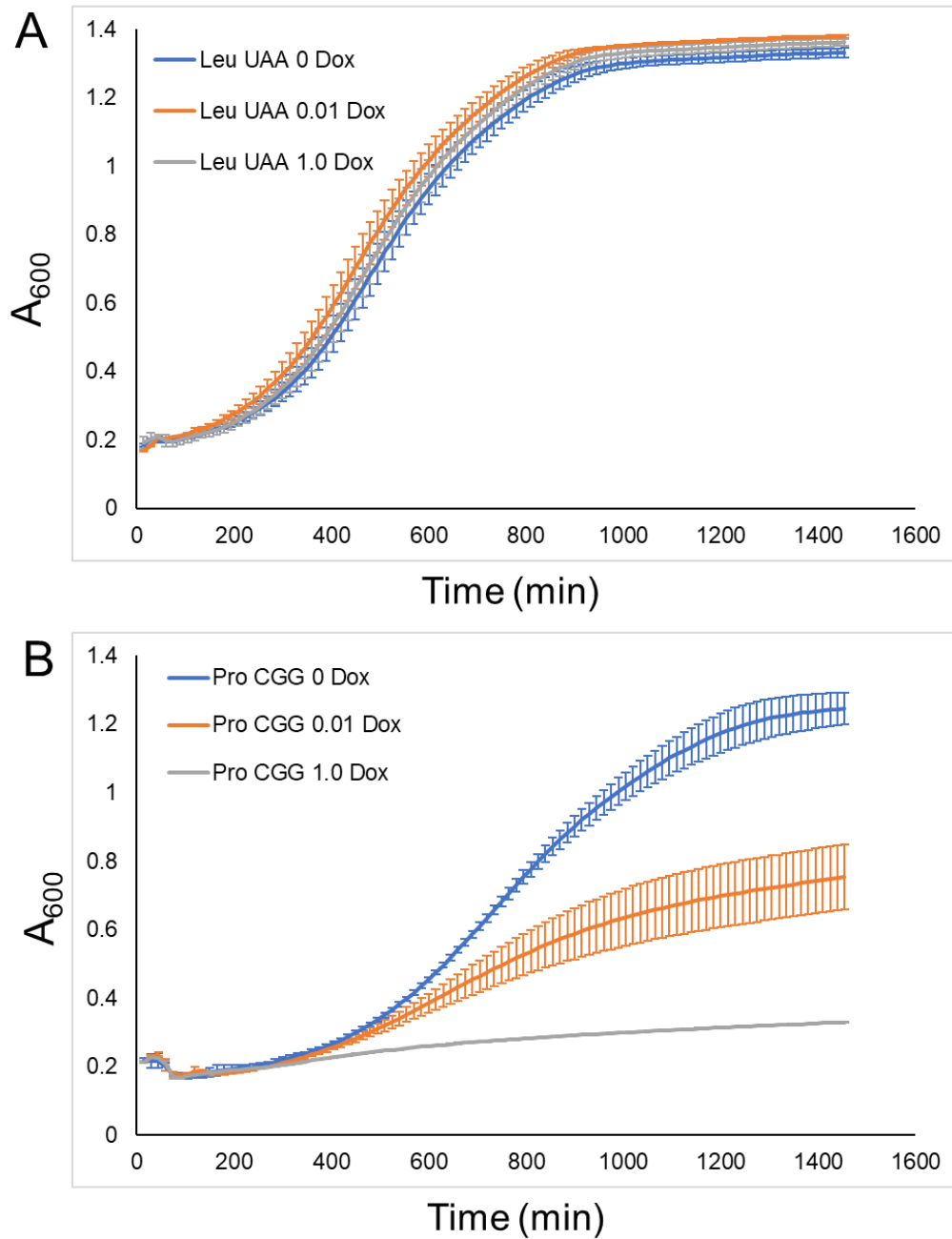


Figure 9: Representative growth curves of yeast cells expressing the wild-type $tRNA^{Leu_{UAA}}$ (A) and the $tRNA^{Leu_{CGG}}$ (Pro) variant (B). Each strain was grown in triplicate ($n = 3$). The A_{600} is represented on the y-axis and the time is represented on the x-axis. The grey curves represent cells grown at 1.0 $\mu\text{g/mL}$ dox, the orange curves represent cells grown at 0.01 $\mu\text{g/mL}$ dox and the blue curve is cells grown at 0 $\mu\text{g/mL}$ dox.

Table 4: Heat map of the growth rate of each tRNA^{Leu} anticodon variant yeast strain. This figure is the same as a codon table, except all the anticodons are represented instead. The fold reduction in doubling time between the mutant strains and the wild-type strains (grown under 1.0 µg/mL dox) is shown on the right of the corresponding anticodon. Each strain was grown in triplicate (n = 3) except tRNA^{Leu}_{UUA} (Stop) (n = 2), tRNA^{Leu}_{UGG} (Pro) (n = 5) and the wild type strain tRNA^{Leu}_{UAA} (n = 5). The color coding is redder if the strain is slow growing and bluer if it is fast growing compared to the wild type. The Welch's t-test was used to calculate significance of the difference in doubling time between the tRNA^{Leu} anticodon variant and wild-type strain. (n.s. = no significant difference, * p < 0.05, ** p < 0.01, *** p < 0.001).

	A		G		U		C	
A	AAA Phe	0.89 n.s.	AGA Ser		AUA Tyr	0.92 **	ACA Cys	
G	GAA Phe		GGA Ser	1.02 n.s.	GUA Tyr		GCA Cys	1 n.s.
U	UAA Leu	1	UGA Ser	1.06 n.s.	UUA stop	0.96 n.s.	UCA stop	1.02 n.s.
C	CAA Leu	1.01 n.s.	CGA Ser	1.04 n.s.	CUA stop		CCA Trp	1.01 n.s.
A	AAG Leu		AGG Pro	1.66 *	AUG His	0.93 n.s.	ACG Arg	
G	GAG Leu		GGG Pro	1.25 *	GUG His		GCG Arg	2.10 *
U	UAG Leu		UGG Pro	1.69 **	UUG Gln	0.95 n.s.	UCG Arg	
C	CAG Leu	0.94 n.s.	CGG Pro	2.00 **	CUG Gln		CCG Arg	1.21 *
A	AAU Ile		AGU Thr		AUU Asn		ACU Ser	
G	GAU Ile	1.11 *	GGU Thr		GUU Asn		GCU Ser	
U	UAU Ile	0.97 n.s.	UGU Thr		UUU Lys	1.03	UCU Arg	1.10 ***
C	CAU Met	1.16 **	CGU Thr	1.10 n.s.	CUU Lys	0.93 n.s.	CCU Arg	1.02 n.s.
A	AAC Val	1.01 n.s.	AGC Ala		AUC Asp	0.94 n.s.	ACC Gly	
G	GAC Val	0.91 **	GGC Ala	1 n.s.	GUC Asp	1.35 *	GCC Gly	
U	UAC Val	1 n.s.	UGC Ala	1.01 ***	UUC Glu		UCC Gly	1.14 ***
C	CAC Val	1.08 n.s.	CGC Ala		CUC Glu	1.14 n.s.	CCC Gly	1.08 n.s.

3.4 Trends in the growth curve data

The data gathered from the 24-hour growth rate of the different tRNA^{Leu} anticodon yeast strains in comparison to the wild-type strain showed that the growth rate of each strain varied depending on the anticodon of the tRNA^{Leu} anticodon variant plasmid. Thus, it was important to see if codon usage in the yeast genome could be correlated with the growth rate corresponding to each tRNA^{Leu} anticodon variant yeast strain. Using the laws of base pairing it was determined how many codons in the yeast genome could base pair to each of the 38 tRNA^{Leu} anticodon variants used in this study. The number of codons in the yeast genome that could base-pair to each tRNA^{Leu} anticodon variant was then plotted against the doubling time of each tRNA^{Leu} anticodon variant strain on a scatter plot. The linear regression analysis from the scatter plot indicated that codon usage was not the primary determinant for the change in growth rate for each tRNA^{Leu} anticodon variant strain as the goodness of fit score was very low ($R^2 = 0.0312$) (Fig. 10.).

If codon usage was not the primary factor, then maybe GC content was as it is another aspect of the anticodon. The GC content of the anticodon is a good indicator of how well it will base pair with its matching codon. This is because the purine guanine and the pyrimidine cytosine form three hydrogen bonds instead of the two that occur between adenine and uridine/thymine (90). Thus, a higher GC content in the anticodon should facilitate a higher degree of mistranslation. A higher degree of mistranslation normally coincides with increased proteotoxic stress, which could explain the slow growth phenotype seen in many of the tRNA^{Leu} anticodon variant plasmids (4). To test the linear correlation between the GC content of the anticodon and the doubling time of the yeast strains, linear regression analysis was used to calculate the goodness of fit score. The goodness of fit score was low ($R^2 = 0.2525$), meaning there is not a strong correlation between GC content of the anticodon and the doubling time of the tRNA^{Leu} anticodon variant yeast strains (Fig. 11.). This means that factors other just GC content are impacting the growth rate of the yeast cells.

If the anticodon was not the primary factor, then maybe the type of amino acid replacement is. The BLOSUM62 matrix is a substitution matrix that is used for sequence alignment (91). It was created by analyzing the conserved regions of protein families with 62% homology and calculating how often each amino acid substitution event occurs (91). The BLOSUM62 scores for leucine substitution events go from -4 to +4, with scores below + 1 indicating less observed

(non-conservative) amino acid replacements and score above + 1 indicating commonly observed (conservative) amino acid replacements (91). When comparing the amino acid replacement scores of the BLOSUM62 matrix with doubling times associated with the tRNA^{Leu} variants, there is no linear correlation as the goodness of fit score is too low ($R^2 = 0.0865$) (Figure 12.). This lack of correlation is because there are several strains with doubling times that are not significantly different from the wild-type that have scores for non-conservative amino acid replacement (BLOSUM62 score ≥ 1).

There are also tRNA^{Leu} anticodon variants like tRNA^{Leu}_{CAU} (Met) and tRNA^{Leu}_{GAU} which have high doubling times (slow-growth) and conservative BLOSUM62 scores. The line of best fit follows the predicted trend where non-conservative amino acid-replacements are correlated with a slow growth phenotype. This is because certain mistranslation events are negative for cell growth, while other do not affect it (92). However, the tRNA^{Leu} variant strain discussed previously removes this correlation. The tRNA^{Leu}_{NGG} (proline) and tRNA^{Leu}_{GCG} (arginine) variants, which have doubling times much higher than the other yeast strains also appear to decrease the goodness of fit score. These strains both have doubling times far greater than the other strains, but their BLOSUM62 scores are not as low as -4 (-2 for Arg and -3 for Pro). There may be something about these amino acid substitution events that make them detrimental to cell growth far more than the BLOSUM62 matrix predicted.

There was also one observation that from the data that appeared to go against the established literature. Less than half of the tRNA^{Leu} anticodon variants have adenine at position 35 of the tRNA. Also, the five tRNA^{Leu} variants with the lowest growth rate do not have adenine at position 35 of the tRNA (middle position of the anticodon). This is interesting as A35 is listed as an identity element for tRNA^{Leu} in *S. cerevisiae* (50) (Table 4.). If mistranslation of leucine is what is inducing the low growth phenotype in the slowest growing strains (i.e., tRNA^{Leu}_{AGG}), then it would confirm that leucylation of the tRNA is possible without the A35 tRNA^{Leu} identity element.

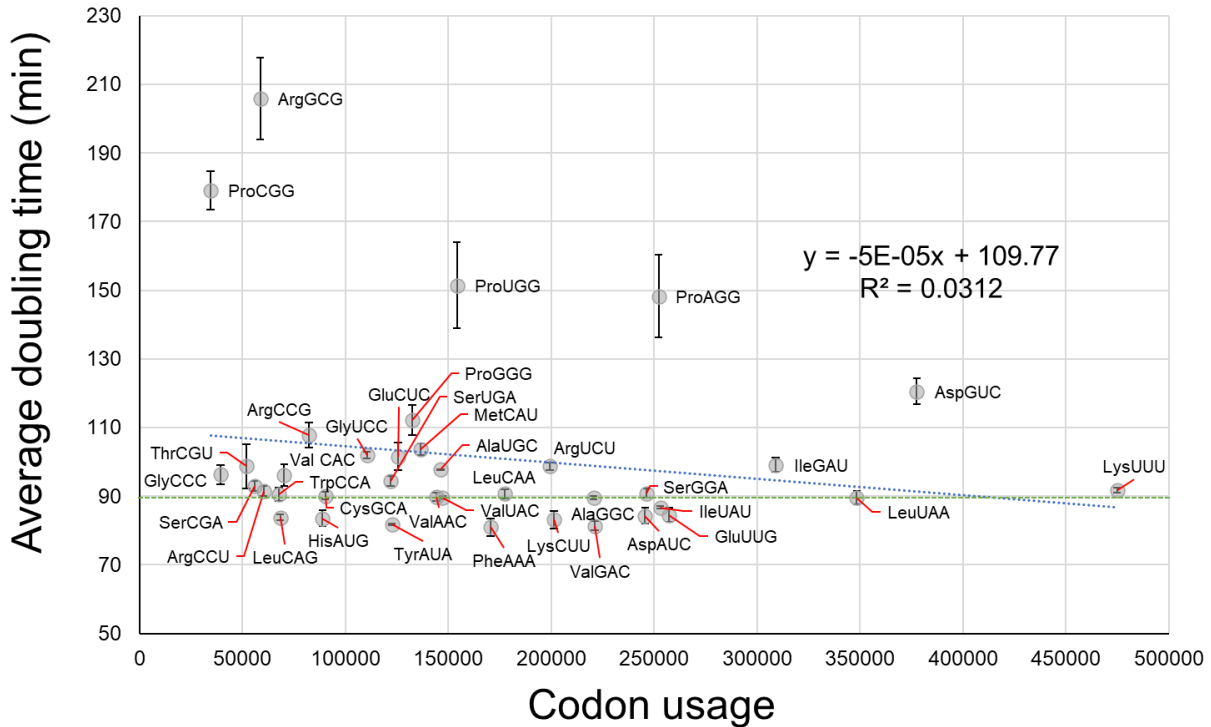


Figure 10: Linear correlation of potential codon usage against the doubling time of the tRNA^{Leu} anticodon variant strain. The potential codons that could base-pair to the tRNAs from each tRNA^{Leu} variant strains was plotted against the average doubling time of each strain grown under 1.0 µg/mL doxycycline. This data is presented as grey dots, with the anticodon of the tRNA^{Leu} variant and the amino acid beside it. The number of biological replicates was 3 for most strains except tRNA^{Leu}_{UUA} (Stop) (n = 2), tRNA^{Leu}_{UGG} (Pro) (n = 5) and the wild type strain tRNA^{Leu}_{UAA} (n = 5). The potential number of codons in the yeast genome that could base-pair to the tRNAs in each tRNA^{Leu} anticodon variant yeast strain is shown on the x-axis. The average doubling time of each tRNA^{Leu} anticodon variant strain is shown on the y-axis. The green line matches the average doubling time of the wild-type strain (tRNA^{Leu}_{UAA}). The equation for the trend line and the goodness of fit score (R²) are shown on the top right of the graph.

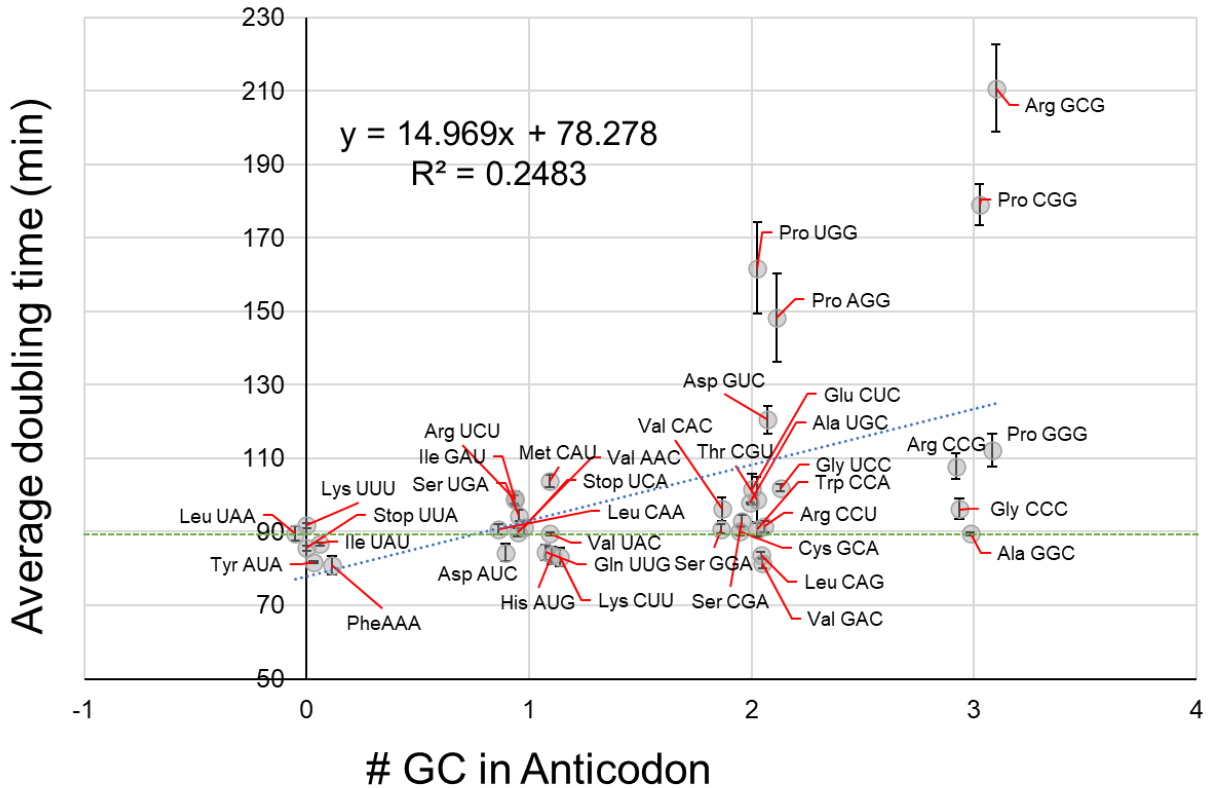


Figure 11: Linear correlation of GC content of the anticodon against the doubling time of the tRNA^{Leu} anticodon variant strain. The GC content of the tRNA^{Leu} anticodon was plotted against the doubling time of the tRNA^{Leu} anticodon strain at 1.0 µg/mL doxycycline. In grey are the points which represent each strain, with the label for the anticodon of the tRNA^{Leu} anticodon variant and the amino acid beside it. The number of biological replicates was 3 for most strains except tRNA^{Leu}_{UUA} (Stop) (n = 2), tRNA^{Leu}_{UGG} (Pro) (n = 5) and the wild type strain tRNA^{Leu}_{UAA} (n = 5). The GC content of the anticodon for each tRNA^{Leu} anticodon variant strain is shown on the x-axis. The average doubling time of each tRNA^{Leu} anticodon variant strain is shown on the y-axis. The green line matches the average doubling time of the wild-type strain (tRNA^{Leu}_{UAA}). The blue dotted line is the line of best fit. The equation for the line of best fit and the goodness of fit score (R²) are shown on the top-left of the graph.

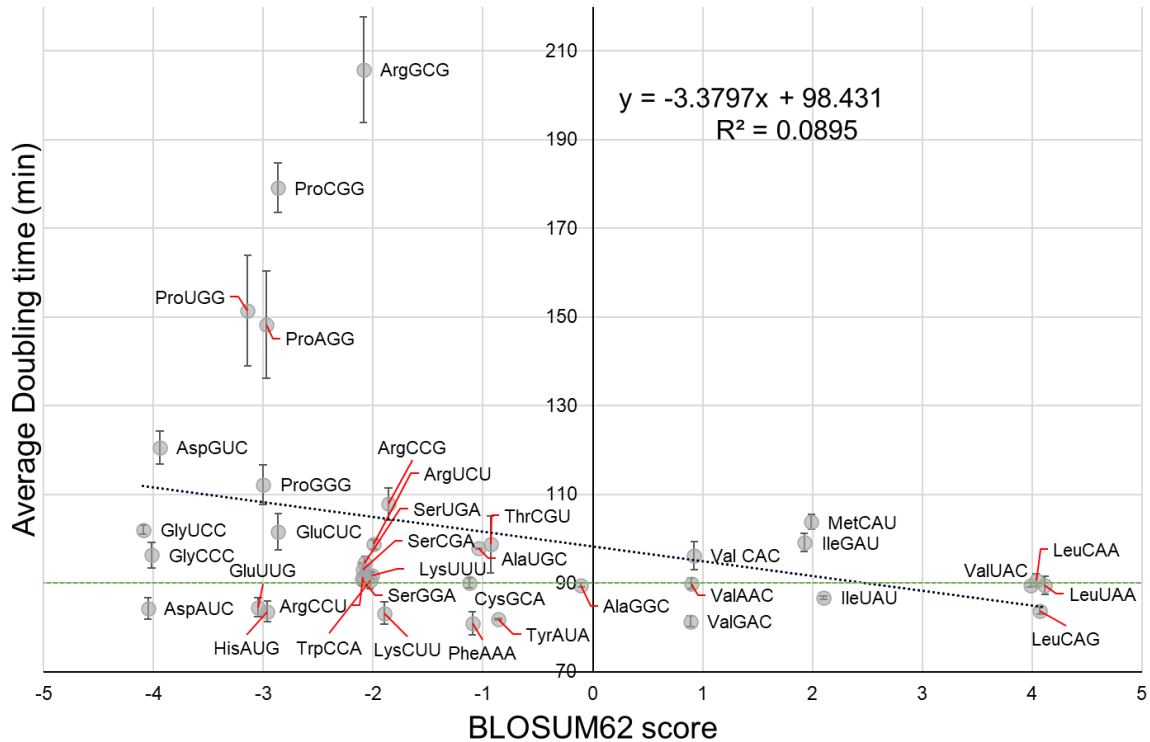


Figure 12: Comparing the doubling time of the tRNA^{Leu} anticodon variants with the BLOSUM62 matrix. To compare the differing growth rates of the tRNA^{Leu} variant yeast strains to the BLOSUM62 scoring matrix both were plotted against each other on a scatter plot. In grey are the points which represent each strain, with the label for the anticodon of the tRNA^{Leu} anticodon variant and the amino acid beside it. The number of biological replicates was 3 for most strains except tRNA^{Leu}_{UUA} (Stop) (n = 2), tRNA^{Leu}_{UGG} (Pro) (n = 5) and the wild type strain tRNA^{Leu}_{UAA} (n = 5). The average doubling times (at 1.0 µg/mL dox) of each yeast strain is on the y-axis and the BLOSUM62 scores for each amino acid replacement were plotted on the x-axis. The green line matches the average doubling time of the wild-type strain (tRNA^{Leu}_{UAA}). The blue dotted line is the trend line. The equation for the trend line is shown on the top right as well as the goodness of fit score (R²).

3.5 Mass spectrometry of tRNA^{Leu} variant yeast strains

To confirm that mistranslation was the main factor that controlled to effect of each tRNA^{Leu} variant on yeast cells, liquid chromatography and tandem mass spectrometry (LC MS/MS) analysis was performed. LC-MS/MS analysis analyzes the protein content of yeast cells and provides an accurate amino acid sequence for every peptide analyzed. The peaks studio software was used to confirm cases where leucine was substituted in the place of other amino acids. Four separate yeast strains were analyzed by LC-MS/MS analysis. These four strains each contained one dox-inducible tRNA^{Leu} plasmid. These tRNA^{Leu} variants were tRNA^{Leu}_{CGG} (proline anticodon), tRNA^{Leu}_{AGG} (proline anticodon), tRNA^{Leu}_{UAC} (valine anticodon) and tRNA^{Leu}_{UAA} (wild-type). tRNA^{Leu}_{CGG} is the strain with the second highest recorded doubling time at 1.0 µg/mL dox (179 min⁻¹), tRNA^{Leu}_{AGG} has the third highest doubling time (148 min⁻¹), tRNA^{Leu}_{UAC} has a doubling time (89.5 min⁻¹) close to the wild type strain and (89.6 min⁻¹) tRNA^{Leu}_{UAA} is the wild type strain. These strains were chosen because it was necessary to confirm that mistranslation was occurring in two of the slow growth phenotype yeast strains. This would support the idea that leucine mistranslation was responsible for the slow growth phenotype. The tRNA^{Leu}_{UAC} was analyzed to see if mistranslation events occurred in a tRNA^{Leu} variant yeast strain without the slow growth phenotype. The wild-type strain was included as a control to confirm that the mistranslation events recorded in the tRNA^{Leu} variant strains did not occur in the wild-type strain.

The whole-cell lysate of these strains was run on an SDS-PAGE gel. Two clear bands at 42 kDa were extracted, and trypsin digested for LC-MS/MS analysis. This was not an analysis of the whole proteome, instead this was an experiment intended to confirm any mistranslation in a group of highly abundant proteins. Upon performing LC-MS/MS analysis there were 23 instances of leucine mistranslation with a -10logp score above 20 (Table 5.). The tRNA^{Leu}_{CGG} strain had 6 peptides with a recorded proline to leucine mistranslation event (Table 5.). In the tRNA^{Leu}_{AGG} strain, there were 13 peptides with a recorded the proline to leucine mistranslation event. In the tRNA^{Leu}_{UAC} strain, there were four peptides with a recorded valine to leucine mistranslation event (Table 5.). The peptide the with highest -10logp (59.61) value came from Enolase 1 according the peaks studio database. This protein came from the tRNA^{Leu}_{AGG} strain. The peptide with the second highest -10logp (53.77) value matched with saccharopepsin, that

was expressed in the tRNA^{Leu}_{CGG} strain (Fig 13.). The peptide with the third highest -10logp (49.96) value also matched with Enolase 1. This peptide came from the tRNA^{Leu}_{CGG} strain. A -10logp score is a measure of how much the observed mass spectrum matches the sequence of the identified peptide. A higher -10logp score indicates that the sequenced peptide is a better match for the reference protein. There were no leucine mistranslation events in the wild-type strain that matched those recorded in the tRNA^{Leu} anticodon variant strains.

The amount of mistranslation events observed in both slow growth phenotype strains (tRNA^{Leu}_{AGG} and tRNA^{Leu}_{CGG}) gives evidence that the slow growth phenotype is due to leucine mistranslation events. It also proves that mistranslation is possible without an adenine present at position 35 of the tRNA^{Leu} anticodon. This is because tRNA^{Leu}_{AGG} and tRNA^{Leu}_{CGG}, had mistranslation events recorded even though they do not have the A35 identity element.

Table 5: Description of proteins with leucine mistranslation identified via LC-MS/MS.

tRNA^{Leu}_{CGG} tRNA^{Leu}_{AGG}, both with proline anticodons, result in yeast misincorporating leucine in place of proline. The tRNA^{Leu}_{UAC} strain misincorporate leucine in place of valine as UAC is a valine anticodon. None of these mistranslation events were found in the wild type strain (tRNA^{Leu}_{UAA}). The numbers beside the strain name indicate which biological replicate the peptide was extracted from.

Strain	Protein	logp	%Area	Spectral counting
tRNA ^{Leu} _{CGG} 1	Saccharopepsin	53.77	0.20%	1 in 3
tRNA ^{Leu} _{CGG} 1	Enolase 1	49.96		1 in 9
tRNA ^{Leu} _{CGG} 1	Saccharopepsin	47.73	4.50%	1 in 6
tRNA ^{Leu} _{CGG} 1	Sphingolipid long chain base-responsive protein	42.86		1 in 2
tRNA ^{Leu} _{CGG} 2	Saccharopepsin	40.91	4.40%	1 in 4
tRNA ^{Leu} _{CGG} 1	Heat shock protein SSA4	28.04		1 in 1
tRNA ^{Leu} _{AGG} 2	Enolase 1	59.61	0.01%	1in11
tRNA ^{Leu} _{AGG} 1	Enolase 1	47.58		1in13
tRNA ^{Leu} _{AGG} 1	Phosphoglycerate kinase	45.11		1in26
tRNA ^{Leu} _{AGG} 1	Phosphoglycerate kinase	43.26	0.49%	1in15
tRNA ^{Leu} _{AGG} 2	Heat shock protein 104	42.44	12.20%	1in2
tRNA ^{Leu} _{AGG} 1	Citrate synthase	40.3	6.70%	1in2
tRNA ^{Leu} _{AGG} 1	Ketol-acid reductoisomerase	40.03	0.50%	1 in 7
tRNA ^{Leu} _{AGG} 3	Phosphoglycerate kinase	38.05	0.07%	1in22
tRNA ^{Leu} _{AGG} 2	Pyruvate kinase	37.3		1in7
tRNA ^{Leu} _{AGG} 1	Fructose-bisphosphate aldolase	27.95		1 in 2
tRNA ^{Leu} _{AGG} 2	Heat shock protein SSA1	26.7	0.55%	1in7
tRNA ^{Leu} _{AGG} 3	Phosphoglycerate kinase	24.07		1in22
tRNA ^{Leu} _{AGG} 2	Small glutamine-rich tetratricopeptide repeat-containing protein 2	23.75	3.40%	1in6
tRNA ^{Leu} _{CAC} 3	Alpha,alpha-trehalose-phosphate synthase [UDP-forming]	36.42		1in4
tRNA ^{Leu} _{CAC} 1	D-3-phosphoglycerate dehydrogenase	35.23		1in1
tRNA ^{Leu} _{CAC} 1	Inositol-3-phosphate synthase	28.73		1in1
tRNA ^{Leu} _{CAC} 3	Inositol-3-phosphate synthase	22.32		1in2

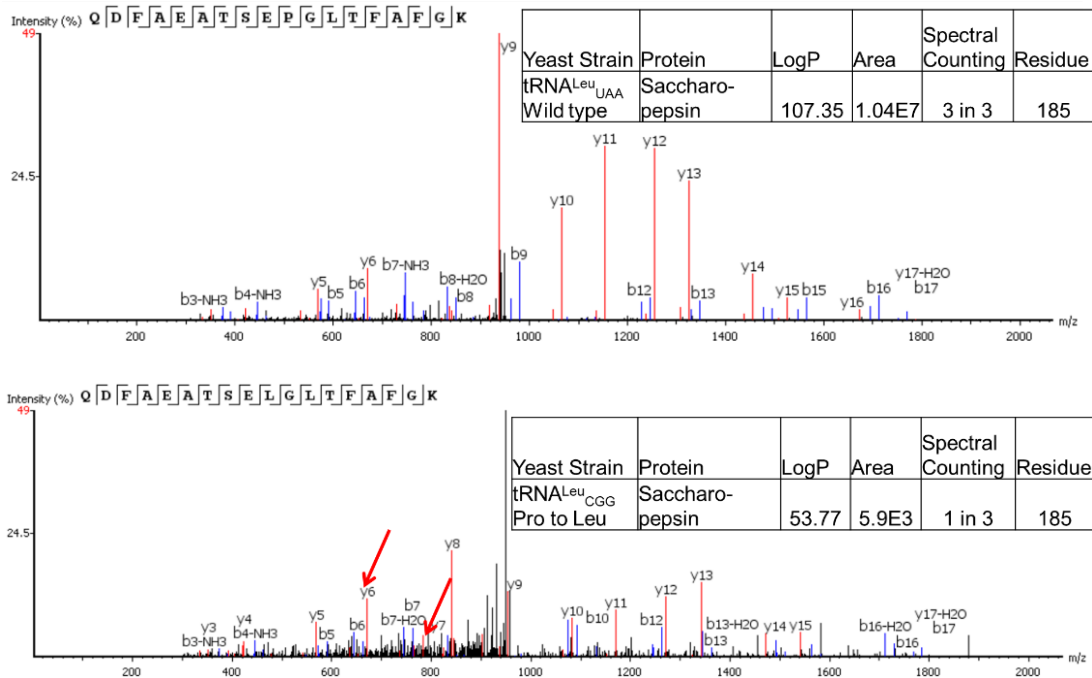


Figure 13: Mass spectrometry profiles of Saccharopepsin peptide found in tRNA^{Leu}_{CGG} and wild type tRNA^{Leu}_{UAA} cells. Above is the mass spectrogram for yeast cells expressing tRNA^{Leu}_{UAA} at 2.0 µg/mL dox A) and below is the mass spectrogram for yeast cells expressing tRNA^{Leu}_{CGG} at 2.0 µg/mL dox B). The protein was identified as Saccharopepsin by the Peaks+ database. The red arrows point to the peaks which correspond to the proline to leucine substitution event.

3.6 Selecting the mammalian tRNA variants

To observe the effects of leucine tRNA variants on mammalian cells, 3 mutant tRNA^{Leu} genes were chosen. This choice was made after searching the GtRNA database for point mutations in the anticodon of human tRNA^{Leu} (13). The three mutant tRNA^{Leu} variants chosen were tRNA^{Leu}_{AAA} (G36A), tRNA^{Leu}_{CCA} (C35A) and tRNA^{Leu}_{GAA} (C34G). tRNA^{Leu}_{AAA} and tRNA^{Leu}_{GAA} both have phenylalanine anticodons, while tRNA^{Leu}_{CCA} has a tryptophan anticodon (Table 6.). All three tRNAs were unique alleles found in a small sample group of individuals (e.g., tRNA^{Leu}_{AAA} was found once in 264690 individuals studied) (93). These mutations could still be significant as they could be linked to diseases found in the select individuals who possess these tRNA^{Leu} variants (94). Thus, it is important to discover if these tRNAs induce mistranslation in mammalian cells, what effect this has on protein synthesis and ultimately how this effects the viability of the mammalian cells.

Table 6: The profiles for the three human tRNA^{Leu} anticodon variants. All information was provided from the GtRNA database and dbSNP (National library of medicine). The leftmost column shows the tRNA present, the column next to it displays the position of the tRNA where the single nucleotide polymorphism occurs in the tRNA^{Leu} anticodon variant. The middle column shows to type of SNP that occurred. The column right of the middle displays the anticodon of the tRNA^{Leu} variant and the change in anticodon identity from leucine to another amino acid. The rightmost column displays the frequency at which the allele was found in a group of human individuals who had their genomes sequenced for a biological study.

Wild-type tRNA	SNP location	SNP	Anticodon shift	Allele Frequency
tRNA-Leu CAA-3-1	34	C -> G	GAA Leu -> Phe	A=0.00000 (0/14050, ALFA)
tRNA-Leu CAA-3-1	35	A -> C	CCA Leu -> Trp	A=0.000004 (1/264690, TOPMED) A=0.000007 (1/140238, GnomAD) G=0.0003 (1/3854, ALSPAC)
tRNA-Leu AAG 3-1	36	G -> A	AAA Leu -> Phe	A=0.000004 (1/264690, TOPMED) A=0.00006 (1/16760, 8.3KJPN)

3.7 Fluorescence of tRNA^{Leu} variant mammalian cells

Lant et al. (65), had observed that the tRNA^{Ser}_{AGA} (G35A) variant which mistranslates serine at phenylalanine codons, caused a reduction in protein synthesis. This was determined after observing that the fluorescent protein mCherry (in the same vector as tRNA^{Ser}_{AAA}) had reduced fluorescence in tRNA^{Ser}_{AAA} compared to the wild-type strain (tRNA^{Ser}_{AGA}) and measuring the reduction in mCherry concentration using LC-MS/MS analysis (65).

To determine if this reduction in protein synthesis also occurs in mammalian cells transfected with tRNA^{Leu} variants, both the wild type and mutant human tRNA^{Leu} were cloned into the WT-PAN vector. The WT-PAN vector expresses both eGFP and mCherry. The cell line used was murine Neuro-2_a (N2_a), which are neuroblastoma cells extracted from *Mus musculus*. After growing N2_a cells for 24 hours, they were transfected with all three tRNA^{Leu} variant plasmids and two wild-type tRNA^{Leu} plasmids (tRNA^{Leu}_{AAG} and tRNA^{Leu}_{CAA}). N2_a cells were also transfected with the same tRNA^{Ser} plasmids used by Lant et al. (65). These were used as control to see if the N2_a cells grown shared the same trend that Lant et al. (65) observed. All the plasmids used did not have the G26A mutation that was used in the yeast trials, as it was unknown how this mutation would affect the N2_a cells.

24 hours post-transfection, the N2_a cells were analyzed for both mCherry and eGFP fluorescence. In the control cell lines, tRNA^{Ser}_{AAA} showed the same reduction in mCherry fluorescence that was observed by Lant et al. (65) (Supp Fig 2.). However, the main goal was to observe any changes in protein synthesis caused by the tRNA^{Leu} variants. There was no significant difference in eGFP fluorescence ($p = 0.56$), or mCherry fluorescence ($p = 0.38$) between the phe-decoding tRNA^{Leu}_{AAA} and tRNA^{Leu}_{AAG} (wild-type) cell lines (Fig 14., Supp Fig 3.). Furthermore, there was a highly significant 9% decrease ($p = 2.9E-07$) in the mean mCherry fluorescence in the trp-decoding tRNA^{Leu}_{CCA} cells compared to the wild type tRNA^{Leu}_{CAA} cells, but no significant ($p = 0.16$) change in eGFP fluorescence (Fig 15., Supp Fig 4.). Lastly, there was a highly significant 21% decrease ($p = 4.1E-51$) in the eGFP fluorescence of N2_a cells transfected with the phe-decoding tRNA^{Leu}_{GAA} compared to cells transfected with the wild-type tRNA^{Leu}_{CAA}, and a highly significant 17% decrease ($p = 7.4E-21$) in mCherry fluorescence (Fig 15, Supp Fig 4.).

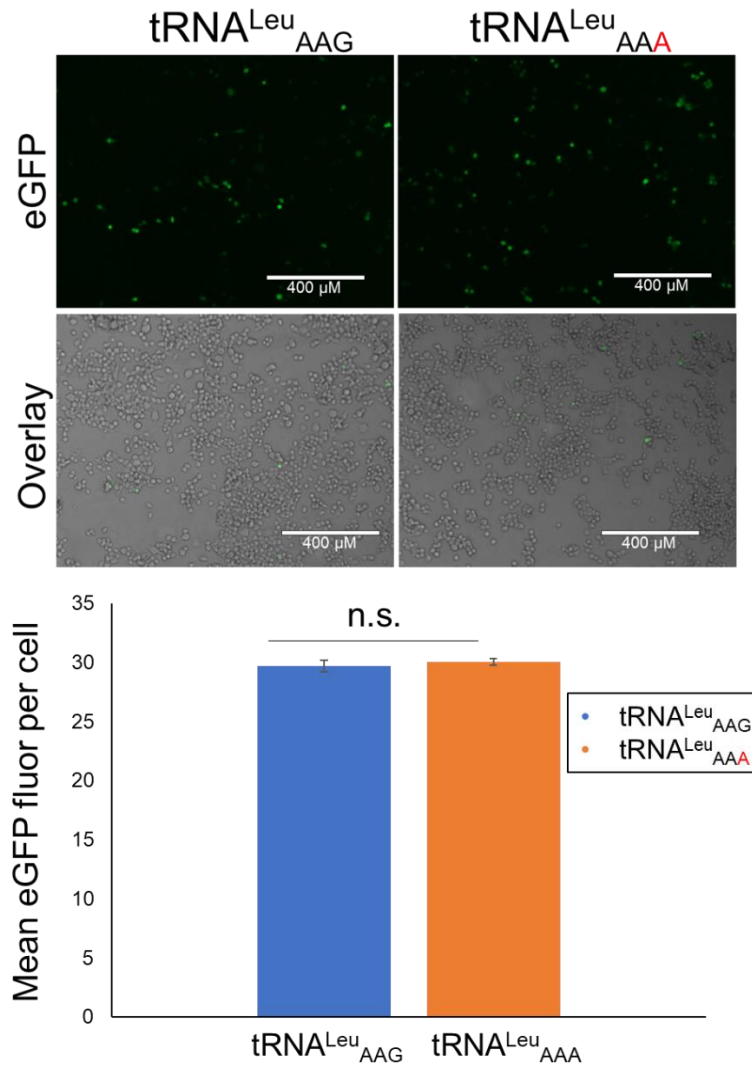


Figure 14: The Comparison of eGFP fluorescence between wild type tRNA^{Leu}_{AAG} and tRNA^{Leu}_{AAA(G36A)} (phenylalanine anticodon) N2_a cells. On top are eGFP fluorescent images of N2_a cells 24 hours after they were transfected with the wild-type tRNA^{Leu}_{AAG} plasmid (n= 1795) and the tRNA^{Leu}_{AAA(G36A)} (Phe) plasmid (n= 3663). On the bottom is a bar plot comparing the average fluorescence per cell of the tRNA^{Leu}_{AAG} and tRNA^{Leu}_{AAA} cell lines quantified using Fiji/ImageJ. The difference in mean fluorescence per cell between the two cell lines is not significant (p = 0.56). Significance was calculated using Welch's t-test.

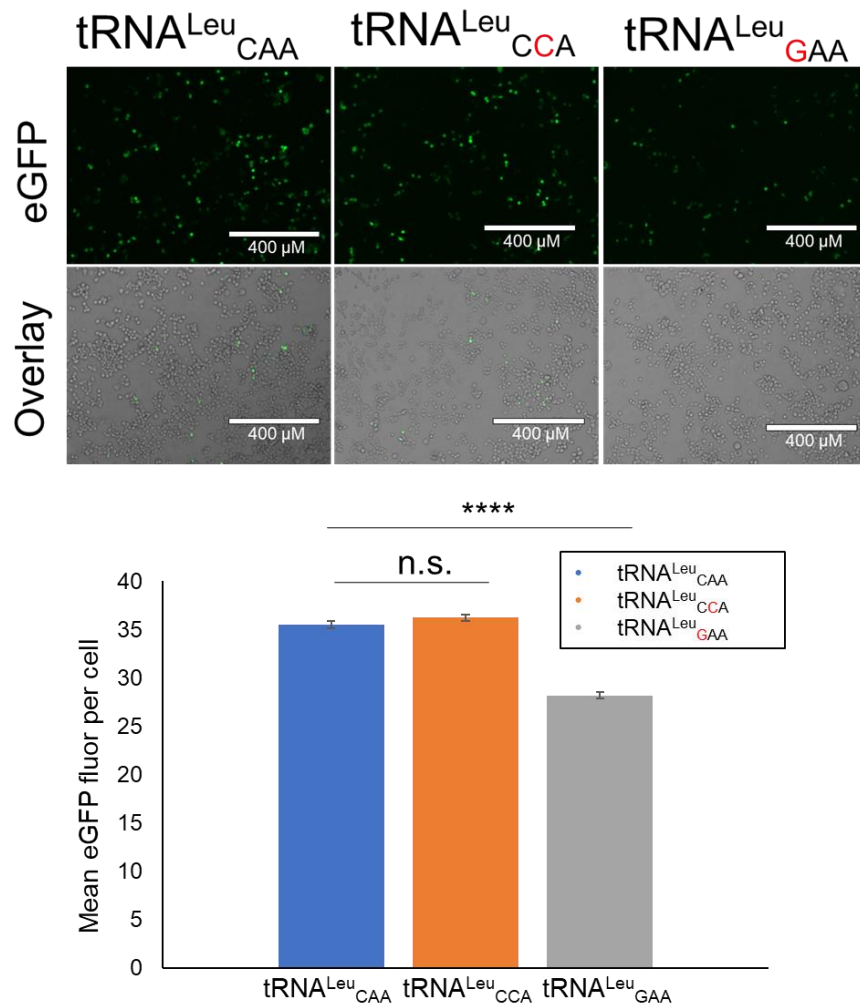


Figure 15: The comparison of GFP fluorescence between the wild type tRNA^{Leu}_{CAA}, tRNA^{Leu}_{CCA} (A35C) (tryptophan anticodon) and tRNA^{Leu}_{GAA} (C34G) (phenylalanine anticodon) N2a cells. On top are images of N2a cells 24 hours post-transfection with tRNA^{Leu}_{CAA} (n= 3670), tRNA^{Leu}_{CCA} (tryptophan anticodon) (n=4663) and tRNA^{Leu}_{GAA} (phenylalanine anticodon) (n=2564) cell lines (all fluoresce eGFP). Below is a comparison of the mean eGFP fluorescence per cell between tRNA^{Leu}_{CAA}, tRNA^{Leu}_{CCA} and tRNA^{Leu}_{GAA} cell lines. The difference between the tRNA^{Leu}_{CAA} and tRNA^{Leu}_{CCA} cell lines was not significant (p = 0.16). The difference between tRNA^{Leu}_{CAA} and tRNA^{Leu}_{GAA} cell lines was highly significant (p = 4.1E-51). Stars indicate p-values from the Welch's t-test. (n.s. = no significant difference, * p < 0.05, ** p < 0.01, *** p < 0.001, **** p < 0.0001)

3.8 Mammalian cell fluorescence after proteasome inhibition

After comparing the mean fluorescence of both eGFP and mCherry per cell of the tRNA^{Leu} anticodon variant cell lines against the wild-type cell lines it became apparent that the degree of perturbation of protein homeostasis was dependent on the anticodon of the tRNA^{Leu} variant. The next step was to see if the tRNA^{Leu} anticodon variants both altered protein homeostasis and were toxic to the N2_a cells during the inhibition of proteome. Lant et al. (65), found that tRNA^{Ser}_{AAA} (Phe anticodon) lowered protein synthesis in N2_a cells and were toxic to the cell line when protein degradation was halted using a MG132 reagent. MG132 is potent proteasome inhibitor, that inadvertently blocks protein synthesis as well (88). As the concentration of this reagent is increased there should be an accumulation of mistranslated and/or misfolded proteins which are toxic to the mistranslating N2_a cells in comparison to the N2_a cells expressing the wild-type tRNA (88). They measured the toxicity of tRNA^{Ser}_{AAA} (phe) by measuring the amount of dead cells in comparison to the wild-type cell line at different MG132 concentrations using the Promega CytoTox-glo cytotoxicity assay (65).

This study replicated Lant et al. (65) results and tested if the tRNA^{Leu} anticodon variants were toxic to N2_a cells in comparison to the wild-type tRNA^{Leu} when the proteasome is inhibited by MG132. The MG132 reagent was added to the tRNA^{Leu} anticodon variant, tRNA^{Leu} wild-type, tRNA^{Ser} anticodon variant and tRNA^{Ser} wild-type cell lines under four different MG132 conditions (10 µg/mL, 1 µg/mL, 0.1 µg/mL and 0 µg/mL). Four hours after treatment the eGFP and mCherry fluorescence were measured again. It was important to see if the concentration of fluorescent proteins in all the cell lines had been altered by MG132 before performing the cytotoxicity assay.

In the control cells lines the mutant cell line (tRNA^{Ser}_{AAA} expressing N2_a cells) had a significant reduction in mCherry synthesis compared to the wild-type cell line (tRNA^{Ser}_{AGA}) under all MG132 concentrations (Supp Fig 5.). At 4 hours after adding the different MG132 concentrations there was still no difference in the mean eGFP fluorescence between tRNA^{Leu}_{AAG} and tRNA^{Leu}_{AAA} N2_a cell lines except at 0.1 µg/mL, where there was a significant 9% decrease (p = 0.008) in the mean eGFP fluorescence (Fig 16.). There was also no significant difference in mCherry fluorescence between the cell lines under any MG132 concentration (Supp Fig 6.).

When comparing the tRNA^{Leu}_{CAA} and tRNA^{Leu}_{CCA} (Trp) cell lines there was a highly significant 15% ($p = 3.4E-07$) increase in eGFP fluorescence at 0 $\mu\text{g/mL}$ MG132, and a significant 8% increase ($p = 0.01$) in eGFP fluorescence at 1.0 $\mu\text{g/mL}$ MG132 (Fig 17.). There was also a significant 6% increase ($p = 0.011$) in mCherry fluorescence under 0 $\mu\text{g/mL}$ MG132 (Supp Fig 7.). Lastly, there was always a highly significant decrease in the eGFP fluorescence of the tRNA^{Leu}_{GAA} transfected N2_a cells compared to tRNA^{Leu}_{CAA} N2_a cells under any MG132 concentration (12% at 1.0 μM ($p = 5.5 E-05$), 22% at 0.1 μM ($p = 6.0 E-15$) and 16% at 0 μM ($p = 4.4E-09$)) (Fig 17.). There was also a significant 22% ($p = 0.0012$) decrease of mCherry fluorescence at 0.1 $\mu\text{g/mL}$ MG132, but no significant difference at any other MG132 concentration (Supp Fig 7.).

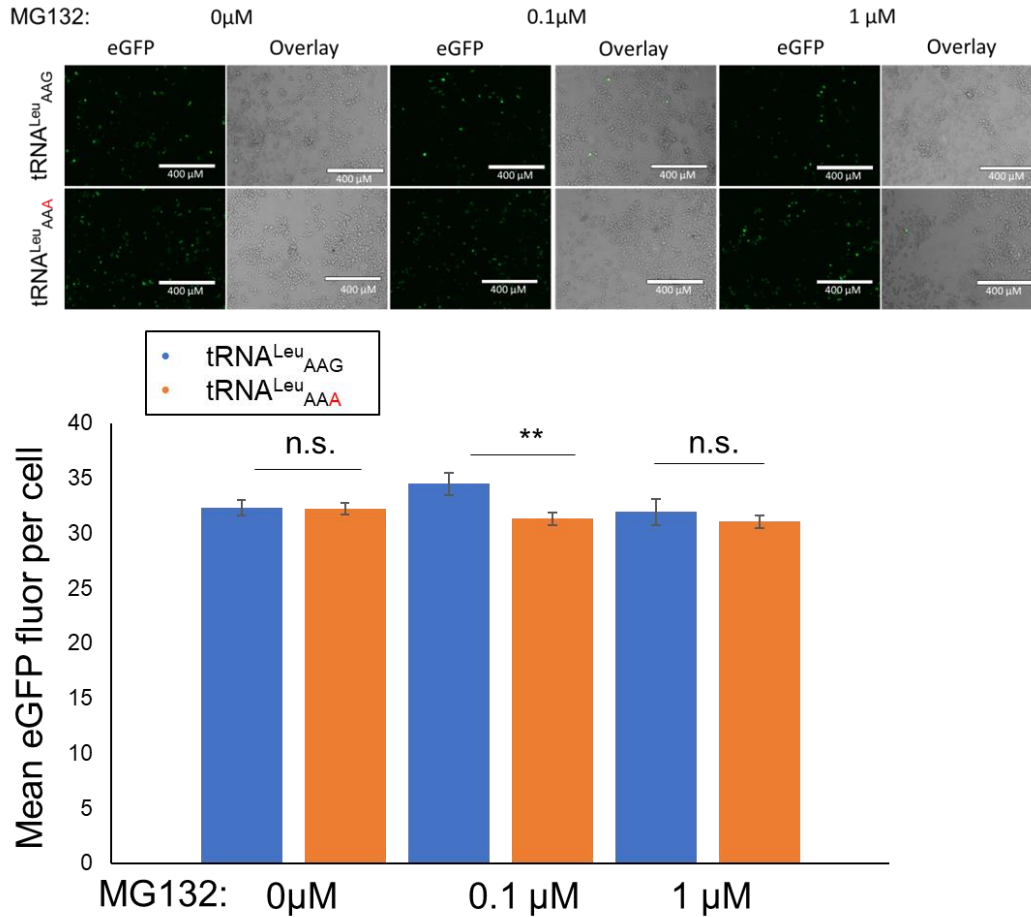


Figure 16: The comparison of eGFP fluorescence in tRNA^{Leu}_{AAG} and tRNA^{Leu}_{AAA} (G36A) (phenylalanine anticodon) N2a cells under different concentrations of MG132. On top are eGFP fluorescent images of N2a cells transfected with tRNA^{Leu}_{AAG} and tRNA^{Leu}_{AAA} plasmids. The cells were treated for 4 hours under 3 different MG132 concentrations (0, 0.1 and 1 μg/mL MG132). On the bottom is a bar graph comparing the mean eGFP fluorescence per cell of the different cell lines under the different MG132 concentrations. At 1.0 μg/mL the difference was non-significant (p= 0.5), at 0.1 μg/mL the difference was significant (p=0.008) and at 0 μg/mL the difference was non-significant (p= 0.9). Stars indicate p-values from the Welch's t-test (n.s. = no significant difference, * p < 0.05, ** p < 0.01, *** p < 0.001, **** p < 0.0001).

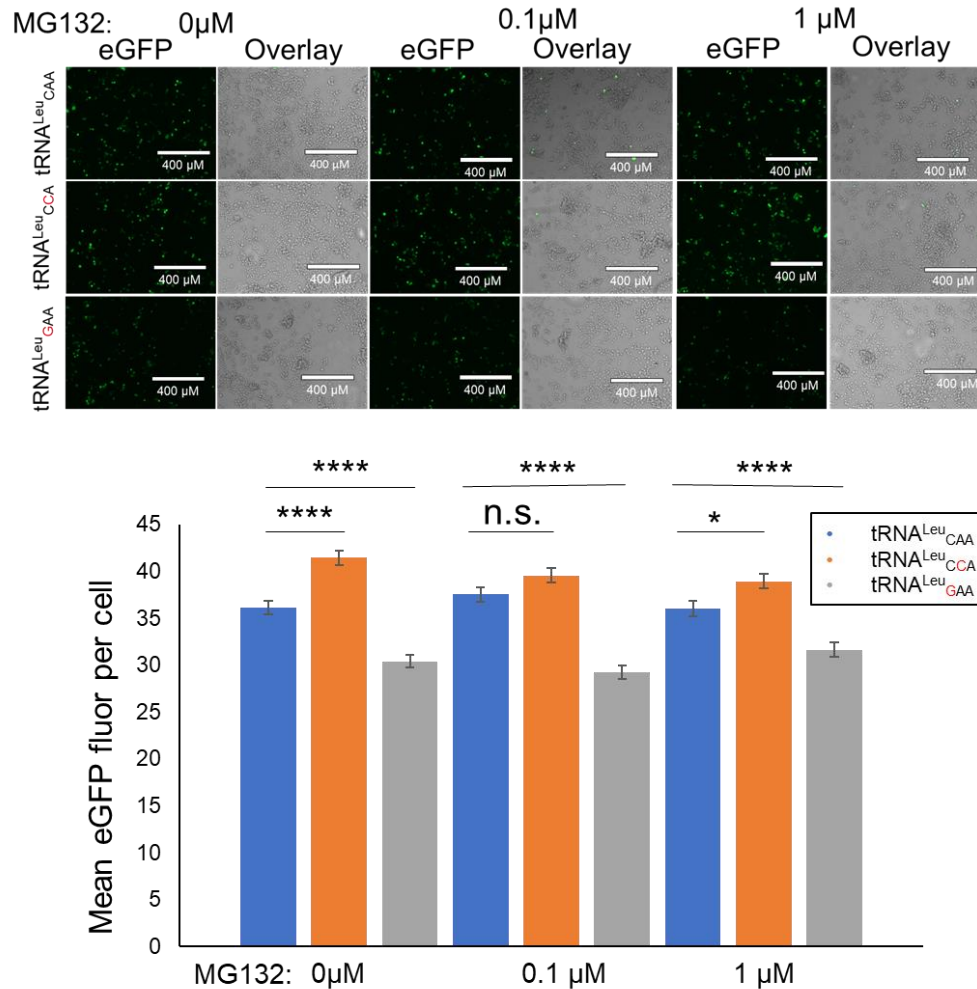


Figure 17: The comparison of eGFP fluorescence in wild-type tRNA^{Leu}_{CAA}, tRNA^{Leu}_{CCA} (A35C) (tryptophan anticodon) and tRNA^{Leu}_{GAA} (C34G) (phenylalanine anticodon) N2a cells under different MG132 concentrations. On the top are images of N2a cells transfected with tRNA^{Leu}_{CAA} (wild-type), tRNA^{Leu}_{CCA} (A35C) and tRNA^{Leu}_{GAA} (C34G) plasmids. On the bottom is a bar graph comparing the mean eGFP fluorescence per cell of the cell lines under the different MG132 concentrations. The cells were treated for four hours with 0, 0.1 and 1.0 μg/mL MG132. There was a highly significant decrease in fluorescence between the tRNA^{Leu}_{GAA} (Phe) and tRNA^{Leu}_{CAA} cell lines at 0 (p= 4.4E-09), 0.1 (p= 6.0 E-15) and 1.0 μg/mL (p= 4.4E-09). There was a significant difference in eGFP fluorescence between tRNA^{Leu}_{CCA} (A35C) (Trp) and tRNA^{Leu}_{CAA} cell lines at 1.0 (p= 0.01) and 0 μg/mL (p= 3.4E-07) MG132. The statistical test performed was the Welch's t-test. Stars indicate p-values from the Welch's t-test. (n.s. = no significant difference, * p < 0.05, ** p < 0.01, *** p < 0.001, **** p < 0.0001).

3.9 Cytotoxicity analysis of tRNA^{Leu} variant cell lines

After analyzing the fluorescence of the MG132 treated cells, a CytoTox-Glo assay (Promega) was used to measure the cellular toxicity of the tRNA^{Leu} variants. Each sample was analyzed with three biological replicates (n=3). A toxic effect induced by the tRNA^{Leu} variants is an indicator that they could promote disease in humans, as any adverse effects on mammalian cells would likely be detrimental to humans as well (95). The data from the 10 µg/mL MG132 treatment was not included as in all samples the cytotoxicity values varied too much between the biological replicates. There was a 19% increase ($p = 0.026$) in cytotoxicity to N2_a cells caused by tRNA^{Leu}_{CCA} compared to tRNA^{Leu}_{CAA} at 0.1 µg/mL MG132, but there was no significant change in cytotoxicity under any other MG132 concentration (Fig 18.). There was no change in toxicity caused by tRNA^{Leu}_{AAA} towards N2_a cells compared to tRNA^{Leu}_{AAG} under any MG132 concentration (Fig 19.). Lastly, there was no change in toxicity caused by tRNA^{Leu}_{GAA} towards N2_a cells compared to tRNA^{Leu}_{CAA} under any MG132 condition (Fig 18.). In the control cell line, tRNA^{Ser}_{AAA} induced a significant increase in cytotoxicity compared the tRNA^{Ser}_{AGA} under 0.1 and 1.0 µg/mL, which was also observed by Lant et al. (65) (supp Fig 8.). The data shows that the only tRNA^{Leu} variant that was significantly more toxic to N2_a cells in comparison to a wild-type tRNA^{Leu} was tRNA^{Leu}_{CCA} (Trp). This was only true at an MG132 concentration of 0.1 µg/mL.

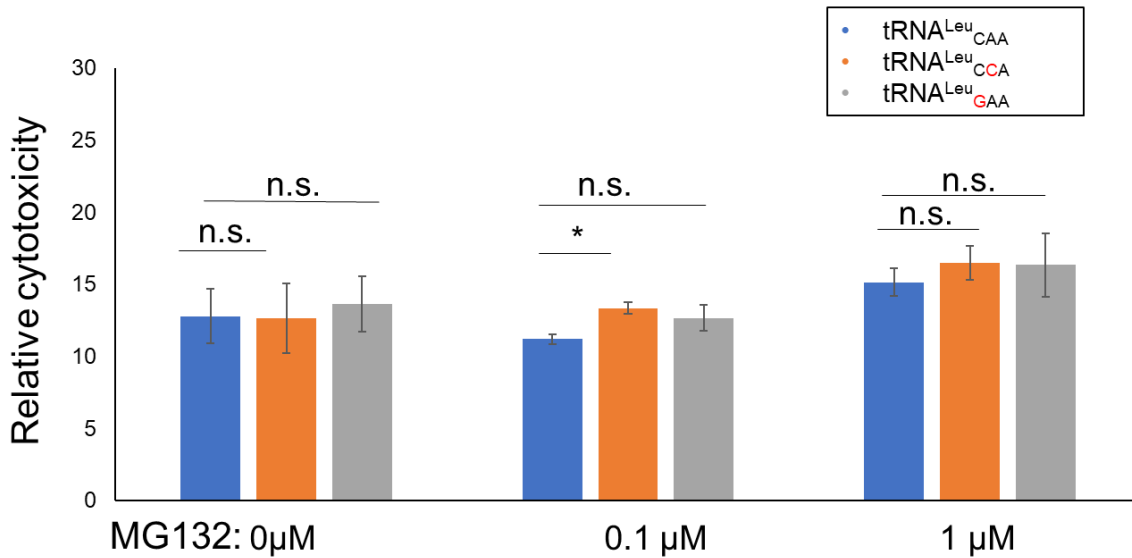


Figure 18: The comparison of relative cytotoxicity caused by wild type tRNA^{Leu}_{CAA}, tRNA^{Leu}_{CCA} (A35C) (tryptophan anticodon) and tRNA^{Leu}_{GAA} (C34G) (phenylalanine anticodon) towards N2_a cells under different MG132 concentrations. This is a bar plot comparing the relative cytotoxicity caused by tRNA^{Leu}_{CAA} (wild-type), tRNA^{Leu}_{CCA} (A35C) and tRNA^{Leu}_{GAA} (C34G) towards N2_a cells at three different MG132 concentrations (0, 0.1 and 1.0 μg/mL). Each cell line was grown with three biological replicates (n = 3). There was no significant difference in cytotoxicity caused by tRNA^{Leu}_{GAA} (C34G) and tRNA^{Leu}_{CAA} to N2_a cells under 0 (p= 0.78), 0.1 (p= 0.26), or 1.0 (p= 0.72) μg/mL MG132. There was also no significant difference between tRNA^{Leu}_{CCA} (A35C) and tRNA^{Leu}_{CAA} expressing N2_a cells at 1.0 (p= 0.72) and 0 (p= 0.94) μg/mL MG132. However, there was a significant difference between cytotoxicity caused by tRNA^{Leu}_{CCA} (A35C) and tRNA^{Leu}_{CAA} to N2_a cells at 0.1 μg/mL (p= 0.03) MG132. The statistical tests performed were Welch's t-test. (n.s. = no significant difference, * p < 0.05, ** p < 0.01, *** p < 0.001)

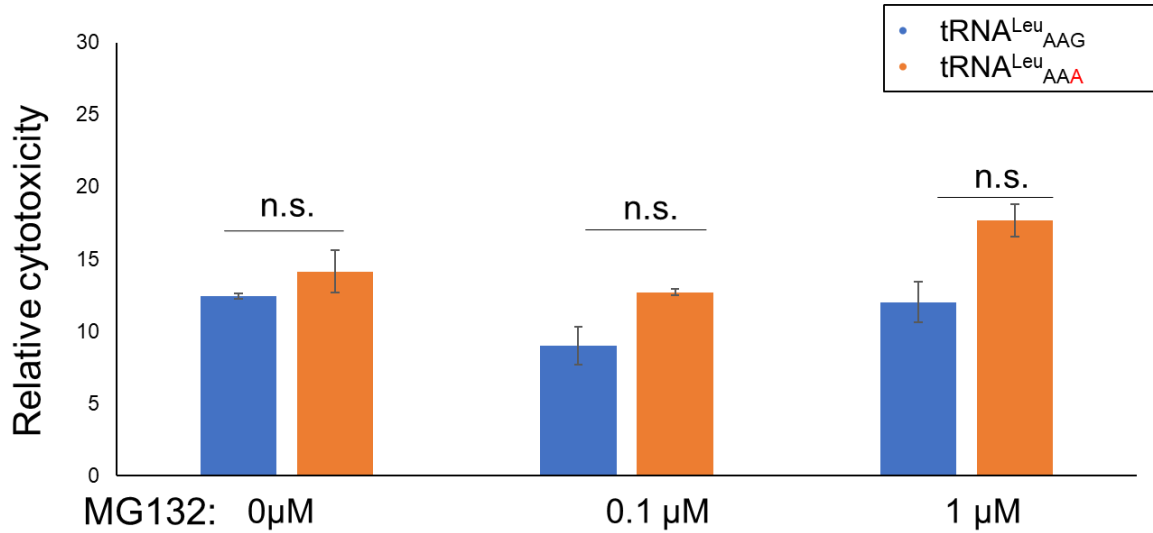


Figure 19: The comparison of relative cytotoxicity induced by tRNA^{Leu}_{AAG} and tRNA^{Leu}_{AAA(G36A)} (phenylalanine anticodon) in N2a cells under different MG132 concentrations. This is a bar plot comparing the relative cytotoxicity between tRNA^{Leu}_{AAG} and tRNA^{Leu}_{AAA} cell lines at three different MG132 concentrations (0, 0.1 and 1.0 μg/mL MG132). The difference in cytotoxicity at 0 (p = 0.47), 0.1 (p = 0.13) and 1.0 (p = 0.08) μg/mL was non-significant. The statistical tests performed using Welch's t-test. (n.s. = no significant difference, * p < 0.05, ** p < 0.01, *** p < 0.001)

Chapter 4 Discussion

4.0 Introduction

For protein synthesis to be achieved, the genetic instructions stored in DNA must be transcribed into mRNA by the appropriate RNA polymerase. This mRNA is then read by the ribosome which samples the cellular amino-acyl tRNA pool until a tRNA that fits with the current codon is in the A site of the ribosome. The ribosome does not read the amino acid attached to the tRNA, only the anticodon sequence.

LeuRS recognizes tRNA^{Leu} based primarily on the acceptor stem, the extended variable arm and G37, but not specifically the anticodon (5). This allows for a tRNA^{Leu} with an anticodon that is not leucine to base-pair with the current codon in the reading frame and transfer leucine to the growing polypeptide chain instead of the amino acid specified by the genetic code. This creates statistical proteins which may have an impact on the cell's internal environment. Statistical proteins are generated by the random mistranslation of one protein encoding gene to create several proteins with differences in their amino acid sequences (42). Mutations which create misfolded proteins may induce stress, while other mutations may cause a situational advantage (96). The purpose of this project was to observe the effect of mistranslation caused by tRNA^{Leu} variants in yeast and mammalian cells.

4.1 Safe expression of tRNA^{Leu} variants in yeast

The results of this study prove that the doxycycline-inducible tRNA expression system developed by Berg et al. (73), can be applied to the selective expression of tRNA^{Leu} variants in yeast. The initial trials involving tRNA^{Leu}_{UGG} (A35G and A36G) and the wild type tRNA^{Leu}_{UAA} show that under low concentrations of doxycycline (0 to 1.0 µg/mL), controlling the expression of the tRNA^{Leu} variants helps alleviate the growth defects caused by them, thereby allowing for the observation of how tRNA^{Leu}_{NNN} affects yeast cells.

In the 12 yeast strains which grew significantly ($p < 0.05$) slower than the wild-type strain at 1.0 µg/mL, the doubling time increased as the doxycycline concentration was raised from 0 to 0.01 µg/mL (half expression) and finally to 1.0 µg/mL (full expression). The doxycycline inducible

expression system was able to limit the expression of toxic tRNAs at 0 $\mu\text{g/mL}$. There was still a noticeable decrease in the growing rate of strains like the tRNA^{Leu}_{GCG} strain (34% increase in doubling time) in comparison to the wild-type stain even at 0 $\mu\text{g/mL}$. This can be attributed to a leakiness in the expression system, whereby some pol-III transcription is permitted even without doxycycline (73). However, when comparing the difference in the doubling time between cells expressing tRNA^{Leu}_{GCG} at 0 and 1.0 $\mu\text{g/mL}$ dox, the doxycycline inducible system still prevented a 75% decrease in growth rate. Therefore, the dox inducible system is working as expected and it could be used to gatekeep the expression of other tRNA anticodon variants at a level that is tolerated by yeast cells.

The G26A mutation that was added to all the tRNA^{Leu} variants also reduced the impact of the tRNAs on yeast cell viability. This occurs because G at position 26, is required to stabilize the tRNA structure. Without this mutation the tRNAs normally are degraded as part of the rapid tRNA decay pathway (43), (57). This helped reduce the negative growth phenotype of tRNA^{Leu} variants like tRNA^{Leu}_{UGG}, as before any concentration of doxycycline above 0 $\mu\text{g/mL}$ would arrest cell growth. This highlights the necessity of certain nucleotides as they can be modified allowing for the tRNA to function properly.

4.2 tRNA^{Leu} identity in yeast

For tRNA^{Leu} to be amino-acylated in yeast, the major identity elements as stated before are adenine at the discriminator base (A73), and guanosine at position 37. Soma et al. (50) have stated that adenine at position 35 is also an identity element in yeast, which causes a decrease in tRNA^{Leu} amino-acylation when removed. The decrease in catalytic efficiency is reported as two-fold when A35 is substituted with G. However, from the data collected it is likely that having adenine at position 35 is not necessary. The mass spectrometry data has shown that the Pro to Leu substitution is still present if the anticodon is changed from UAA to CGG or AGG. Furthermore, of the 12 yeast strains with a significant increase in doubling time compared to the wild-type strain, only two strains (Met CAU and Ile GAU) have adenine at position 35. This indicates that the detrimental effects of mistranslation occur without A at position 35 and it is likely that the tRNA^{Leu} variants are being amino-acylated by LeuRS without A35.

4.3 The link between GC content and mistranslation

After expressing tRNA^{Leu} variants in *S. cerevisiae* under three separate conditions (no expression, half expression and full expression), it was apparent that several tRNA^{Leu} plasmids in yeast negatively impacted cell growth and the rest grew at a rate close (within a ten-minute difference of doubling time) to the wild type (tRNA^{Leu}_{UAA}). The yeast cells transformed with the tRNA^{Leu} plasmids with the NGG (any proline anticodon) and the GCG (for arginine) anticodon have the slowest growing rate under any dox concentration. The yeast strains transformed with tRNA^{Leu} plasmids that gave the shortest doubling time had the anticodons AAA (Phe), GAC (Val), AUA (Tyr) and CTT (Lys). Except for valine (GAC) and lysine (CTT), the difference between the yeast strains with the highest and lowest doubling time is the GC content of the anticodon.

The GC content of the anticodon is important for its binding affinity to its corresponding codon (97). If higher GC content will increase the binding affinity, then maybe it could give the tRNA^{Leu} variant a greater affinity for its codon, thus making misincorporation of leucine at the codon more likely. However, when the GC content of the anticodon was plotted along side the doubling time of the yeast strains, there was no strong linear correlation observed. This indicates that there are other factors aside from GC content that contribute the effect of the tRNA^{Leu} variants on the growth rate of the yeast cells.

4.4 Certain amino acid replacements have major effects

After confirming that the GC content of the anticodon was not the main contributor to the effect of each tRNA^{Leu} variant on yeast cell growth, the next step was to explore if the type of amino acid substitution played a greater role. According to the genetic code, substituting one amino acid for another of similar structure is a conservative substitution that should not affect the function of the protein (98). Since structure influences the function of the protein, this lack of change should not affect the yeast cells (99). However, a substitution of one amino acid for another without a similar molecular structure is a non-conservative mutation. This mutation changes the structure of the protein, which could change the proteins' function (98). This change in function may contribute to the growth defect seen in the yeast cells.

The BLOSUM62 matrix was created by analyzing the conserved regions of protein families and scoring the likelihood of amino acids substitutions at this position (91). Of the ten yeast strains with the slowest growing rate, the BLOSUM62 index indicates that all except 1 amino acid substitution are unlikely to occur. However, the yeast strain with the highest doubling time (210.78 min^{-1} at 1.0 dox) Arg (GCG) has a score of -2 which is not even the most negative score (which is -4) (91). Furthermore, among the strains with lowest doubling time, there are several which also have negative scores with some as low as -4. The middle growing strains all seem to have an average score of -1 or -2 (Supp Table 3.). When the doubling time of the tRNA^{Leu} yeast strains was plotted against the BLOSUM62 matrix, there was no linear correlation. This could mean that multiple factors contribute to the affect of the amino acid substitution on the growth rate of yeast cells.

If the growth rate of the tRNA^{Leu} anticodon variants does not correlate with the BLOSUM62 matrix, could it be something to do with the amino acid associated with anticodon in question? tRNA^{Leu} variants with the anticodon (NGG) for proline have some of the lowest growth scores (doubling time is 1.25-2.05-fold higher than the wild-type). Prolines as an amino acid is crucial in turns in the protein secondary structure (100). This is thanks to proline creating a ϕ angle at about -65° (101). Thus, removing this structure defining amino acid may interrupt turns in the protein. This could prevent the interaction of key amino acids in the proteins structure, thereby destabilizing the protein. Furthermore, arginine contains a positively charged guanidium group that increases the polarity at one end of the molecule, while the rest is a hydrophobic amino acid chain. Thanks to these properties arginine is an important surface amino acid which stretches out and interacts with other polar molecules (102).

However, lysine is another amino acid with a similar charge to arginine and both tRNA^{Leu} variants with a lysine anticodon (UUU and CUU) share a growth rate close to the wild-type. All serine, threonine, and tyrosine anticodon tRNA^{Leu} variants recorded, caused a negligible change in growth rate as well, even though the variants could remove important phosphorylation sites (103). This even more so indicates that the effects of tRNA^{Leu} mistranslation by tRNA^{Leu} anticodon variants is multifactorial.

4.5 tRNA competition and codon context

The overall impact of tRNA^{Leu} variants is highly variable depending on the anticodon. It does not appear to follow a clear pattern based on amino acid substitution scores according to the BLOSUM 62 index, or the GC content of the anticodon. It could be that not all the variants are amino-acylated, or certain variants are outcompeted at the A site of the ribosome by other tRNAs. However Chu et al. (104) found that competition for the ribosome by mRNA is the primary factor that effects the rate of translation, but they also did find that competition for aminoacylation among tRNAs was a moderate factor. Chu et al. (104) found that tRNA competition was important among rare tRNAs (like tRNA^{Arg}_{UCU} and tRNA^{Arg}_{CCU}) that are critical for lowly-expressed mRNA.

Furthermore, some of the anticodons that the tRNA^{Leu} adopted had no tRNA equivalent in *S. cerevisiae*. There is no tRNA^{Arg} with a GCG anticodon in *S. cerevisiae* (13). This anticodon would potentially base-pair with the CGC and CGU codons. Neither CGC and CGU are common codons among highly expressed proteins found in *S. cerevisiae* (105). This could mean that these negative growth phenotypes are occurring in part due to mistranslation of less-expressed genes that are still critical for cell function. The anticodons Pro CGG and GGG also have no equivalent tRNAs in yeast and they are in the top ten slowest growing strains. The two corresponding codons are also less commonly found in the yeast genome (105).

However, the scatter plot which compared codon usage to the doubling time of each tRNA^{Leu} anticodon variant strain made it clear that there is no correlation between codon usage and the growth rate of a tRNA^{Leu} anticodon variant yeast strain. Furthermore, tRNAs with the anticodon GUC (Asp) are commonly found in yeast (16 tRNA^{Asp}_{GUC}) and the corresponding codon (GAC) is somewhat common in the yeast genome. The tRNA^{Leu}_{GUC} expressing strain is among the top ten slowest growing tRNA^{Leu} anticodon strains. The fast-growing AAA (Phe) codon also has no equivalent tRNA, but the matching UUU codon is highly expressed. Therefore, once again the effect which tRNA^{Leu} anticodon variants have on yeast cells is likely multifactorial.

It instead could be that the mistranslation caused by certain tRNA^{Leu} variants are targeting specific genes. The genes may have a high amount of the codons that base-pair with the tRNA^{Leu} variants that alter the growth rate of yeast cells. It maybe that some proteins in yeast have

arginine, or proline at critical structural points and mistranslation of leucine at these sites destabilizes the protein, causing a loss of function and potentially protein aggregation. This would be detrimental to cell as the function of a critical protein is lost and protein aggregation is unhealthy for the cell. This could explain the slow growth phenotype in certain tRNA^{Leu} variants.

4.6 Changes in protein synthesis and the toxic effect of human tRNA^{Leu} variants

The tRNA^{Leu} variants tRNA^{Leu}_{AAA} (phenylalanine anticodon), tRNA^{Leu}_{CCA} (tryptophan anticodon) and tRNA_{GAA} (phenylalanine codon) and the wild-type tRNAs (tRNA^{Leu}_{AAG} and tRNA^{Leu}_{CAA}) were all cloned into the WT-PAN vector. The WT-PAN vector allows the expression of mCherry and eGFP fusion protein when transfected in mammalian cells. The amount of fluorescence per cell in the wild-type and the tRNA^{Leu} variant strains is used to quantitate protein synthesis levels in each transfected cell. Lant et al. (65) observed that tRNA variants can alter the level of protein synthesis in N2_a cells. It could be that certain mistranslation events caused by the tRNA variants lower protein synthesis in the cells that express them. The tRNA^{Leu} variants and the wild-type tRNA^{Leu} were transfected into N2_a cells to compare the difference in protein synthesis between the two cell lines. The MG132 treatment of the wild-type and tRNA^{Leu} variant cell lines reduced proteasome activity as well as protein synthesis. This prevented the degradation of mCherry, eGFP and any mistranslated proteins. Lant et al. (65) found that tRNA^{Ser}_{AAA} was toxic to N2_a cells when treated with MG132. They theorized that the MG132 prevented the degradation of mistranslated proteins that became toxic to the cells.

The results of this study indicate that tRNA^{Leu}_{GAA} causes a reduction in protein synthesis. Under all MG132 concentrations, tRNA^{Leu}_{GAA} causes a large decrease in eGFP expression in comparison to tRNA^{Leu}_{CAA}. There is also a significant decrease in mCherry expression for tRNA^{Leu}_{GAA} cells under 0.1 ug/mL and 0 µg/mL MG132 concentrations. Thus, tRNA^{Leu}_{GAA} reduced protein synthesis in N2_a cells just like tRNA^{Ser}_{AAA}. tRNA^{Leu}_{GAA} has the same anticodon as the wild-type tRNA^{Phe} expressed in *Mus musculus*. Furthermore, GAA is the only anticodon for tRNA^{Phe} in *Mus musculus* (13). The two codons that GAA can base-pair with (UUU and UUG) are also highly used codons in the *Mus musculus* genome (106). This is all points to tRNA^{Leu}_{GAA} being expressed in N2_a cells and potentially allowing leucine misincorporation at

phenylalanine codons. However, tRNA^{Leu}_{GAA} did not cause any significant change in cytotoxicity compared to tRNA^{Leu}_{CAA} under any MG132 concentration. This indicates that tRNA^{Leu}_{GAA} is not toxic to N2_a cells.

tRNA^{Leu}_{AAA} is another tRNA^{Leu} variant with a phenylalanine codon. The results indicate that there was no significant change in eGFP, or mCherry fluorescence when tRNA^{Leu}_{AAA} was expressed in N2_a cells. However, there was a significant increase in eGFP fluorescence at 0.1 µg/mL of MG132. Furthermore, tRNA^{Leu}_{AAA} did not cause any significant change in cytotoxicity compared to tRNA^{Leu}_{CAA} at 0, 0.1, or 1.0 µg/mL MG132. In *S. cerevisiae* the yeast tRNA^{Leu}_{AAA} strain grew at a similar rate to the wild-type strain. This would point toward tRNA^{Leu}_{AAA} not being a toxic tRNA^{Leu} variant. This agrees with the lack of toxicity induced by tRNA^{Leu}_{GAA} which also potentially mistranslated leucine at phenylalanine codons. There is also no tRNA with an AAA anticodon expressed in *Mus musculus* (13). Schwartz and Curran (107), reported that there is frequent frameshifting at UUU, the only codon which the AAA anticodon can bind to. However, this does not seem to occur, as these frameshift mutations are usually detrimental to the host organism (4).

Lastly, there is tRNA^{Leu}_{CCA} which has a tryptophan anticodon. tRNA^{Leu}_{CCA} (A35C) causes a significant decrease in mCherry fluorescence in the initial fluorescence reading trials. There is also no significant difference in eGFP fluorescence between tRNA^{Leu}_{CCA} and tRNA^{Leu}_{CAA} in the initial fluorescence reading trials. In the MG132 trials performed 4 hours after the initial fluorescence reading there was a highly significant increase in eGFP fluorescence of tRNA^{Leu}_{CCA} compared to tRNA^{Leu}_{CAA} expressing N2_a cells under the 0 µg/mL MG132 condition. This increase in fluorescence is likely due to the cells expressing more eGFP in that 4-hour period, as no MG132 was present in these samples. There was also a significant increase in mCherry fluorescence at 0 µg/mL MG132. However, there was no significant change in m-Cherry or eGFP fluorescence in tRNA^{Leu}_{CAA} compared to tRNA^{Leu}_{CCA} expressing N2_a cells at any MG132 concentration higher than 0 µg/mL. Thus, there may be an increase in protein synthesis when tRNA^{Leu}_{CCA} is expressed, but only when no MG132 is present. tRNA^{Leu}_{CCA} is the only tRNA that has shown to cause a significant increase in protein synthesis in N2_a cells in comparison to the wild-type tRNA.

Furthermore, tRNA^{Leu}_{CCA} is the only cell lines that caused a significant increase in cytotoxicity in comparison to the wild-type tRNA^{Leu}_{CAA} (p=0.03) at 0.1 µg/mL MG132, but not at 0 or 1µg/mL MG132. However, in yeast cells tRNA^{Leu}_{CCA} does not cause a significant change in growth rate compared to the wild-type cells (tRNA^{Leu}_{UAA}). It could be that tRNA^{Leu}_{CCA} is not toxic under normal cell conditions, but under proteasome inhibition by MG132, the proteins with leucine mis-incorporated for tryptophan may be toxic to the cells. However, this is disputable since there is no change in cytotoxicity at 1.0 µg/mL.

In future studies mistranslation could be confirmed by performing LC MS/MS with both wild type and mutant human tRNA^{Leu} strains. Either the expressed eGFP or mCherry could be captured using an antibody column. This collected protein could then be purified by running it on an 0.8% SDS PAGE gel. The gels could then be cut and sent for LC-MS/MS sequencing. This would give an efficient way of comparing the amount of mistranslation in the mutant strains to the wild-type strains.

4.7 Conclusion

The results prove that tRNA^{Leu} anticodon variants can be safely expressed in yeast cells via the control of the doxycycline inducible system. After analyzing the effect of 38 different tRNA^{Leu} variants in yeast cells, I have concluded it is likely that multiple factors influence the effect of tRNA^{Leu} anticodon variants on *S. cerevisiae*. The BLOSUM 62 index, GC content of the anticodon or overall codon usage by each tRNA^{Leu} anticodon variant did not correlate well with the doubling time of each yeast strain. The nature of the amino acid being replaced is important as replacing the leucine anticodon with proline and arginine anticodons gave by far the largest decrease in growth rate. Lastly, LC-MS/MS data showed that A at position 35 is not necessary for tRNA^{Leu} aminoacylation.

Furthermore, the results from the mammalian cells showed that the effects of the tRNA^{Leu} variants vary greatly depending on the anticodon. tRNA^{Leu}_{AAG} (G36A) (phenylalanine anticodon) did not alter protein synthesis in N2_a cells, nor did it show significant toxicity towards N2_a cells compared to the wild-type tRNA^{Leu}_{CAA}. Furthermore, tRNA^{Leu}_{CAA}(C34G) (phenylalanine anticodon) appeared to alter protein synthesis at any MG132 concentration compared to tRNA^{Leu}_{CAA} N2_a cells and there was no toxic effect observed. Lastly, N2_a cells expressing

tRNA^{Leu}_{CCA} increased protein synthesis at 0 µg/mL MG132 and appeared to be toxic at 0.1 µg/mL MG132, but not under any other concentration of MG132.

In future studies LC-MS/MS should be used on more yeast strains expressing different tRNA^{Leu} variants to confirm mistranslation at different codons. Furthermore, the tRNA^{Leu} variant N2_a cell lines should also be analyzed by mass spec to observe mistranslation at phenylalanine and tryptophan codons in eGFP. It would also be helpful to look at the whole proteome of both organisms and observe which proteins are being mistranslated when certain tRNA^{Leu} variants and which codons this occurs at. Many tRNA^{Leu} variants negatively affect the viability of yeast and mammalian cells, while others are neutral. This is likely due to a combination of the codon context, other tRNAs expressed in the host organism and the nature of the amino acid being replaced. It may be possible that some of these tRNA^{Leu} variant adversely affect human health. The neutral tRNA variants could possibly change the amino acid context of certain codons by allowing ambiguous translation of leucine and another amino acid (only in certain organisms). Lastly, the LC-MS/MS with the tRNA^{Leu}_{CGG} and tRNA^{Leu}_{AGG} strains proved that leucine could be incorporated at proline codons to create statistical proteins.

Works Cited

1. Moghal, A., Mohler, K., and Ibba, M. (2014) Mistranslation of the genetic code. *FEBS Letters* **588**, 4305-4310
2. Ribas de Pouplana, L., Santos, M. A., Zhu, J. H., Farabaugh, P. J., and Javid, B. (2014) Protein mistranslation: friend or foe? *Trends Biochem Sci* **39**, 355-362
3. Berg, M. D., Hoffman, K. S., Genereaux, J., Mian, S., Trussler, R. S., Haniford, D. B., O'Donoghue, P., and Brandl, C. J. (2017) Evolving Mistranslating tRNAs Through a Phenotypically Ambivalent Intermediate in *Saccharomyces cerevisiae*. *Genetics* **206**, 1865-1879
4. Paredes, J. A., Carreto, L., Simões, J., Bezerra, A. R., Gomes, A. C., Santamaria, R., Kapushesky, M., Moura, G. R., and Santos, M. A. S. (2012) Low level genome mistranslations deregulate the transcriptome and translome and generate proteotoxic stress in yeast. *BMC Biology* **10**, 55
5. Giege, R., Sissler, M., and Florentz, C. (1998) Universal rules and idiosyncratic features in tRNA identity. *Nucleic Acids Res* **26**, 5017-5035
6. Tocchini-Valentini, G., Saks, M. E., and Abelson, J. (2000) tRNA leucine identity and recognition sets 1 Edited by D. E. Draper. *Journal of Molecular Biology* **298**, 779-793
7. Woese, C. R. (1965) On the evolution of the genetic code. *Proceedings of the National Academy of Sciences* **54**, 1546-1552
8. Schwartz, M. H., and Pan, T. (2017) Function and origin of mistranslation in distinct cellular contexts. *Critical Reviews in Biochemistry and Molecular Biology* **52**, 205-219
9. Finsterer, J. (2007) Genetic, pathogenetic, and phenotypic implications of the mitochondrial A3243G tRNA^{Leu}(UUR) mutation. *Acta Neurologica Scandinavica* **116**, 1-14
10. Schwartz, M. H., and Pan, T. (2017) tRNA Misacylation with Methionine in the Mouse Gut Microbiome in Situ. *Microbial Ecology* **74**, 10-14
11. Leuker, C. E., and Ernst, J. F. (1994) Toxicity of a heterologous leucyl-tRNA (anticodon CAG) in the pathogen *Candida albicans*: in vivo evidence for non-standard decoding of CUG codons. *Molecular and General Genetics MGG* **245**, 212-217

12. Cherry, J. M., Hong, E. L., Amundsen, C., Balakrishnan, R., Binkley, G., Chan, E. T., Christie, K. R., Costanzo, M. C., Dwight, S. S., Engel, S. R., Fisk, D. G., Hirschman, J. E., Hitz, B. C., Karra, K., Krieger, C. J., Miyasato, S. R., Nash, R. S., Park, J., Skrzypek, M. S., Simison, M., Weng, S., and Wong, E. D. (2012) Saccharomyces Genome Database: the genomics resource of budding yeast. *Nucleic Acids Research* **40**, D700-D705
13. Chan, P. P., and Lowe, T. M. (2016) GtRNADB 2.0: an expanded database of transfer RNA genes identified in complete and draft genomes. *Nucleic Acids Research* **44**, D184-D189
14. Moore, M. J., and Proudfoot, N. J. (2009) Pre-mRNA Processing Reaches Back to Transcription and Ahead to Translation. *Cell* **136**, 688-700
15. Ghosh, A., and Lima, C. D. (2010) Enzymology of RNA cap synthesis. *WIREs RNA* **1**, 152-172
16. Takahashi, N., Nagai, S., Fujita, A., Ido, Y., Kato, K., Saito, A., Moriya, Y., Tomimatsu, Y., Kaneta, N., Tsujimoto, Y., and Tamura, H. (2020) Discrimination of psychrotolerant Bacillus cereus group based on MALDI-TOF MS analysis of ribosomal subunit proteins. *Food Microbiology* **91**, 103542
17. Hoagland, M. B., Stephenson, M. L., Scott, J. F., Hecht, L. I., and Zamecnik, P. C. (1958) A SOLUBLE RIBONUCLEIC ACID INTERMEDIATE IN PROTEIN SYNTHESIS. *Journal of Biological Chemistry* **231**, 241-257
18. Ben-Shem, A., Garreau de Loubresse, N., Melnikov, S., Jenner, L., Yusupova, G., and Yusupov, M. (2011) The Structure of the Eukaryotic Ribosome at 3.0 Å Resolution. *Science* **334**, 1524-1529
19. Jackson, R. J., Hellen, C. U. T., and Pestova, T. V. (2010) The mechanism of eukaryotic translation initiation and principles of its regulation. *Nature Reviews Molecular Cell Biology* **11**, 113-127
20. Oakes, M., Henderson, E., Scheinman, A., Clark, M., and Lake, J. A. (1986) Ribosome Structure, Function, and Evolution: Mapping Ribosomal RNA, Proteins, and Functional Sites in Three Dimensions. in *Structure, Function, and Genetics of Ribosomes* (Hardesty, B., and Kramer, G. eds.), Springer New York, New York, NY. pp 47-67

21. Petry, S., Weixlbaumer, A., and Ramakrishnan, V. (2008) The termination of translation. *Current Opinion in Structural Biology* **18**, 70-77
22. Watson, J. D., and Crick, F. H. C. (1953) Genetical Implications of the Structure of Deoxyribonucleic Acid. *Nature* **171**, 964-967
23. Crick, F. H. C. (1966) Codon—anticodon pairing: The wobble hypothesis. *Journal of Molecular Biology* **19**, 548-555
24. Breitschopf, K., Achsel, T., Busch, K., and Gross, H. J. (1995) Identity elements of human tRNA^{Leu}: structural requirements for converting human tRNA^{Ser} into a leucine acceptor in vitro. *Nucleic Acids Research* **23**, 3633-3637
25. Brown, A., Shao, S., Murray, J., Hegde, R. S., and Ramakrishnan, V. (2015) Structural basis for stop codon recognition in eukaryotes. *Nature* **524**, 493-496
26. Giegé, R., and Frugier, M. (2000) Transfer RNA Structure and Identity.
27. Lorenz, C., Lünse, C. E., and Mörl, M. (2017) tRNA Modifications: Impact on Structure and Thermal Adaptation. *Biomolecules* **7**
28. Xiong, Y., and Steitz, T. A. (2006) A story with a good ending: tRNA 3'-end maturation by CCA-adding enzymes. *Current Opinion in Structural Biology* **16**, 12-17
29. Sharp, S. J., Schaack, J., Cooley, L., Burke, D. J., and Soil, D. (1985) Structure and Transcription of Eukaryotic tRNA Gene. *Critical Reviews in Biochemistry* **19**, 107-144
30. Nissen, P., Kjeldgaard, M., Thirup, S., Polekhina, G., Reshetnikova, L., Clark, B. F. C., and Nyborg, J. (1995) Crystal Structure of the Ternary Complex of Phe-tRNA^{Phe}, EF-Tu, and a GTP Analog. *Science* **270**, 1464-1472
31. Shi, H., and Moore, P. (2000) The crystal structure of yeast phenylalanine tRNA at 1.93 Å resolution: A classic structure revisited. *RNA (New York, N.Y.)* **6**, 1091-1105
32. Berg, M. D., and Brandl, C. J. (2021) Transfer RNAs: diversity in form and function. *RNA Biology* **18**, 316-339
33. Hingerty, B., Brown, R. S., and Jack, A. (1978) Further refinement of the structure of yeast tRNA^{Phe}. *Journal of Molecular Biology* **124**, 523-534
34. Boccaletto, P., Machnicka, M. A., Purta, E., Piątkowski, P., Bagiński, B., Wirecki, T. K., de Crécy-Lagard, V., Ross, R., Limbach, P. A., Kotter, A., Helm, M., and Bujnicki, J. M. (2018) MODOMICS: a database of RNA modification pathways. 2017 update. *Nucleic Acids Research* **46**, D303-D307

35. Kato, N., Hoshino, H., and Harada, F. (1983) Minor serine tRNA containing anticodon NCA (C4 RNA) from human and mouse cells. *Biochem Int* **7**, 635-645
36. Chou, H.-J., Donnard, E., Gustafsson, H., Garber, M., and Rando, O. (2017) Transcriptome-wide Analysis of Roles for tRNA Modifications in Translational Regulation. *Molecular Cell* **68**
37. Klassen, R., Bruch, A., and Schaffrath, R. (2016) Independent suppression of ribosomal +1 frameshifts by different tRNA anticodon loop modifications. *RNA Biol*, 1-8
38. Johansson, M. J. O., Esberg, A., Huang, B., Björk, G. R., and Byström, A. S. (2008) Eukaryotic wobble uridine modifications promote a functionally redundant decoding system. *Molecular and Cellular Biology* **28**, 3301-3312
39. Phizicky, E., and Hopper, A. (2010) tRNA biology charges to the front. *Genes & development* **24**, 1832-1860
40. Suzuki, T. (2021) The expanding world of tRNA modifications and their disease relevance. *Nature Reviews Molecular Cell Biology* **22**, 375-392
41. Schaefer, M., Pollex, T., Hanna, K., Tuorto, F., Meusburger, M., Helm, M., and Lyko, F. (2010) RNA methylation by Dnmt2 protects transfer RNAs against stress-induced cleavage. *Genes & development* **24**, 1590-1595
42. Berg, M. D., Zhu, Y., Genereaux, J., Ruiz, B. Y., Rodriguez-Mias, R. A., Allan, T., Bahcheli, A., Villén, J., and Brandl, C. J. (2019) Modulating Mistranslation Potential of tRNA^{Ser} in *Saccharomyces cerevisiae*. *Genetics* **213**, 849-863
43. Dewe, J. M., Whipple, J. M., Chernyakov, I., Jaramillo, L. N., and Phizicky, E. M. (2012) The yeast rapid tRNA decay pathway competes with elongation factor 1A for substrate tRNAs and acts on tRNAs lacking one or more of several modifications. *Rna* **18**, 1886-1896
44. Cusack, S. (1997) Aminoacyl-tRNA synthetases. *Current Opinion in Structural Biology* **7**, 881-889
45. Trobro, S., and Åqvist, J. (2005) Mechanism of peptide bond synthesis on the ribosome. *Proceedings of the National Academy of Sciences of the United States of America* **102**, 12395-12400

46. Alexander, R. W., and Hendrickson, T. L. (2020) Chapter Three - Putting amino acids onto tRNAs: The aminoacyl-tRNA synthetases as catalysts. in *The Enzymes* (Ribas de Pouplana, L., and Kaguni, L. S. eds.), Academic Press. pp 39-68
47. Perona, J. J., and Gruic-Sovulj, I. (2014) Synthetic and Editing Mechanisms of Aminoacyl-tRNA Synthetases. in *Aminoacyl-tRNA Synthetases in Biology and Medicine* (Kim, S. ed.), Springer Netherlands, Dordrecht. pp 1-41
48. O'Donoghue, P., and Luthey Schulten, Z. (2004) On the Evolution of Structure in Aminoacyl-tRNA Synthetases. *Microbiology and molecular biology reviews : MMBR* **67**, 550-573
49. Carter, C. W., Jr. (2017) Coding of Class I and II Aminoacyl-tRNA Synthetases. *Adv Exp Med Biol* **966**, 103-148
50. Soma, A., Kumagai, R., Nishikawa, K., and Himeno, H. (1996) The Anticodon Loop is a Major Identity Determinant of *Saccharomyces cerevisiae* tRNA^{Leu}. *Journal of Molecular Biology* **263**, 707-714
51. Joazeiro, C. A. P. (2017) Ribosomal Stalling During Translation: Providing Substrates for Ribosome-Associated Protein Quality Control. *Annual Review of Cell and Developmental Biology* **33**, 343-368
52. Ishimura, R., Nagy, G., Dotu, I., Zhou, H., Yang, X.-L., Schimmel, P., Senju, S., Nishimura, Y., Chuang, J. H., and Ackerman, S. L. (2014) Ribosome stalling induced by mutation of a CNS-specific tRNA causes neurodegeneration. *Science* **345**, 455-459
53. Masuda, I., Hwang, J.-Y., Christian, T., Maharjan, S., Mohammad, F., Gamper, H., Buskirk, A. R., and Hou, Y.-M. (2021) Loss of N1-methylation of G37 in tRNA induces ribosome stalling and reprograms gene expression. *eLife* **10**, e70619
54. Chen, C.-W., and Tanaka, M. (2018) Genome-wide Translation Profiling by Ribosome-Bound tRNA Capture. *Cell reports* **23**, 608-621
55. Lee, J. Y., Kim, D. G., Kim, B.-G., Yang, W. S., Hong, J., Kang, T., Oh, Y. S., Kim, K. R., Han, B. W., Hwang, B. J., Kang, B. S., Kang, M.-S., Kim, M.-H., Kwon, N. H., and Kim, S. (2014) Promiscuous methionyl-tRNA synthetase mediates adaptive mistranslation to protect cells against oxidative stress. *Journal of Cell Science* **127**, 4234-4245

56. Ruan, B., Palioura, S., Sabina, J., Marvin-Guy, L., Kochhar, S., LaRossa, R. A., and Söll, D. (2008) Quality control despite mistranslation caused by an ambiguous genetic code. *Proceedings of the National Academy of Sciences* **105**, 16502-16507
57. Hoffman, K. S., Berg, M. D., Shilton, B. H., Brandl, C. J., and O'Donoghue, P. (2017) Genetic selection for mistranslation rescues a defective co-chaperone in yeast. *Nucleic Acids Research* **45**, 3407-3421
58. Lant, J. T., Berg, M. D., Sze, D. H. W., Hoffman, K. S., Akinpelu, I. C., Turk, M. A., Heinemann, I. U., Duennwald, M. L., Brandl, C. J., and O'Donoghue, P. (2018) Visualizing tRNA-dependent mistranslation in human cells. *RNA Biology* **15**, 567-575
59. Wals, K., and Ovaas, H. (2014) Unnatural amino acid incorporation in E. coli: current and future applications in the design of therapeutic proteins. *Front Chem* **2**
60. Santos, M. A. S., and Tuite, M. F. (1995) The CUG codon is decoded in vivo as serine and not leucine in *Candida albicans*. *Nucleic Acids Research* **23**, 1481-1486
61. Miranda, I., Silva-Dias, A., Rocha, R., Teixeira-Santos, R., Coelho, C., Gonçalves, T., Santos, M. A. S., Pina-Vaz, C., Solis, N. V., Filler, S. G., Rodrigues, A. G., and Berman, J. (2013) *Candida albicans* CUG Mistranslation Is a Mechanism To Create Cell Surface Variation. *mBio* **4**, e00285-00213
62. Goto, Y., and Suga, H. (2009) Translation Initiation with Initiator tRNA Charged with Exotic Peptides. *Journal of the American Chemical Society* **131**, 5040-5041
63. Santos, M., Pereira, P. M., Varanda, A. S., Carvalho, J., Azevedo, M., Mateus, D. D., Mendes, N., Oliveira, P., Trindade, F., Pinto, M. T., Bordeira-Carriço, R., Carneiro, F., Vitorino, R., Oliveira, C., and Santos, M. A. S. (2018) Codon misreading tRNAs promote tumor growth in mice. *RNA Biology* **15**, 773-786
64. Yasukawa, T., Suzuki, T., Suzuki, T., Ueda, T., Ohta, S., and Watanabe, K. (2000) Modification Defect at Anticodon Wobble Nucleotide of Mitochondrial tRNAs^{Leu(UUR)} with Pathogenic Mutations of Mitochondrial Myopathy, Encephalopathy, Lactic Acidosis, and Stroke-like Episodes*. *Journal of Biological Chemistry* **275**, 4251-4257
65. Lant, J. T., Kiri, R., Duennwald, M. L., and O'Donoghue, P. (2021) Formation and persistence of polyglutamine aggregates in mistranslating cells. *Nucleic Acids Research* **49**, 11883-11899

66. Parisien, M., Wang, X., and Pan, T. (2013) Diversity of human tRNA genes from the 1000-genomes project. *RNA Biology* **10**, 1853-1867
67. Berg, M. D., Giguere, D. J., Dron, J. S., Lant, J. T., Genereaux, J., Liao, C., Wang, J., Robinson, J. F., Gloor, G. B., Hegele, R. A., O'Donoghue, P., and Brandl, C. J. (2019) Targeted sequencing reveals expanded genetic diversity of human transfer RNAs. *RNA Biology* **16**, 1574-1585
68. Schultz, D. W., and Yarus, M. (1994) Transfer RNA Mutation and the Malleability of the Genetic Code. *Journal of Molecular Biology* **235**, 1377-1380
69. Mühlhausen, S., Findeisen, P., Plessmann, U., Urlaub, H., and Kollmar, M. (2016) A novel nuclear genetic code alteration in yeasts and the evolution of codon reassignment in eukaryotes. *Genome Research* **26**, gr.200931.200115
70. Massey, S. E., Moura G Fau - Beltrão, P., Beltrão P Fau - Almeida, R., Almeida R Fau - Garey, J. R., Garey Jr Fau - Tuite, M. F., Tuite Mf Fau - Santos, M. A. S., and Santos, M. A. (2003) Comparative evolutionary genomics unveils the molecular mechanism of reassignment of the CTG codon in *Candida* spp. *Genome Res* **4**, 544-557
71. Suzuki, T., Ueda, T., and Watanabe, K. (1997) The 'polysemous' codon - A codon with multiple amino acid assignment caused by dual specificity of tRNA identity. *The EMBO journal* **16**, 1122-1134
72. Berg, M. D., Genereaux, J., Zhu, Y., Mian, S., Gloor, G. B., and Brandl, C. J. (2018) Acceptor Stem Differences Contribute to Species-Specific Use of Yeast and Human tRNAs^{er}. *Genes* **9**
73. Berg, M. D., Isaacson, J. R., Cozma, E., Genereaux, J., Lajoie, P., Villén, J., and Brandl, C. J. (2021) Regulating Expression of Mistranslating tRNAs by Readthrough RNA Polymerase II Transcription. *ACS Synthetic Biology* **10**, 3177-3189
74. Hughes, T. R., Marton, M. J., Jones, A. R., Roberts, C. J., Stoughton, R., Armour, C. D., Bennett, H. A., Coffey, E., Dai, H., He, Y. D., Kidd, M. J., King, A. M., Meyer, M. R., Slade, D., Lum, P. Y., Stepaniants, S. B., Shoemaker, D. D., Gachotte, D., Chakraborty, K., Simon, J., Bard, M., and Friend, S. H. (2000) Functional Discovery via a Compendium of Expression Profiles. *Cell* **102**, 109-126
75. Sprouffske, K., and Wagner, A. (2016) Growthcurver: an R package for obtaining interpretable metrics from microbial growth curves. *BMC Bioinformatics* **17**, 172

76. Rizzardi, L. F., Dorn, E. S., Strahl, B. D., and Cook, J. G. (2012) DNA Replication Origin Function Is Promoted by H3K4 Di-methylation in *Saccharomyces cerevisiae*. *Genetics* **192**, 371-384
77. Andreadis, A., Hsu, Y. P., Hermodson, M., Kohlhaw, G., and Schimmel, P. (1984) Yeast LEU2. Repression of mRNA levels by leucine and primary structure of the gene product. *Journal of Biological Chemistry* **259**, 8059-8062
78. Spaller, T., Groth, M., Glöckner, G., and Winckler, T. (2017) TRE5-A retrotransposition profiling reveals putative RNA polymerase III transcription complex binding sites on the *Dictyostelium* extrachromosomal rDNA element. *PLOS ONE* **12**, e0175729
79. Kory, N., uit de Bos, J., van der Rijt, S., Jankovic, N., Güra, M., Arp, N., Pena, I. A., Prakash, G., Chan, S. H., Kunchok, T., Lewis, C. A., and Sabatini, D. M. (2020) MCART1/SLC25A51 is required for mitochondrial NAD transport. *Science Advances* **6**, eabe5310
80. Sambrook J Fau - Russell, D. W., and Russell, D. W. (2006) Preparation of Plasmid DNA by Alkaline Lysis with SDS: Miniprep. LID - [pdb.prot4084 \[pii\]](https://pubmed.ncbi.nlm.nih.gov/16759661/) LID - [10.1101/pdb.prot4084 \[doi\]](https://doi.org/10.1101/pdb.prot4084) FAU - Sambrook, Joseph.
81. Berg, M. D., Isaacson, J. R., Cozma, E., Genereaux, J., Lajoie, P., Villen, J., and Brandl, C. J. (2021) Regulating Expression of Mistranslating tRNAs by Readthrough RNA Polymerase II Transcription. *ACS Synth Biol* **10**, 3177-3189
82. Nowakowski, A., Wobig, W., and Petering, D. (2014) Native SDS-PAGE: High Resolution Electrophoretic Separation of Proteins With Retention of Native Properties Including Bound Metal Ions. *Metallomics : integrated biometal science* **6**
83. Laemmli, U. K. (1970) Cleavage of Structural Proteins during the Assembly of the Head of Bacteriophage T4. *Nature* **227**, 680-685
84. Mellacheruvu, D., Wright, Z., Couzens, A. L., Lambert, J.-P., St-Denis, N. A., Li, T., Miteva, Y. V., Hauri, S., Sardi, M. E., Low, T. Y., Halim, V. A., Bagshaw, R. D., Hubner, N. C., al-Hakim, A., Bouchard, A., Faubert, D., Fermin, D., Dunham, W. H., Goudreault, M., Lin, Z.-Y., Badillo, B. G., Pawson, T., Durocher, D., Coulombe, B., Aebersold, R., Superti-Furga, G., Colinge, J., Heck, A. J. R., Choi, H., Gstaiger, M., Mohammed, S., Cristea, I. M., Bennett, K. L., Washburn, M. P., Raught, B., Ewing, R.

- M., Gingras, A.-C., and Nesvizhskii, A. I. (2013) The CRAPome: a contaminant repository for affinity purification–mass spectrometry data. *Nature Methods* **10**, 730-736
85. Gomes, A. C., Kordala, A. J., Strack, R., Wang, X., Geslain, R., Delaney, K., Clark, W. C., Keenan, R., and Pan, T. (2016) A dual fluorescent reporter for the investigation of methionine mistranslation in live cells. *Rna* **22**, 467-476
86. Schneider, C. A., Rasband, W. S., and Eliceiri, K. W. (2012) NIH Image to ImageJ: 25 years of image analysis. *Nature Methods* **9**, 671-675
87. Rueden, C. T., Schindelin, J., Hiner, M. C., DeZonia, B. E., Walter, A. E., Arena, E. T., and Eliceiri, K. W. (2017) ImageJ2: ImageJ for the next generation of scientific image data. *BMC Bioinformatics* **18**, 529
88. Han, Y. H., Moon, H. J., You, B. R., and Park, W. H. (2009) The effect of MG132, a proteasome inhibitor on HeLa cells in relation to cell growth, reactive oxygen species and GSH. *Oncol Rep* **22**, 215-221
89. Zimmerman, D. W., and Zumbo, B. D. (1993) Rank transformations and the power of the Student t test and Welch t' test for non-normal populations with unequal variances. *Canadian Journal of Experimental Psychology / Revue canadienne de psychologie expérimentale* **47**, 523-539
90. Gospodinov, A., and Kunnev, D. (2020) Universal Codons with Enrichment from GC to AU Nucleotide Composition Reveal a Chronological Assignment from Early to Late Along with LUCA Formation. *Life (Basel)*. 10.3390/life10060081
91. Henikoff, S., and Henikoff, J. G. (1992) Amino acid substitution matrices from protein blocks. *Proceedings of the National Academy of Sciences* **89**, 10915-10919
92. Nangle, L. A., Motta, C. M., and Schimmel, P. (2006) Global Effects of Mistranslation from an Editing Defect in Mammalian Cells. *Chemistry & Biology* **13**, 1091-1100
93. Sherry, S. T., Ward, M., and Sirotkin, K. (1999) dbSNP-database for single nucleotide polymorphisms and other classes of minor genetic variation. *Genome Res* **9**, 677-679
94. Lant, J. T., Berg, M. D., Heinemann, I. U., Brandl, C. J., and O'Donoghue, P. (2019) Pathways to disease from natural variations in human cytoplasmic tRNAs. *J Biol Chem* **294**, 5294-5308
95. Berg, M. D., Zhu, Y., Ruiz, B. Y., Loll-Kripplbeber, R., Isaacson, J., San Luis, B.-J., Genereaux, J., Boone, C., Villén, J., Brown, G. W., and Brandl, C. J. (2021) The amino

- acid substitution affects cellular response to mistranslation. *G3 Genes/Genomes/Genetics* **11**
96. Mohler, K., and Ibba, M. (2017) Translational fidelity and mistranslation in the cellular response to stress. *Nature Microbiology* **2**, 17117
 97. Xia, T., SantaLucia, J., Jr., Burkard, M. E., Kierzek, R., Schroeder, S. J., Jiao, X., Cox, C., and Turner, D. H. (1998) Thermodynamic Parameters for an Expanded Nearest-Neighbor Model for Formation of RNA Duplexes with Watson–Crick Base Pairs. *Biochemistry* **37**, 14719-14735
 98. Bueno, M., Campos, L. A., Estrada, J., and Sancho, J. (2006) Energetics of aliphatic deletions in protein cores. *Protein Science* **15**, 1858-1872
 99. Orengo, C. A., Todd, A. E., and Thornton, J. M. (1999) From protein structure to function. *Current Opinion in Structural Biology* **9**, 374-382
 100. Morgan, A. A., and Rubenstein, E. (2013) Proline: The Distribution, Frequency, Positioning, and Common Functional Roles of Proline and Polyproline Sequences in the Human Proteome. *PLOS ONE* **8**, e53785
 101. Morris, A. L., MacArthur, M. W., Hutchinson, E. G., and Thornton, J. M. (1992) Stereochemical quality of protein structure coordinates. *Proteins: Structure, Function, and Bioinformatics* **12**, 345-364
 102. Ngola, S. M., Kearney, P. C., Mecozzi, S., Russell, K., and Dougherty, D. A. (1999) A Selective Receptor for Arginine Derivatives in Aqueous Media. Energetic Consequences of Salt Bridges That Are Highly Exposed to Water. *Journal of the American Chemical Society* **121**, 1192-1201
 103. Urbanska, A. S., Janusz-Kaminska, A., Switon, K., Hawthorne, A. L., Perycz, M., Urbanska, M., Bassell, G. J., and Jaworski, J. (2017) ZBP1 phosphorylation at serine 181 regulates its dendritic transport and the development of dendritic trees of hippocampal neurons. *Scientific Reports* **7**, 1876
 104. Chu, D., Barnes, D. J., and von der Haar, T. (2011) The role of tRNA and ribosome competition in coupling the expression of different mRNAs in *Saccharomyces cerevisiae*. *Nucleic Acids Research* **39**, 6705-6714
 105. Kliman, R. M., Irving, N., and Santiago, M. (2003) Selection Conflicts, Gene Expression, and Codon Usage Trends in Yeast. *Journal of Molecular Evolution* **57**, 98-109

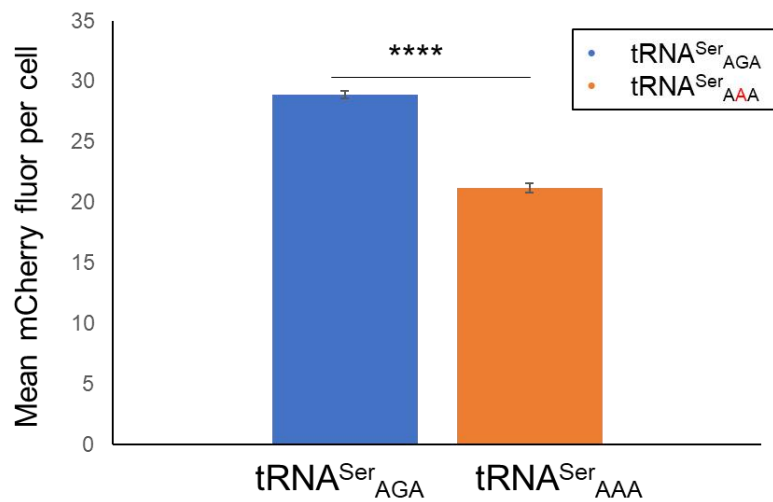
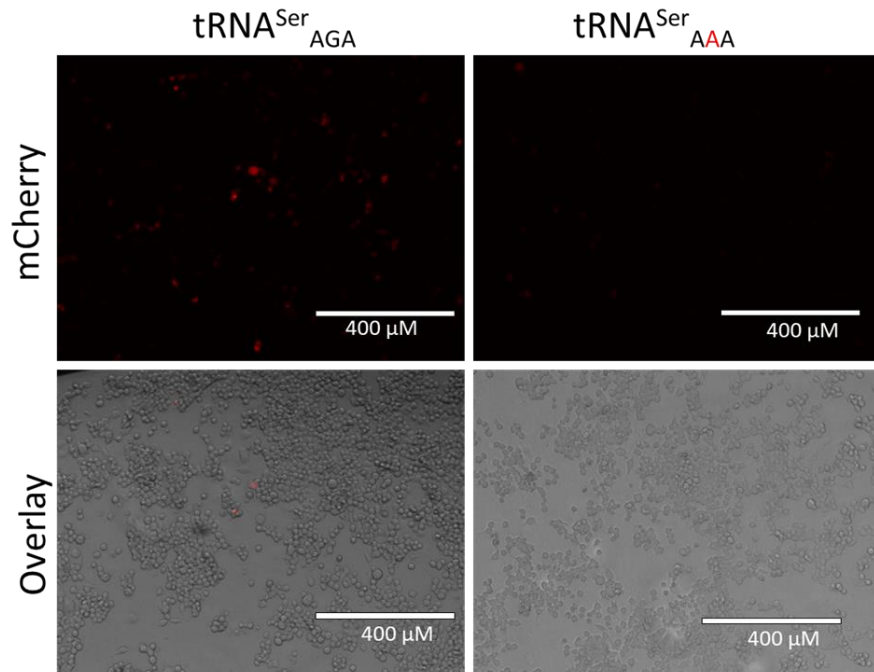
106. Shirasawa, K., Isobe, S., Tabata, S., and Hirakawa, H. (2014) Kazusa Marker DataBase: a database for genomics, genetics, and molecular breeding in plants. *Breeding science* **64**, 264-271
107. Schwartz, R., and Curran, J. F. (1997) Analyses of frameshifting at UUU-pyrimidine sites. *Nucleic Acids Research* **25**, 2005-2011

Appendices

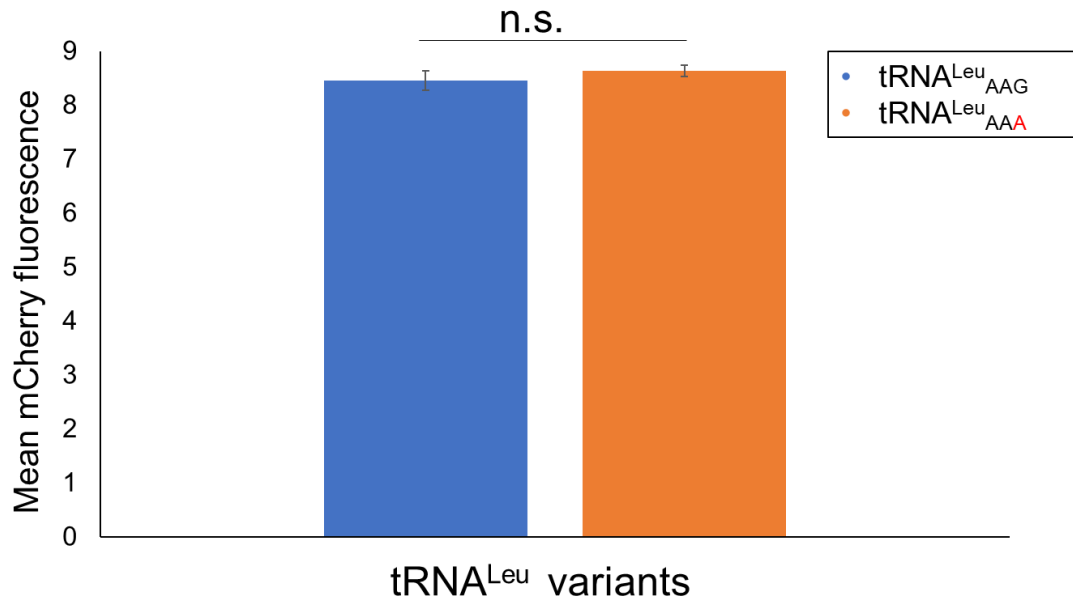
Supplemental figures:

5'TGTTGGAATTCAGTGGCTCCACGACCAATACCTGGTACGTAACCTGCAGGTGGTTC
TTGATCCAAAAAAGATGGCCTCTCCATAAAATGTGACGTTTTCTTGCTGTAAACTCTT
TATGTCAACTCACCCGTATATTTTCTGAAATTTTTCGTTTTTTTTTGCTTAATAGAACAA
TCTGACACACTATAAATGTACTGGTTAAATTAGCCCAAGGTTCTATCAACGGTAAAGAA
GACTTTTAAAAATACTTTCGTTACATTATTTATTAAGAAGAAACGCCATCATTTCATA
AAGGTCTCCGGAGGAGCTACTAAAGAAAGAGTGCTGCAATTAATAACAATTAATATAAG
TGTGGTTATTGAAAATAACTATTCATTTATACGGAGGGTTGGCCGAGTGGTCTAAGGCA
GCAGACTNNNGATCTGTTGGACGGTTGTCCGCGGAGTTCGAACCTCGCATCCTTCAG
TAATATTTTTTAATATACATTTTCTCTGCCATCATGGCTTAAAAAATGCTTAAAAGAAG
GGAATTAGGGGGGATGGATGAACTAAGACATAACTTTCTTTTCTTCAATTCGAACTCTG
TTGGGAAGAGTTGCTTTAAAAAAGACTCTCTATCCATCTATAAAATTTATTAAACTTTT
GAACTGCACAGAATGATTGGCTCACTTAGAAACAAATTTGAGCATTTCAAAGTTTCTGA
AAAGGGAGGTCAAAATTTATCTACAACACTACCGAAACTACCCCTGCGGCCGCCCTT 3'

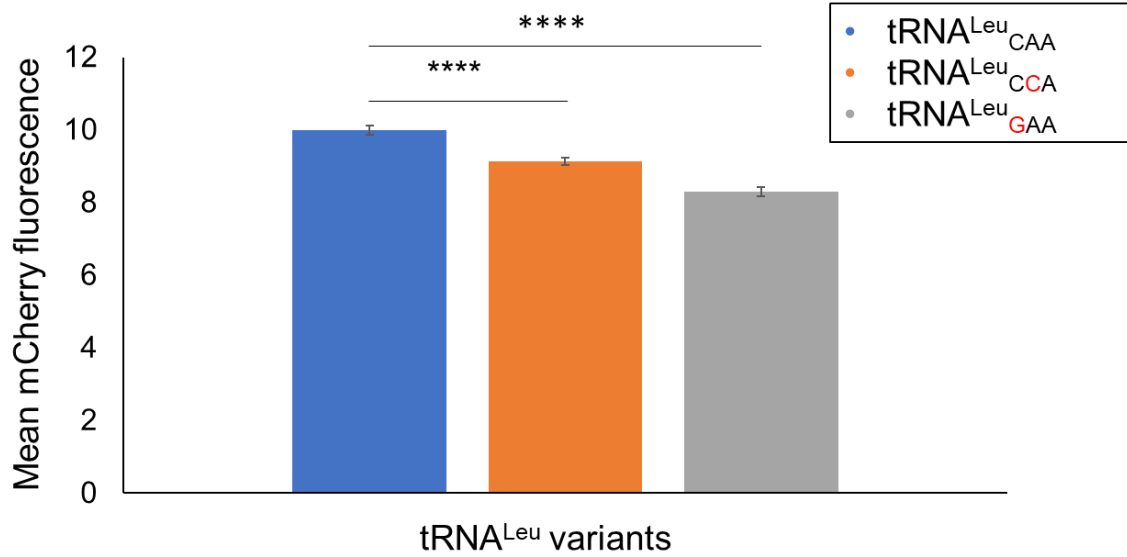
Supplemental figure 1: Random tRNA^{Leu} oligo purchased from geneart. The sequence for tRNA^{Leu}_{XXX} is highlighted in yellow and the anticodon is highlighted in purple



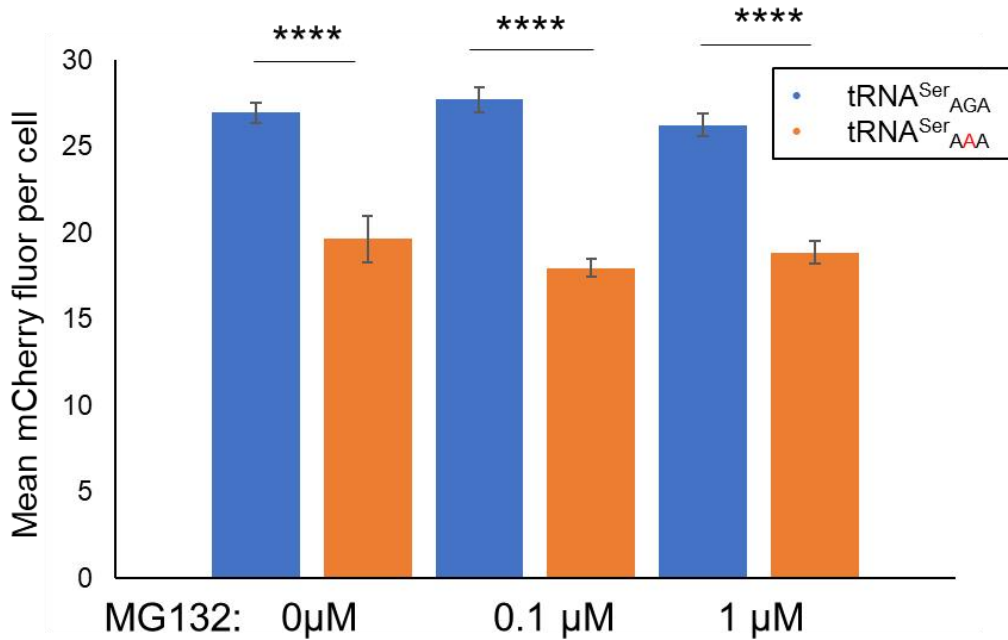
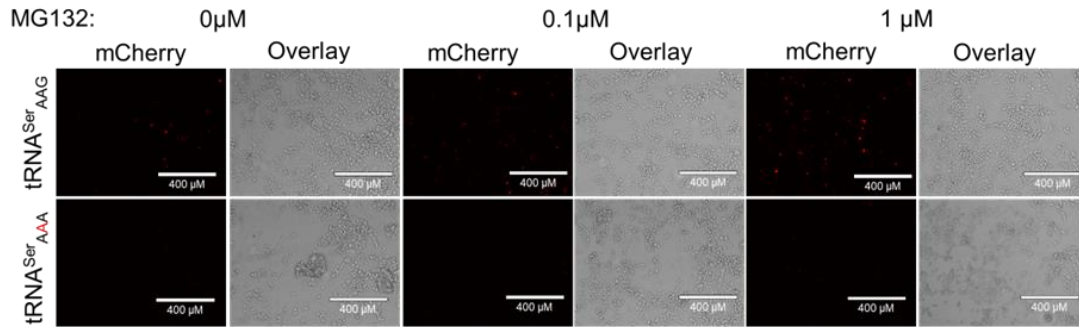
Supplemental Figure 2: Comparing the mean mCherry fluorescence of N2_a cells transfected with tRNA^{Ser}_{AGA} and tRNA^{Ser}_{AAA} (G35A) (phenylalanine) plasmids. Above is the images taken of the N2_a cells 24 hours post transfection of the tRNA^{Ser} plasmids (WT-PAN backbone with eGFP removed). Below is the bar graph comparing the fluorescence between tRNA^{Ser}_{AGA} and tRNA^{Ser}_{AAA} expressing cells. Statistical analysis was done using Welch's t-test. (n.s. = no significant difference, * p < 0.05, ** p < 0.01, *** p < 0.001, **** p < 0.0001)



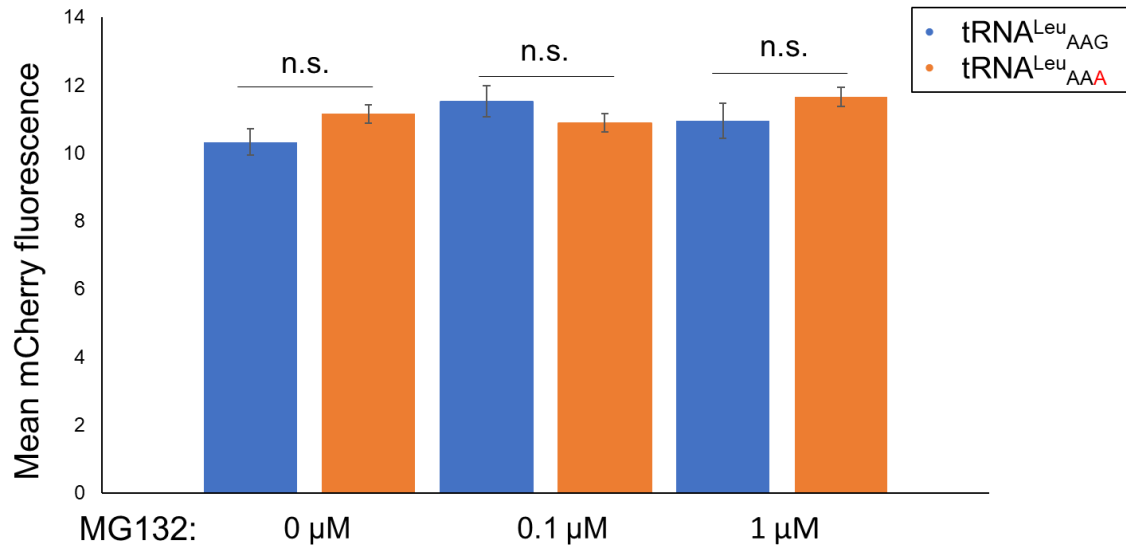
Supplemental figure 3: The mean mCherry fluorescence of N2_a cells expressing tRNA^{Leu}_{AAG} and tRNA^{Leu}_{AAA}(G36A) (phenylalanine anticodon). This is a bar plot comparing the mean mCherry fluorescence between tRNA^{Leu}_{AAG}, and tRNA^{Leu}_{AAA} expressing N2_a cell lines. the statistical test used the Welch's t-test. (n.s. = no significant difference, * p < 0.05, ** p < 0.01, *** p < 0.001, **** p < 0.0001).



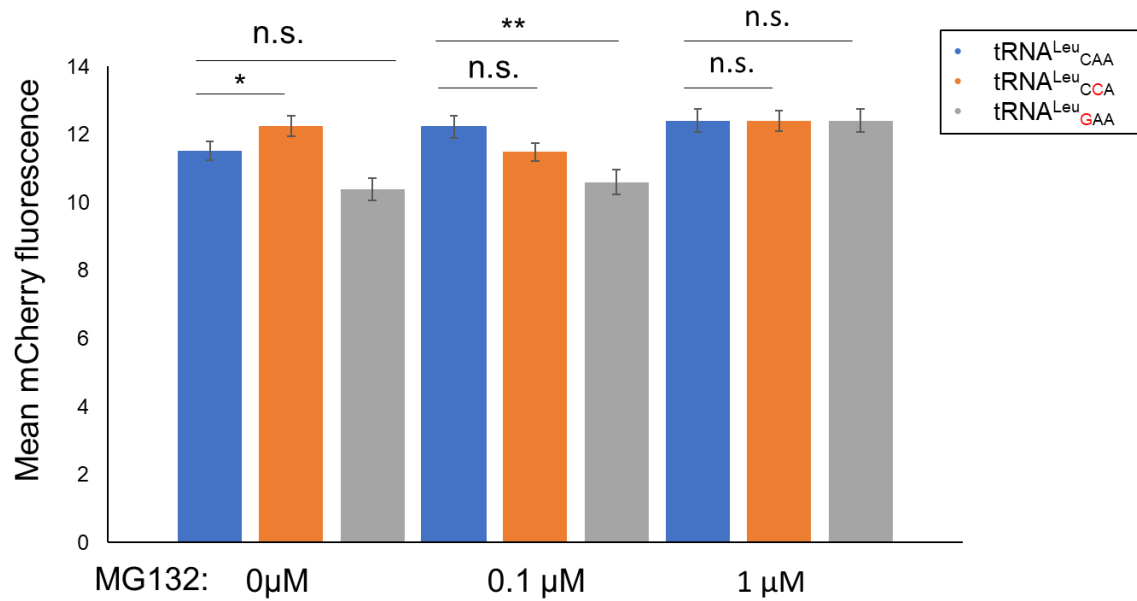
Supplemental Figure 4: The mean mCherry fluorescence of N2_a cells expressing tRNA^{Leu}_{CAA}, tRNA^{Leu}_{CCA} (A35C) (tryptophan anticodon) and tRNA^{Leu}_{GAA} (C34G) (phenylalanine anticodon). This plot compares the mean mCherry fluorescence in N2_a cells expressing tRNA^{Leu}_{CAA}, tRNA^{Leu}_{CCA} and tRNA^{Leu}_{GAA}. the statistical test was Welch's t-test. (n.s. = no significant difference, * p < 0.05, ** p < 0.01, *** p < 0.001, **** p < 0.0001).



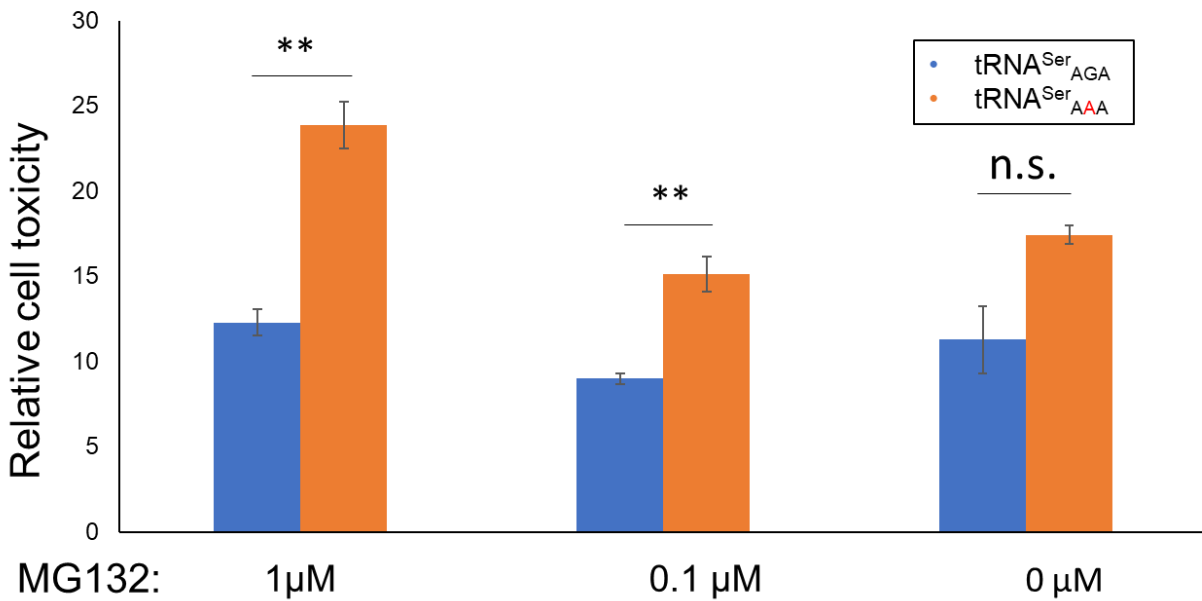
Supplemental Figure 5: Comparing the mean mCherry fluorescence of N2_a cells transfected with tRNA^{Ser}_{AGA} and tRNA^{Ser}_{AAA} (G35A) (phenylalanine) plasmids 4 hours after MG132 treatment. Above are the images of N2_a cells transfected with tRNA^{Ser}_{AGA} and tRNA^{Ser}_{AAA} plasmids under four different MG132 concentrations (0, 0.1 and 1.0 μg/mL). Below is a bar plot comparing the mCherry fluorescence between tRNA^{Ser}_{AGA} and tRNA^{Ser}_{AAA} cells under the different MG132 treatments (0, 0.01 and 1.0 μg/mL). The statistical test used was Welch's t-test. (n.s. = no significant difference, * p < 0.05, ** p < 0.01, *** p < 0.001, **** p < 0.0001)



Supplemental Figure 6: The mean mCherry fluorescence of N2_a cells expressing tRNA^{Leu}_{AAG} and tRNA^{Leu}_{AAA} (G36A) (phenylalanine anticodon) 4 hours post MG132 treatment. This bar plot compares the fluorescence between tRNA^{Leu}_{AAG}, and tRNA^{Leu}_{AAA} expressing N2_a cell lines. There are four different MG132 conditions (0, 0.01 and 1.0 μg/mL MG132). the statistical test was Welch's t-test. (n.s. = no significant difference, * p < 0.05, ** p < 0.01, *** p < 0.001, **** p < 0.0001)



Supplemental figure 7: The mean mCherry fluorescence of N2_a cells expressing tRNA^{Leu}_{CAA}, tRNA^{Leu}_{CAA} (A35C) (tryptophan anticodon) and tRNA^{Leu}_{CAA} (C34G) (phenylalanine anticodon) 4 hours post MG132 treatment. This plot compares the mean fluorescence of tRNA^{Leu}_{CAA}, tRNA^{Leu}_{CCA} and tRNA^{Leu}_{GAA} expressing N2_a cell lines. There are four separate MG132 conditions (0, 0.01 and 1.0 μg/mL). the statistical used test was Welch's t-test. (n.s. = no significant difference, * p < 0.05, ** p < 0.01, *** p < 0.001, **** p < 0.0001)



Supplemental Figure 8: Comparing the cytotoxicity of N2_a cells transfected with tRNA^{Ser} plasmids 4 hours post MG132 treatment. This is a bar plot comparing the cytotoxicity in N2_a cells caused by tRNA^{Ser}_{AGA} vs. tRNA^{Ser}_{AAA} under three different MG132 conditions (0, 0.1 and 1.0 μg/mL MG132). the statistical test used was Welch's t-test. (n.s. = no significant difference, * p < 0.05, ** p < 0.01, *** p < 0.001).

Supplemental tables:

Supplemental table 1: Description of plasmids transformed into *S. cerevisiae*

Yeast tRNA plasmids	Description
CB4043	YCPlac111(leu2) gene with tRNA ^{Leu} _{UAA} B2 gene cloned in
CB4045	YCPlac111(leu2) gene with tRNA ^{Leu} _{UGG} gene cloned in
CB4718	YCPlac111(leu2) gene with the tetO promoter cloned in and the tRNA ^{Leu} _{UAA} B2 gene cloned in upstream
CB4727	YCPlac111(leu2) gene with the tetO promoter cloned in with tRNA ^{Leu} _{UGG} gene cloned in upstream
CB4744	YCPlac111(leu2) gene with the tetO promoter cloned in with random tRNA ^{Leu} _{NNN} gene cloned in upstream
CB4919	YCplac111(leu2) gene with the tetO promoter cloned in and the tRNA ^{Leu} _{CCC} (G26A) gene cloned upstream of the tetO gene
CB4920	Same as 4919 except the anticodon is Ser CGA
CB4921	Same as 4919 except the anticodon is His ATG
CB4923	Same as 4919 except the anticodon is Ala GGC
CB4924	Same as 4919 except the anticodon is Leu CAG

CB4926	Same as 4919 except the anticodon is Ser GGA
CB4927	Same as 4919 except the anticodon is Phe AAA
CB4928	Same as 4919 except the anticodon is Ala TGC
CB4929	Same as 4919 except the anticodon is Lys TTT
CB4930	Same as 4919 except the anticodon is Tyr ATA
CB4931	Same as 4919 except the anticodon is Glu TTG
CB4932	Same as 4919 except the anticodon is Asp ATC
CB4933	Same as 4919 except the anticodon is Arg GCG
CB4934	Same as 4919 except the anticodon is Stop TTA
CB4936	Same as 4919 except the anticodon is Lys CTT
CB4937	Same as 4919 except the anticodon is Val GAC
CB4938	Same as 4919 except the anticodon is Ser TGA
CB4939	Same as 4919 except the anticodon is Leu CAA
CB4940	Same as 4919 except the anticodon is Arg TCT
CB4941	Same as 4919 except the anticodon is Gly TCC

CB4951	Same as 4919 except the anticodon is Glu CTC
CB4952	Same as 4919 except the anticodon is Asp GTC
CB4953	Same as 4919 except the anticodon is Trp CCA
CB4954	Same as 4919 except the anticodon is Arg CCT
CB4955	Same as 4919 except the anticodon is Pro UGG
CB4966	Same as 4919 except the anticodon is Thr CGT
CB4967	Same as 4919 except the anticodon is Ile TAT
CB4968	Same as 4919 except the anticodon is Pro CGG
CB4969	Same as 4919 except the anticodon is Val AAC
CB4970	Same as 4919 except the anticodon is Pro AGG
CB4971	Same as 4919 except the anticodon is Stop TCA
CB4972	Same as 4919 except the anticodon is Val TAC
CB4973	Same as 4919 except the anticodon is Ile GAT
CB4987	Same as 4919 except the anticodon is Leu UAA
CB5019	Same as 4919 except the anticodon is Met CAT

CB5074	Same as 4919 except the anticodon is Arg CCG
CB5075	Same as 4919 except the anticodon is Pro GGG
CB5076	Same as 4919 except the anticodon is Val CAC
CB5090	Same as 4919 except the anticodon is Cys GCA
CB5109	Same as 4919 except the anticodon is Met CAU

Supplemental table 2: Primers used in synthesizing human tRNA^{Leu}

Mammalian tRNA oligos	MW	Tm	Sequence
F-tL-AAG-3-1-RD1	9449	72.9	CCACAGCGAACCTGCGAAC
R-tL-AAG-3-1-RD1	6464	61.8	TGAGCACACTACAGAGAGGCT
F-tL-AAG-3-1-Rd2-PciI	10067	72.1	<u>CAGACTACATGTTTACATCGGTGACGCAA</u> G
R-tL-AAG-3-1-Rd2-PciI	9007	74.9	<u>CAGACTACATGTGGCAGGAGAATGGCTTG</u>
F-tL-AAG2AAA	8332	73.9	<u>GGATTAAAGCTCCAGTCTCTTCGGGGG</u>
R-tL-AAG2AAA	8334	72	<u>GAAGAGACTGGAGCTTTAATCCAGCGC</u>
F-tL-CAA-3-1-Rd1 F	5942	67.4	CTCAAACAATCCTCCCCGCT

R-tL-CAA-3-1- RD1 R	7119	68.9	CTCCACCTTCATCTTTTCCAACCA
F-tL-CAA-3-1- Rd2-PciI	1006 7	72.1	<u>CAGACTACATGTTTTTCCTCTTGGCTTTTT</u> GAG
R-tL-CAA-3-1- Rd2-PciI	9449	72.9	<u>CAGACTACATGTGTCCCTCTAGCCAGGAA</u> AC
F-tL- CAA2CCA	7732	73.4	<u>GAAGTAGCAACTGGAGTCTGGCGCC</u>
R-tL- CAA2CCA	7578	69.8	<u>CAGACTCCAGTTGCTACTTCCCAGG</u>
F-tL-CAA-3-1- Rd1	8334	72	CTCAAACAATCCTCCCCGCT
R-tL-CAA-3-1- Rd1	7119	68.9	CTCCACCTTCATCTTTTCCAACCA
F-tL-CAA-3-1- Rd2 F	1006 7	72.1	<u>CAGACTACATGTTTTTCCTCTTGGCTTTTT</u> GAG
R-tL-CAA-3-1- Rd2 R	9449	72.9	<u>CAGACTACATGTGTCCCTCTAGCCAGGAA</u> AC
F- tLCAA2GAA	7732	73.4	<u>GAAGTAGCAACTTCAGTCTGGCGCC</u>
R- tLCAA2GAA	7642	67.9	<u>CAGACTGAAGTTGCTACTTCCCAGG</u>
F-tL-TAA-4-1- RD1	7352	60.9	TTAGGTAGAACATCCACTTAGGCT
R-tL-TAA-4-1- RD1	7678	61.9	ACTCTTCTGTATGTCAATGTATGGG

F-tL-TAA-4-1-Rd2 F	1114 7	70.9	<u>CAGACTACATGGTGATAGGAATGTATTCA</u> AGACTTG
R-tL-TAA-4-1-Rd2 R	9535	76.4	<u>CAGACTACATGCATTGACAGGCGTGGATT</u> TC
F-tL-TAA2TAAA	7881	71	<u>CCATTGGATCTTTAAGTCCAACGCCT</u>
R-tL-TAA2TAAA	8043	66.4	<u>GTTGGACTTAAAGATCCAATGGACAG</u>
F-WT-PAN-PCI1	6035	64.8	GTTTCGCCACCTCTGATTG
R-WT-PAN-PCI1	7070	63.6	GGGCCATTTACCGTAAGTTATGT

Supplemental Table 3: Table of the doubling times of the tRNA^{Leu} variants with the plasmids on the leftmost column of the table. These are doubling times of strains at 0, 0.01 and 1.0µg/mL dox. The BLOSUM62 score for the amino acid replacement is also listed on the rightmost column.

Plasmid no.	Anticodon	0 dox	0.01 dox	1.0 dox	BLOSUM62
4923	Ala GGC	89.5	91.1	89.4868	-1
4928	Ala UGC	88.0	94.3	97.8	-1
5074	Arg CCG	99.2	102.8	107.8	-2
4954	Arg CCU	89.7	92.4	91.3	-2
4933	Arg GCG	122.7	179.1	205.9	-2
4940	Arg UCU	97.5	96.9	98.7	-2
4932	Asp AUC	84.7	85.5	84.3	-4
4952	Asp GUC	102.7	111.2	120.6	-4
5090	Cys GCA	91.3	90.5	90.1	-1
4951	Glu CUC	99.2	99.5	101.6	-3
4931	Glu UUG	84.8	82.2	84.5	-3
4919	Gly CCC	85.7	92.1	96.3	-4
4941	Gly UCC	97.3	101.0	102.0	-4
4921	His AUG	82.9	82.8	83.6	-3
4973	Iso GAU	93.3	97.1	99.1	2
4967	Iso UAU	85.3	87.1	86.7	2

4939	Leu CAA	92.5	91.3	90.7	4
4924	Leu CAG	83.3	83.1	83.8	4
4987 W.T.	Leu UAA	89.2	90.2	89.5	4
4936	Lys CUU	84.0	84.0	83.2	-2
4929	Lys UUU	89.2	92.0	91.7	-2
5109	Met CAU	91.5	101.1	103.4	2
4927	Phe AAA	83.6	81.3	80.9	-1
4970	Pro AGG	115.0	128.0	148.3	-3
4968	Pro CGG	117.6	129.3	179.2	-3
5075	Pro GGG	100.3	108.7	112.2	-3
4955	Pro UGG	121.1	135.2	151.5	-3
4920	Ser CGA	89.5	92.8	93.0	-2
4926	Ser GGA	87.9	90.9	90.8	-2
4938	Ser UGA	91.6	94.4	94.4	-2
4971	Stop UCA	89.5	91.5	91.2	
4934	Stop UUA	87.4	87.0	85.6	
4966	Thr CGU	88.5	91.5	98.7	-1
4953	Trp CCA	89.9	90.8	90.6	-2
4930	Tyr AUA	81.0	79.7	81.9	-1

5076	Val CAC	102.8	92.9	96.2	1
4969	Val AAC	87.3	91.9	89.9	1
4937	Val GAC	83.7	82.7	81.4	1
4972	Val UAC	88.8	88.9	89.5	1

CURRICULUM VITAE

Name Peter Anderson Hall

Post-Secondary Education Queen's University – Kingston, Ontario

- Fall 2015 to December 2019

Publication

- DeVaux, RS, Ropri, AS, Grimm, SL, et al. Long noncoding RNA BHLHE40-AS1 promotes early breast cancer progression through modulating IL-6/STAT3 signaling. J Cell Biochem. 2020; 121: 3465– 3478. <https://doi.org/10.1002/jcb.29621>

Related work experience

- Research Assistant
London Research and development centre
1391 Sandford St, London
August 2019

Presentations and Posters

- Gave presentation titled “BHLHE40-AS1 regulates levels of IL6 and p-STAT3 in breast cancer progression” to both researchers at the SUNY Cancer Research Centre and Queen's biochemistry faculty members (December 2018 and January 2019)

- Presented poster titled “Elucidating the function of NucG” to Queen’s life sciences and biochemistry professors (April 2019)
 - Presented “Probing the genetic code with tRNA variants” at the London Health Research Day (May 11th – May 12th)
 - Presented “Probing the genetic code with tRNA variants” at the Toronto RNA Enthusiasts Day (July 28th, 2021 – July 29th, 2021)
-